

University of Mississippi

eGrove

---

Electronic Theses and Dissertations

Graduate School

---

1-1-2015

## Influence of novel techniques on solubility, mechanical properties and permeability via hot melt extrusion technology

Eman A. Ashour

*University of Mississippi*

Follow this and additional works at: <https://egrove.olemiss.edu/etd>



Part of the [Pharmacy and Pharmaceutical Sciences Commons](#)

---

### Recommended Citation

Ashour, Eman A., "Influence of novel techniques on solubility, mechanical properties and permeability via hot melt extrusion technology" (2015). *Electronic Theses and Dissertations*. 1464.

<https://egrove.olemiss.edu/etd/1464>

This Dissertation is brought to you for free and open access by the Graduate School at eGrove. It has been accepted for inclusion in Electronic Theses and Dissertations by an authorized administrator of eGrove. For more information, please contact [egrove@olemiss.edu](mailto:egrove@olemiss.edu).

INFLUENCE OF NOVEL TECHNIQUES ON SOLUBILITY, MECHANICAL PROPERTIES  
AND PERMEABILITY VIA HOT MELT EXTRUSION TECHNOLOGY

A Dissertation  
presented in partial fulfillment of requirements  
for the degree of Doctor of Philosophy  
in the Department of Pharmaceutics and Drug Delivery  
The University of Mississippi

by

EMAN A. ASHOUR

December 2015

Copyright<sup>©</sup> by Eman A. Ashour  
All rights reserved

## ABSTRACT

Hot melt extrusion (HME) was evaluated as a continuous processing technology for the manufacture of solid dispersions. The aim of the current research project was to study the effect of pressurized carbon dioxide (P-CO<sub>2</sub>) on the physico-mechanical properties of three different grades of cellulose polymers, Klucel™ ELF, EF and LF hydroxypropylcellulose (HPC) resulting from hot melt extrusion techniques, and to assess the plasticization effect of P-CO<sub>2</sub> on the tested polymers. The physico-mechanical properties as well as the tablet characteristics of the extrudates with and without injection of P-CO<sub>2</sub> and with non-extruded polymers were examined. P-CO<sub>2</sub> acted as plasticizer for Klucel™ LF, EF and ELF and allowed for a reduction in processing temperature during the extrusion process by 20°C as compared to the processing temperature without injecting P-CO<sub>2</sub>. Furthermore, the CO<sub>2</sub> served as a pore former and produced foam-like structure extrudates. This morphological change resulted in an increase in bulk and tap density as well as surface area and porosity. Additionally, the hardness of the tablets of the polymers with P-CO<sub>2</sub> was increased compared to polymer processed without P-CO<sub>2</sub> and the non-extruded polymer. Moreover, the % friability of the tablets improved using P-CO<sub>2</sub> processed polymer. Thus good binding properties and compressibility of the extrudates were positively influenced utilizing P-CO<sub>2</sub> processing.

The interest to incorporate a model was increased to investigate the effect of pressurized carbon dioxide (P-CO<sub>2</sub>) on the physico-mechanical properties as well as the drug release behavior.

Ketoprofen (KTP), used as a model drug, was incorporated with hydroxypropylcellulose (HPC) (Klucel™ ELF, EF and LF) as a polymeric carrier to produce KTP amorphous solid dispersion using HME technique. Thermal gravimetric analysis (TGA) was used to evaluate and confirm the formulations thermal stability. Differential Scanning Calorimetry (DSC) was performed to evaluate the physical state of KTP in the extrudates. The microscopic morphology of the extrudates was changed to a foam-like structure due to expansion of the CO<sub>2</sub> at the extrusion die. The foamy extrudates demonstrated enhanced KTP release compared to the extrudates processed without P-CO<sub>2</sub> due to the increase in porosity and surface area of those extrudates. The moisture content of the extrudates processed with P-CO<sub>2</sub> was slightly increased and this played a significant role in increasing KTP tablet hardness and decreasing percent friability.

A concern with HME is the limitation of the drug loading due to drug-polymer miscibility. In order to solve this issue, we investigated the effect of foam like structure produced by pre P-CO<sub>2</sub> on the drug loading and the dissolution profile of carbamazepine (CBZ) and low molecular weight hydroxypropylcellulose (HPC) matrices using HME technique. The resulted extrudates with P-CO<sub>2</sub> injection exhibited higher surface area and porosity compared to the extrudates processed without P-CO<sub>2</sub>. Moreover, the CBZ release profile of the 20-50% drug load formulations processed with P-CO<sub>2</sub> injection showed almost complete drug release within 2 hours. In contrast, the drug release profiles of 20%, 30%, 40% and 50% CBZ/ Klucel™ ELF formulations processed without P-CO<sub>2</sub> injection exhibited 90%, 86%, 80% and 73% CBZ drug release, respectively. In conclusion, HME processing assisted with P-CO<sub>2</sub> increased the drug loading capability of CBZ in Klucel™ ELF polymeric matrix as well as optimized CBZ drug-release profiles.

Drug permeability and dissolution rate are considered as key to predict the drug bioavailability. HME was used as an approach to improve solubility and permeability of the psychoactive natural product piperine. Piperine 10–40% w/w formulated in Eudragit<sup>®</sup> EPO/ Kollidon<sup>®</sup> VA 64 or Soluplus<sup>®</sup> formulation was used in this study to investigate the efficiency of various polymers to enhance the solubility and permeability of piperine via HME technique to ultimately increase its systemic absorption of the compound. Scanning electron microscopy (SEM) images showed absence of crystals in 10% w/w piperine/Soluplus<sup>®</sup> indicating that piperine was dispersed in the Soluplus<sup>®</sup> polymer carrier in its amorphous form. However, crystals were evident in all other formulations with different ratios. Solubility of 10% and 20% piperine/Soluplus<sup>®</sup> was increased more than 160 and 45 folds in water, respectively. Furthermore, permeability studies using non- everted rat intestinal sac model demonstrated the enhancement in piperine absorption of the 10% w/w piperine/Soluplus<sup>®</sup> extrudates up to 158.9 µg/5mL compared to 1.4 µg/5mL in the case of pure piperine within 20 minutes.

## **DEDICATION**

This dissertation is dedicated to my mom, Mrs. Amal Mekky and the spirit of my father Mr. Abdellatif Ashour, who made education and hard work priority for me. This is also dedicated to my lovely husband Dr. Mohamed Radwan and my sweet children Ali, Renad, and Reem who have encouraged and supported me during this journey.

## ACKNOWLEDGEMENTS

I would never have been able to finish my dissertation without the support of several people. I would like to express my deepest gratitude to all of them. I would like to express my sincere gratitude to my advisor, Dr. Michael A. Repka, Chair & Professor of Pharmaceutics and Drug Delivery for his excellent guidance, caring, patience, and providing me with an excellent atmosphere for doing research. Dr. Repka has been supportive and has given me the freedom to pursue different projects without exception.

I would like to express my sincerest thanks and appreciation to Dr. Mahmoud A. ElSohly, for his support and guidance throughout the last ten years. He was and remains my best role model for a scientist. Dr. ElSohly was the reason why I decided to go and pursue my Ph.D. His continued support led me to the right way. I would like also to thank him for being a member in my dissertation committee.

I would also like to extend my appreciation to my other dissertation committee members Dr. Soumyajit Majumdar and Dr. Samir Ross for their valuable advice and suggestions. My special thanks to Dr. Majumdar for his scientific advices and support in the research projects.

I would like to thank Dr. Sejal Shah, Dr. Vijay Kulkarni and the graduate students in the Department of Pharmaceutics and Drug Delivery for their help and friendship. I would also express my sincere thanks to Ms. Deborah King for her help and patience during my graduate studies.



I am very thankful Dr. Mohammad Khalid Ashfaq for his help with the permeability assay, Dr. Iklas Khan for allowing me to use of FTIR, Dr. Ahmed Galal and Dr. Vijayasankar Raman for their help with the microscopical and SEM images.

My deepest thanks go to my mom. I thank you Mom for all of the sacrifices that you've made on my behalf. Your prayers for me are what sustained me thus far.

Last, but certainly not least, I must acknowledge with tremendous and deep thanks my great husband Dr. Mohamed Radwan who spent sleepless nights with me and was always my support in the moments when there was no one to answer my queries.

## TABLE OF CONTENTS

ABSTRACT .....	ii
DEDICATION .....	v
ACKNOWLEDGEMENTS .....	vi
TABLE OF CONTENTS .....	viii
LIST OF TABLES .....	xiv
LIST OF FIGURES .....	xvi
CHAPTER I	
INTRODUCTION .....	1
CHAPTER II	
RESEARCH PROJECTS AND OBJECTIVES .....	7
2.1. Effect of Pressurized Carbon Dioxide on the Physico-Mechanical Properties of Hot Melt Extruded Cellulose Polymers .....	7
2.1.1. Objective.....	7
2.2. Influence of Pressurized Carbon Dioxide on Ketoprofen-Incorporated Hot-Melt Extruded Low Molecular Weight Hydroxypropylcellulose .....	7
2.2.1. Objective .....	7
2.3. Influence of Pressurized Carbon Dioxide on drug loading of High Melting Point Carbamazepine and Low Molecular Weight Hydroxypropylcellulose Matrices Using Hot Melt Extrusion .....	8

2.3.1. Objective .....	8
2.4. Dissolution Enhancement of the Psychoactive Natural Product- Piperine Using Hot Melt Extrusion Techniques .....	8
2.4.1. Objective .....	8
<b>CHAPTER III</b>	
Effect of Pressurized Carbon Dioxide on the Physico-Mechanical Properties of Hot Melt Extruded Cellulose Polymers .....	9
3.1. Introduction .....	9
3.2. Materials .....	12
3.3. Methodology .....	12
3.3.1. Thermogravimetric Analysis (TGA) .....	12
3.3.2. Hot Melt Extrusion (HME) .....	12
3.3.3. Light Microscopy .....	16
3.3.4. Milling .....	16
3.3.5. Tableting .....	16
3.4. Results and Discussion .....	18
3.4.1. Thermal Analysis .....	18
3.4.2. Hot Melt Extrusion .....	19
3.4.3. Tablets evaluation .....	26
3.5. Conclusion .....	29
<b>CHAPTER IV</b>	
Influence of Pressurized Carbon Dioxide on Ketoprofen-Incorporated Hot-Melt Extruded Low Molecular Weight Hydroxypropylcellulose .....	30

4.1. Introduction .....	30
4.2. Material .....	31
4.3. Method .....	32
4.3.1. Thermal Analysis .....	32
4.3.1.1. Thermogravimetric Analysis (TGA) .....	32
4.3.1.2. Differential Scanning Calorimetry (DSC) .....	32
4.3.2. Physical Mixture .....	32
4.3.3. Hot Melt Extrusion .....	32
4.3.4. Microscopical images .....	36
4.3.5. Milling .....	36
4.3.6. High-Performance Liquid Chromatography (HPLC) .....	36
4.3.7. In Vitro Drug Release .....	36
4.3.8. Tableting .....	37
4.3.8.1. Tablets Preparation .....	37
4.3.8.2. Tablets Evaluation .....	38
4.3.9. Moisture Analysis .....	38
4.3.10. Stability Study .....	38
4.4. Results and discussions .....	38
4.4.1. Thermal Analysis .....	38
4.4.2. Hot melt extrusion .....	41
4.4.3. Drug Content .....	44
4.4.4. <i>In-vitro</i> Drug Release .....	44
4.4.5. Tablets Evaluation .....	47

4.5. Conclusion .....	53
CHAPTER V	
Influence of Pressurized Carbon Dioxide on drug loading of High Melting Point Carbamazepine and Low Molecular Weight Hydroxypropylcellulose Matrices Using Hot Melt Extrusion .....	
	54
5.1. Introduction .....	54
5.2. Materials .....	55
5.3. Methods .....	56
5.3.1. Thermal Analysis .....	56
5.3.1.1. Thermogravimetric Analysis (TGA) .....	56
5.3.1.2. Differential Scanning Calorimetry (DSC) .....	56
5.3.2. Hot Melt Extrusion (HME) .....	56
5.3.3. Density .....	58
5.3.4. Surface Area .....	58
5.3.5. Scanning Electron Microscopy (SEM) .....	58
5.3.6. High-Performance Liquid Chromatography (HPLC) .....	59
5.3.7. <i>In-Vitro</i> Drug Release .....	59
5.4. Results and Discussions .....	61
5.4.1. Thermal Analysis .....	61
5.4.2. Hot Melt Extrusion (HME) .....	65
5.4.3. Density .....	68
5.4.4. Surface Area .....	70
5.4.5. Scanning electron microscopy (SEM) .....	72

5.4.6. CBZ Drug Content and Uniformity .....	74
5.4.7. <i>In- vitro</i> Drug Release .....	74
5.5. Conclusion .....	81
CHAPTER VI	
Dissolution Enhancement of the Psychoactive Natural Product- Piperine Using Hot Melt Extrusion Techniques .....	
	82
6.1. Introduction .....	82
6.2. Materials .....	84
6.3. Methods .....	85
6.3.1. Thermogravimetric Analysis (TGA) .....	85
6.3.2. Differential Scanning Calorimetry (DSC) .....	85
6.3.3. Hot Melt Extrusion (HME) .....	85
6.3.4. Scanning electron microscopy (SEM) .....	87
6.3.5. Fourier transforms infrared spectroscopy (FTIR) .....	87
6.3.6. High-Performance Liquid Chromatography (HPLC) .....	87
6.3.7. Solubility test .....	88
6.3.8. In Vitro Drug Release .....	88
6.3.9. Ex vivo permeability model (non-everted intestinal sac) .....	88
6.4. Results and Discussions .....	89
6.4.1. Pre-formulation Studies .....	89
6.4.2. Hot Melt Extrusion (HME) .....	92
6.4.3. Scanning electron microscopy (SEM) .....	95
6.4.4. Fourier transforms infrared spectroscopy (FTIR) .....	98

6.4.5. Solubility Evaluation .....	102
6.4.6. <i>In Vitro</i> Release Profiles .....	104
6.4.7. Ex vivo permeability model (non-everted intestinal sac) .....	106
6.5. Conclusion .....	108
Bibliography .....	109
Vita .....	123

## LIST OF TABLES

Table 3-1: Formulation composition of HME .....	14
Table 3-2: Placebo tablet composition for non-API extrudates with and without P-CO <sub>2</sub> injection and physical mixture of non-extruded polymers .....	17
Table 3-3: Processing parameters for hot melt extrusion process of K <sub>1</sub> - K <sub>9</sub> .....	21
Table 3-4: Bulk and tap density (g/mL) of milled extrudates with and without P-CO <sub>2</sub> injection .....	25
Table 3-5: Bulk and Tap density of placebo tablet blends (g/mL) .....	26
Table 4-1: Formulation composition of HME .....	33
Table 4-2: Processing parameters for hot melt extrusion process of K <sub>10</sub> - K <sub>15</sub> .....	34
Table 4-3: KTP tablet composition of extrudates with and without P-CO <sub>2</sub> injection .....	37
Table 4-4: Bulk and tap density (g/mL) of milled extrudates with and without P-CO <sub>2</sub> injection .....	44
Table 4-5: Bulk and Tap density of KTP tablet blends (g/mL) .....	47
Table 4-6: Moisture content of KTP/ Klucel™ ELF, EF, and LF extrudates .....	51
Table 5-1: CBZ formulation composition of HME .....	57
Table 5-2: Processing parameters for hot melt extrusion process of C <sub>1</sub> -C <sub>8</sub> .....	66
Table 5-3: Bulk and tap density of CBZ /Klucel™ ELF with and without P-CO <sub>2</sub> injection ± Standard deviation n=3 .....	69
Table 5-4: Surface area and % porosity of different drug loading CBZ /Klucel™ ELF	



with and without P-CO <sub>2</sub> .....	71
Table 5-5: Similarity factor of 20%, 30%, 40% and 50% CBZ /Klucel™ ELF formulations with and without P-CO <sub>2</sub> .....	80
Table 5-6: Dissolution efficiency and mean dissolution time of 20%, 30%, 40% and 50% CBZ /Klucel™ ELF formulations with and without P-CO <sub>2</sub> .....	80
Table 6-1: Piperine formulation composition of HME .....	86
Table 6-2: Processing parameters for hot melt extrusion of PIP/ Eudragit® PEO, PIP/ Soluplus® and PIP/ Kollidon® VA formulations .....	94
Table 6-3: Solubility of piperine and piperine formulation in Water, pH 1.2 and pH 6.8 ...	103

## LIST OF FIGURES

Figure 1-1: Phase diagram of carbon dioxide (CO <sub>2</sub> ) .....	2
Figure 1-2: Schematic diagram for the formation of foamy extrudates via hot melt extrusion process .....	4
Figure 1-3: Biopharmaceutics classification system .....	5
Figure 3-1: Chemical structure of Hydroxypropylcellulose (HPC) .....	11
Figure 3-2: Types of screw elements and the screw configuration .....	13
Figure 3-3: Schematic diagram for P-CO <sub>2</sub> injection in hot melt extrusion processing .....	15
Figure 3-4: TGA thermogram of that Klucel™ ELF, EF and LF .....	18
Figure 3-5: HME extrudates processed with and without P-CO <sub>2</sub> injection .....	20
Figure 3-6: Microscopy photographs of Klucel™ (ELF, EF, and LF) extrudates with and without P-CO <sub>2</sub> injection, or with PG injection (Magnification 3X) .....	23
Figure 3-7: Failed milling of Klucel™ (ELF, EF, and LF) extrudates with PG injection ...	24
Figure 3-8: Hardness in (kp) of Klucel™ ELF/EF/LF placebo tablets .....	27
Figure 3-9: % Friability of Klucel™ ELF/EF/LF placebo tablets .....	28
Figure 4-1: Chemical structure of Ketoprofen (KTP) .....	31
Figure 4-2: 16 mm Prism EuroLab, ThermoFisher Scientific .....	35
Figure 4-3: P-CO <sub>2</sub> injection port .....	35
Figure 4-4: TGA thermogram of that Ketoprofen and Klucel™ ELF, EF and LF .....	39
Figure 4-5: DSC thermogram of Ketoprofen, physical mixture and extrudates with and	

without P-CO <sub>2</sub> injection at 0, 1, 2, 3 months .....	40
Figure 4-6: KTP/ Klucel <sup>TM</sup> extrudates with and without P-CO <sub>2</sub> injections .....	41
Figure 4-7: Microscopy photographs of TS sections of KTP and Klucel <sup>TM</sup> ELF, EF and LF extrudates with and without P-CO <sub>2</sub> injections (Magnification 3X) .....	42
Figure 4-8: Milling processing and milled extrudates .....	43
Figure 4-9: Dissolution profiles of KTP/Klucel <sup>TM</sup> ELF extrudates with and without P-CO <sub>2</sub> injection and physical mixture .....	45
Figure 4-10: Dissolution profiles of KTP/Klucel <sup>TM</sup> EF extrudates with and without P-CO <sub>2</sub> injection and physical mixture .....	46
Figure 4-11: Dissolution profiles of KTP/Klucel <sup>TM</sup> LF extrudates with and without P-CO <sub>2</sub> injection and physical mixture .....	46
Figure 4-12: Ketoprofen tablets .....	48
Figure 4-13: Hardness in (kp) of KTP/Klucel <sup>TM</sup> ELF/EF/LF tablets, with and without P-CO <sub>2</sub> injection and physical mixture .....	49
Figure 4-14: Hardness in (kp) of KTP/Klucel <sup>TM</sup> ELF/EF/LF tablets, with and without P-CO <sub>2</sub> injection and physical mixture .....	50
Figure 4-15: Dissolution profiles of KTP/Klucel <sup>TM</sup> EF tablets with and without P-CO <sub>2</sub> injection .....	52
Figure 5-1: Chemical structure of Carbamazepine (CBZ) .....	55
Figure 5-2: TGA thermogram of carbamazepine (CBZ) and Klucel <sup>TM</sup> ELF .....	61
Figure 5-3: DSC thermogram of CBZ/ Klucel <sup>TM</sup> ELF physical mixtures showing the drug- polymer miscibility at different drug loading .....	62
Figure 5-4: DSC thermogram of 20%, 30%, 40% and 50% of CBZ/ Klucel <sup>TM</sup> ELF	

extrudates with and without P-CO <sub>2</sub> injection and pure CBZ .....	63
Figure 5-5: DSC thermogram showing the $\Delta H$ values of 50% CBZ/ Klucel <sup>TM</sup> ELF extrudates with and without P-CO <sub>2</sub> injection as well as pure CBZ .....	64
Figure 5-6: Photographic picture of CBZ /Klucel <sup>TM</sup> ELF extrudates with and without P- CO <sub>2</sub> injection .....	67
Figure 5-7: SEM image of LS of CBZ /Klucel <sup>TM</sup> ELF extrudates a) without P-CO <sub>2</sub> injection, b) with P-CO <sub>2</sub> injection .....	73
Figure 5-8-a: Dissolution profiles of 20% CBZ/Klucel <sup>TM</sup> ELF extrudates with and without P-CO <sub>2</sub> injection and pure CBZ .....	75
Figure 5-8-b: Dissolution profiles of 30% CBZ/Klucel <sup>TM</sup> ELF extrudates with and without P-CO <sub>2</sub> injection and pure CBZ .....	76
Figure 5-8-c: Dissolution profiles of 40% CBZ/Klucel <sup>TM</sup> ELF extrudates with and without P-CO <sub>2</sub> injection and pure CBZ .....	77
Figure 5-8-d: Dissolution profiles of 50% CBZ/Klucel <sup>TM</sup> ELF extrudates with and without P-CO <sub>2</sub> injection and pure CBZ .....	78
Figure 6-1: Chemical structure of piperine .....	84
Figure 6-2: DSC thermogram of 10%, 20% and 40% of PIP/ Eudragit <sup>®</sup> PEO, PIP/ Soluplus <sup>®</sup> and PIP/ Kollidon <sup>®</sup> VA 64 physical mixtures .....	90
Figure 6-3: DSC thermogram of 10%, 20% and 40% of Piperine/ Eudragit <sup>®</sup> PEO, Piperine/ Soluplus <sup>®</sup> and PIP/ Kollidon <sup>®</sup> VA 64 extrudates .....	91
Figure 6-4: Standard screw configuration of Process 11 Twin Screw Extruder, Thermo Fisher Scientific .....	93

Figure 6-5: SEM of extrudates: a) 10% w/w piperine/Soluplus<sup>®</sup>, b) 20% w/w piperine/Soluplus<sup>®</sup>, c) 40% w/w piperine/Soluplus<sup>®</sup> ..... 96

Figure 6-6: SEM of extrudates: a) 20% piperine/Eudragit<sup>®</sup> EPO, b) 20% piperine/Kollidon<sup>®</sup> VA6 ..... 97

Figure 6-7: FTIR spectra of Soluplus<sup>®</sup>, piperine, 10% piperine /Soluplus<sup>®</sup>, 20% piperine /Soluplus<sup>®</sup>, 40% piperine /Soluplus<sup>®</sup> extrudates ..... 99

Figure 6-8: FTIR spectra of Eudragit<sup>®</sup> EPO, piperine, 20% piperine / Eudragit<sup>®</sup> EPO physical mixture and extrudates ..... 100

Figure 6-9: FTIR spectra of Kollidon<sup>®</sup> VA 64, piperine, 20% piperine / Kollidon<sup>®</sup> VA 64 physical mixture and extrudates ..... 101

Figure 6-10: *In-vitro* release profiles of 10% w/w piperine/Soluplus<sup>®</sup>, 20% w/w piperine/Soluplus<sup>®</sup>, 40% w/w piperine/Soluplus<sup>®</sup>, 20% piperine/Eudragit<sup>®</sup> EPO, 20% piperine/Kollidon<sup>®</sup> VA64 and pure piperine ..... 105

Figure 6-11: Piperine absorption characteristics using jejunum non-everted sac under normal physiological conditions ..... 107

## **CHAPTER I**

### **INTRODUCTION**

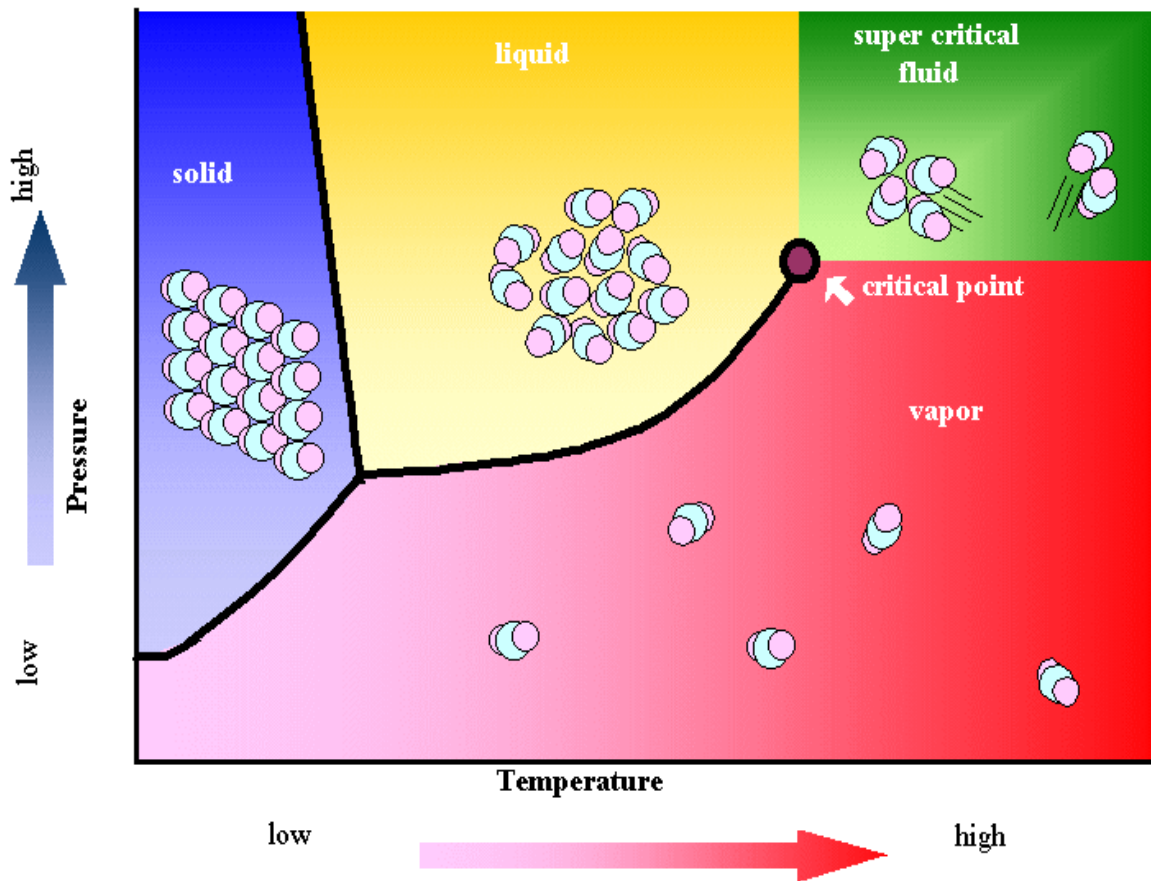
Hot melt extrusion (HME) is a well-known processing technology which represents a novel method to prepare solid dispersions. HME can simply be defined as a mixture of one or more active pharmaceutical ingredients and at least one polymeric carrier forced through extrusion die under controlled conditions to form a solid solution [1]. Being fast, simple, continuous and a solvent free process, HME has received great attention in the pharmaceutical industry [2].

On the other hand most of the polymeric carriers have a high glass transition temperature ( $T_g$ ) of 150 °C or more. Therefore, incorporation of a plasticizer is required in order to facilitate the processing conditions as well as enhance the stability of the extrudates. The use of plasticizers will lower the polymer viscosity due to the reduction in polymer  $T_g$  and therefore, increases the thermal stability and minimizes the material thermal decomposition. There are many factors to be considered to choose the suitable plasticizer such as the plasticizer efficiency, the plasticizer-polymer compatibility and the plasticizer stability. The resulting extrudates exhibit an elastic smooth surface and low porosity. These extrudates properties may lower the formulation drug release and also decrease the milling efficiency of those extrudates. The percentage of the plasticizers in the formulation varies depending on the type of polymeric carrier as well as the plasticizer efficacy. Incorporating plasticizers in pharmaceutical formulations will increase the formulations final weight and result in patients complaints. Therefore, the use of a physical

blowing agent as a reversible plasticizer has gained a great interest in HME processing technology.

Carbon dioxide (CO<sub>2</sub>) is considered as a great example for a physical blowing agent. It acts as a reversible plasticizer and foaming agent [3]. CO<sub>2</sub> is chemically inert and present in four different state, with the change from state to state mainly depends on its temperature and the pressure.

Figure 1-1 shows the phase diagram of CO<sub>2</sub> and its critical point of 31°C and 1073 Psi.



**Figure 1-1: Phase diagram of carbon dioxide (CO<sub>2</sub>) [4]**

There are many pharmaceutical applications for supercritical CO<sub>2</sub> (SC-CO<sub>2</sub>) such as a replacement to organic solvents in extraction, micro and nano particales formation, co-solvents, co-precipitating agent, co-crystalizing agent, and in co-precipitation and solid dispersion formation [5]. Additionally, there are also future prospects for the use of CO<sub>2</sub> as a sterilizing agent [6].

As hot melt extrudates have very low porosity structure which may slow down the penetration of dissolution medium and alter the drug release, P-CO<sub>2</sub> could be used as a blowing agent to provide foamy extrudates with solid porous structure, therefore enhance the drug release.

Generally, production of foamed extrudates includes three main steps with in the drug polymer mixtures; cell nucleation, cell growth and finally, the stabilization step [7]. At the first step, the blowing gas implemented the melted mixture then the cell nucleation of the foam is initiated. At the second step, expansion of the gas takes place, in which the growth of the foam structure occurs. On the stabilization step, the foam formation is completed and the excess gas escapes at the extrusion die.

Formation of foamy hot melt extrudates is described schematically in Figure 1-2. At the P-CO<sub>2</sub> injection site, the sudden reduction in pressure and the increase in the temperature allows for the diffusion of CO<sub>2</sub> into the melted material. This condition helps to start the foam nucleation and the foam structure growth [8].



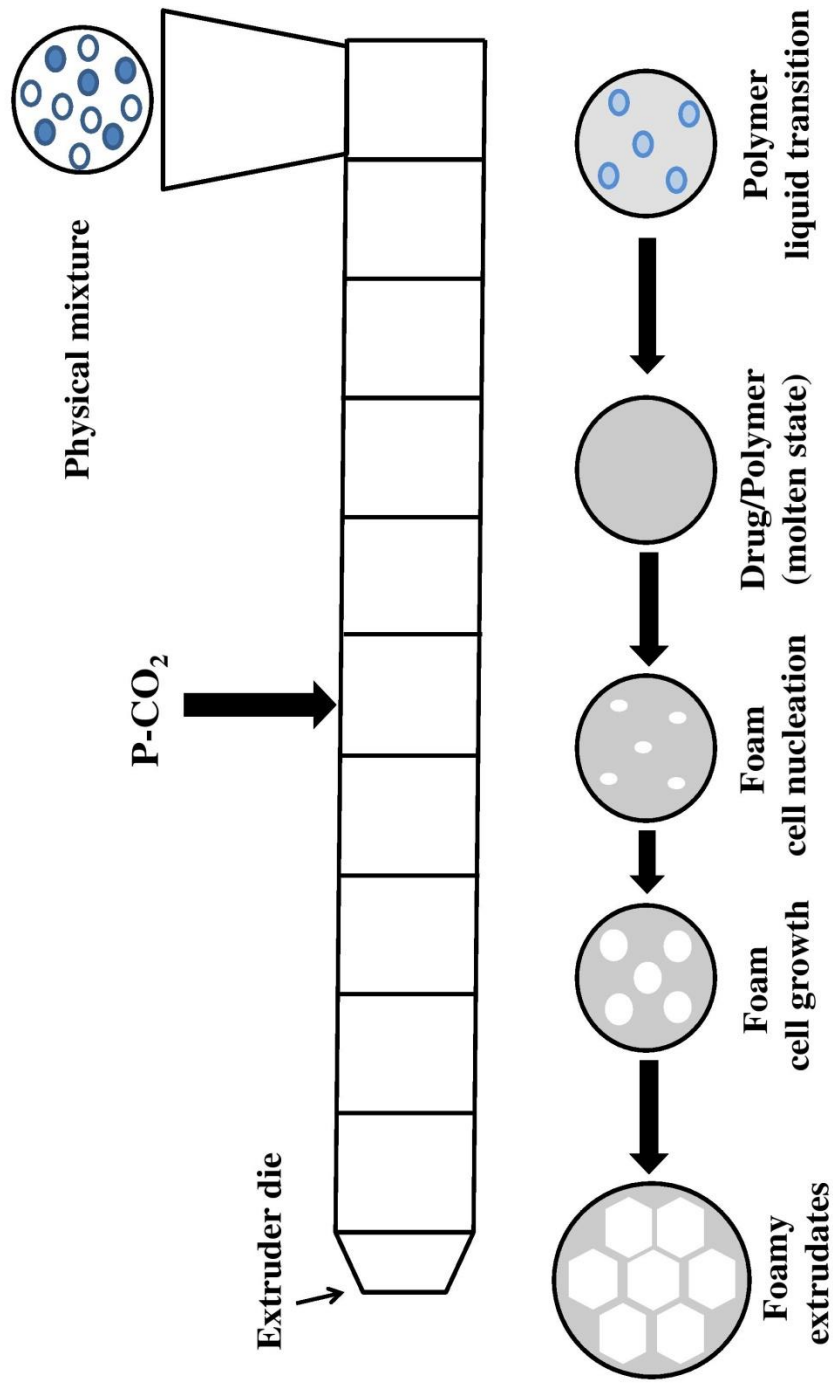


Figure 1-2: Schematic diagram for the formation of foamy extrudates via hot melt extrusion process.

Biopharmaceutics classification system divides the drug into four classes (figure 1-3) depending on two important factors, solubility and permeability. These factors play a big role in the drug absorption and bioavailability. Class I drug having no bioavailability issues as they have good solubility and permeability and hence are easy to formulate for oral administration. While class IV is considered the most difficult one as it represents the drug category which has poor solubility and poor permeability. On the other hand, the biopharmaceutical properties of class II (poor solubility/good permeability) and class III (good solubility and poor permeability) can be modified to develop enhanced bioavailability oral formulations. These modifications can be through enhancing the solubility via HME and other techniques or enhancing the permeability of those drugs. Depending on the drug permeability mechanism of action, different methods can be used to enhance the permeability. Permeability enhancers can be used in case of active transportation mechanism while the HME can be used in case of passive transportation mechanism.

	High Solubility	Low Solubility
High Permeability	<b><u>Class 1</u></b> High Solubility High Permeability Rapid Dissolution	<b><u>Class 2</u></b> Low Solubility High Permeability
Low Permeability	<b><u>Class 3</u></b> High Solubility Low Permeability	<b><u>Class 4</u></b> Low Solubility Low Permeability

**Figure 1-3: Biopharmaceutics classification system by Shugarts *et al.* [9]**

The specific objectives to the current research projects were to study the effect of P-CO<sub>2</sub> on the drug release and drug loading capacity using Ketoprofen (KTP) and Carbamazepine as drug models. In addition, investigate the effect of different polymeric carriers using HME on the solubility and permeability of a model drug piperine, is investigated.

## **CHAPTER II**

### **RESEARCH PROJECTS AND OBJECTIVES**

#### **2.1. Effect of Pressurized Carbon Dioxide on the Physico-Mechanical Properties of Hot Melt Extruded Cellulose Polymers**

##### **2.1.1. Objectives:**

The aims of the this research project were

1. To study the effect of Pressurized carbon dioxide (P-CO<sub>2</sub>) on the physico-mechanical properties of cellulose polymers, Klucel™ LF, EF and ELF hydroxypropylcellulose (HPC) resulting from hot melt extrusion techniques.
2. To assess the plasticization effect of P-CO<sub>2</sub> on the polymers tested (Klucel™ LF, EF and ELF hydroxypropylcellulose (HPC)).

#### **2.2. Influence of Pressurized Carbon Dioxide on Ketoprofen-Incorporated Hot-Melt Extruded Low Molecular Weight Hydroxypropylcellulose**

##### **2.2.1. Objective:**

The goals of the current research project were to:

1. Investigate the effect of pressurized carbon dioxide (P-CO<sub>2</sub>) on the physicomechanical properties of Ketoprofen (KTP) and hydroxypropylcellulose (HPC) matrices produced using hot-melt extrusion (HME) techniques.

2. Study the tablet characteristics of (KTP) and cellulose polymers prepared by Hot-Melt Extrusion (HME) with and without injection of pressurized carbon dioxide (P-CO<sub>2</sub>).

### **2.3. Influence of Pressurized Carbon Dioxide on drug loading of High Melting Point Carbamazepine and Low Molecular Weight Hydroxypropylcellulose Matrices Using Hot Melt Extrusion**

#### **2.3.1. Objective**

The main objective of this research was to investigate the effect of foam like structure produced by pressurized carbon dioxide (P-CO<sub>2</sub>) on the drug loading and the dissolution profile of carbamazepine (CBZ) and low molecular weight hydroxypropylcellulose (HPC) matrices using hot-melt extrusion techniques.

### **2.4. Dissolution Enhancement of the Psychoactive Natural Product- Piperine Using Hot Melt Extrusion Techniques**

#### **2.4.1. Objective**

The aims of the current research project were to:

1. Investigate the efficiency of various polymers to enhance the solubility and dissolution rate of piperine using hot melt extrusion techniques.
2. Increase the systemic absorption of piperine via enhancing its permeability.

## **CHAPTER III**

### **Effect of Pressurized Carbon Dioxide on the Physico-Mechanical Properties of Hot Melt Extruded Cellulose Polymers**

#### **3.1. Introduction**

Solubility is considered one of the most important factors to determine the oral bioavailability of any active pharmaceutical ingredient (API) [10]. Over 40% of APIs are poorly water soluble and result in low oral bioavailability[11]. Thus, enhancement of the solubility and oral bioavailability of APIs has received much interest within the pharmaceutical research community. Various techniques are used to overcome the poor water solubility of APIs such as salt formation, solubilization by cosolvents, particle size reduction, pro-drug approaches, as well as the most successful one to date, solid dispersion technique [10, 12] Solid dispersion is defined as “The dispersion of one or more active ingredients in an inert carrier matrix at solid-state”[13]. There are many methods to prepare solid dispersions such as the fusion method, ball milling, solvent evaporation, lyophilization, hot melt extrusion (HME) and supercritical fluid methods [14-16]

HME has received increasing attention in the pharmaceutical industry over the last few decades as a beneficial technique to produce solid dispersions[17]. There are many advantages of using HME over the conventional pharmaceutical processing methods, such as it is a relatively fast, continuous manufacturing process [18, 19] and it can convert an active pharmaceutical ingredient (API) into its amorphous state [20]. Moreover, another important advantage of HME is that no

solvent is required, so it is considered a “green method” to enhance the solubility and oral bioavailability of poorly water soluble drugs [21, 22]. However, a concern of HME is drug and polymer degradation due to potential high processing temperature. Thus, in case of thermo-labile drugs, processing aids or plasticizers might be added to reduce the viscosity and lower the minimum processing temperature, thus decreasing both drug and polymer degradation [23]. Choice of plasticizers as processing aids in HME depends on the compatibility between the drug and other excipients in the formulation. Use of plasticizers may affect the physico-mechanical properties and drug release profiles of the hot melt extrudates. Plasticizers often increase the elasticity and flexibility of the extrudates [23]. Some plasticizers adversely affect the storage stability of pharmaceutical formulations resulting in changes within their release profiles [24].

It has been reported that P-CO<sub>2</sub> can act as a reversible plasticizer and foaming agent [25]. CO<sub>2</sub> is non-toxic, nonflammable and chemically inert in nature [26, 27]. These properties could increase the interest in the combination of P-CO<sub>2</sub> and HME [28]. Previous investigations have shown that P-CO<sub>2</sub> when injected during HME processing acts as a plasticizer for some pharmaceutically utilized polymers, such as Eudragit® E100, polyvinylpyrrolidone-co-vinylacetate 64 (PVP-VA 64) and ethylcellulose 20 centipoise (EC 20 cps), (allowing for a decrease in their T<sub>g</sub>) [29] and thus, reduction in the extrusion processing temperatures [3, 30-33]. Within the HME process, P-CO<sub>2</sub> changes the microscopic morphology of the extrudates to foam-like structures due to its expansion characteristics at the extrusion die [25, 34]. This morphological change could result in increasing the surface area and porosity, thereby, enhancing the milling efficiency of hot melt extrudates [30, 35]. In the recent past, several studies have evaluated the effect of supercritical CO<sub>2</sub> on HME processing. However, limited studies have been conducted to study the effect of





### **3.2. Materials**

Klucel™ LF, EF and ELF hydroxypropylcellulose (HPC) and polypladone XL™ were obtained as gift samples from Ashland Inc (Wilmington, DW 19808 USA). Propylene glycol and Magnesium Stearate were purchased from Spectrum Chemicals (14422 S. San Pedro Street Gardena, CA 90248 USA). CO<sub>2</sub> was supplied in gas cylinders (pure clean) from Airgas (902 Rockefeller St, Tupelo, MS 38801 USA), Avicel®102 was received as a gift sample from FMC biopolymers (1735 Market Street, Philadelphia PA 19103 USA). Aerosil® was obtained as a gift sample from Evonik degussa Corporation (379 Interpace Parkway, Parsippany, NJ 07054 USA). All other chemicals and reagents used in the present study were of analytical grade and obtained from Fisher scientific (Fair Lawn, NJ 07410 USA).

### **3.3. Methodology**

#### **3.3.1. Thermogravimetric Analysis (TGA)**

TGA studies were performed for Klucel™ LF, EF and ELF hydroxypropylcellulose (HPC) to determine their stability at the extrusion temperatures using a Perkin Elmer Pyris 1 TGA equipped with Pyris manager software (PerkinElmer Life and Analytical Sciences, 710 Bridgeport Ave., Connecticut, USA).

#### **3.3.2. Hot Melt Extrusion (HME)**

The HME processes were performed using a twin-screw extruder (16 mm Prism Euro Lab, ThermoFisher Scientific). The extruder is divided into 10-barrel segments adjacent to the gravimetric feeder. Thermo Fisher Scientific standard screw configuration was used for this study, which consists of four conveying segments and three mixing zones and all of the injections

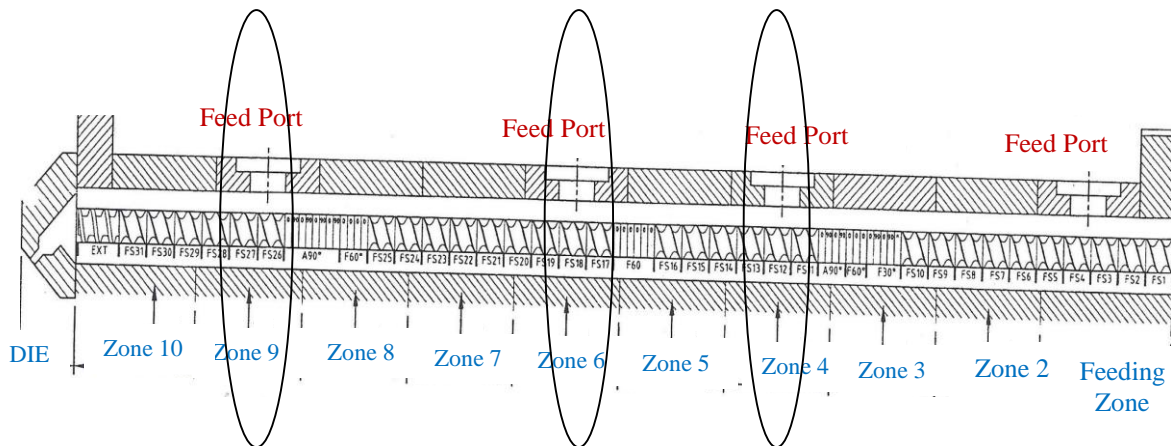
were made through the injection port at the conveying zones of the screw configuration (Figure 3-2).



Conveying elements



Mixing elements



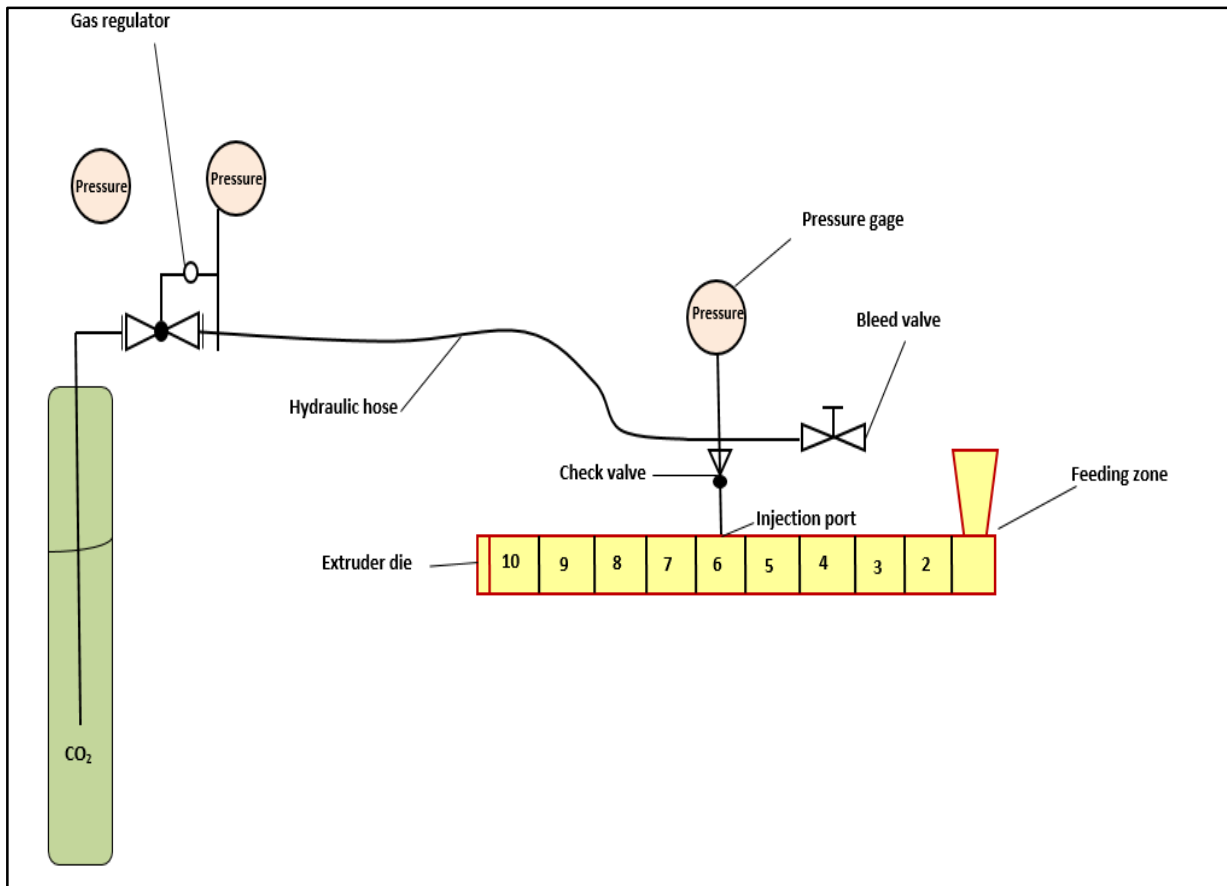
**Figure 3-2: Types of screw elements and the screw configuration.**

All of the formulations as mentioned in (Table 3-1) were extruded at maximum torque possible. The screw speed was 100 rpm at a temperature range from 90-140°C and, at a feed rate of ~ 0.7Kg/hr. The propylene glycol was injected in a barrel segment 4 using Watson-Marlow 520S IP31 Pump.

**Table 3-1: Formulation composition of HME**

<b>Formulation</b>	<b>Klucel™ ELF (%)</b>	<b>Klucel™ EF (%)</b>	<b>Klucel™ LF (%)</b>	<b>Propylene- glycol (PG) (%)</b>	<b>CO<sub>2</sub> Injection Zone</b>
<b>K<sub>1</sub></b>	100	-	-	-	-
<b>K<sub>2</sub></b>	-	100	-	-	-
<b>K<sub>3</sub></b>	-	-	100	-	-
<b>K<sub>4</sub></b>	100	-	-	-	Zone 4
<b>K<sub>5</sub></b>	-	100	-	-	Zone 4
<b>K<sub>6</sub></b>	-	-	100	-	Zone 4
<b>K<sub>7</sub></b>	95	-	-	5	-
<b>K<sub>8</sub></b>	-	95	-	5	-
<b>K<sub>9</sub></b>	-	-	95	5	-

CO<sub>2</sub> was pressurized and injected into the extruder using a high-pressure regulator connected to flexible stainless steel hose with armor casing. The other end of the hose was connected to the four-way connection, fitted with a pressure gauge, bleed valve, check valve (ball type for unidirectional flow of gas), with the later being connected to the injection port seating on the extruder in barrel segment 4 or 6 (Figure 3-3). Metering of CO<sub>2</sub> was regulated using the regulator knob.



**Figure 3-3: Schematic diagram for P-CO<sub>2</sub> injection in hot melt extrusion processing.**

### 3.3.3. Light Microscopy

To evaluate the microscopic morphology of the extrudates with and without P-CO<sub>2</sub> injection and, with the addition of 5% PG, light microscope with camera was used. Thin transverse section (TS) of extrudates were placed on glass slides and observed under the microscope. Photographs of TS samples were taken with zoom power 3x.

### 3.3.4. Milling

The hot melt extrudates were milled and passed through ASTM mesh sieve #35 using a comminuting mill (Fitzpatrick, Model L1A).

### 3.3.5. Tableting

The milled extrudates were used to prepare the tablet blends using microcrystalline cellulose (Avicel<sup>®</sup>102) as diluent, colloidal silicon dioxide (Arosil<sup>®</sup>) as flowability enhancer, polyplasedone XL<sup>™</sup> as a disintegrant and magnesium stearate as a lubricant (Table 1-2). The tablet blends were compressed with the same compression force (1.5-1.6 kN) on a manual tablet press using 8 mm biconcave punch to a final tablet weighing 175mg. The tablet properties such as thickness, hardness and tablets percent friability were performed. A digital caliper was used to obtain the tablet thickness. Optimal control tablet hardness tester was used for the tablet hardness determination. The percent friability was calculated for each batch using a Vanderkamper friability tester by applying the following equation.

$$F = \frac{W_1 - W_2}{W_1} \times 100 \quad \text{(Equation 3-1)}$$

Where F is percent friability, and W1 and W2 are the initial and final tablet weights, respectively.

**Table 3-2: Placebo tablet composition for non-API extrudates with and without P-CO<sub>2</sub> injection and physical mixture of non-extruded polymers**

<b>Excipients</b>	<b>% (w/w)</b>	<b>Weight (mg/tablet)</b>
<b>Klucel™ (ELF/EF/LF)</b>	28.57	50.00
<b>Avicel® 102</b>	68.00	119.00
<b>Aerosil®</b>	0.57	1.00
<b>Polyplasdone™ XL</b>	2.29	4.00
<b>Magnesium stearate</b>	0.57	1.00

### 3.4. Results and Discussions

#### 3.4.1. Thermal Analysis

Thermogravimetric Analysis (TGA) is a technique in which the material sample weight is monitored as a function of temperature. TGA is an essential laboratory tool used to determine the material decomposition temperature and the moisture content. The TGA data demonstrated that Klucel™ ELF, EF and LF degradation temperatures were about 300 °C in which the polymers start losing weight with increasing the temperature. From the TGA thermogram we can conclude that all the polymers used in this study were stable under the employed extrusion processing temperature (120 °C- 140 °C) which is way lower than their decomposing temperatures (Figure 3-4).

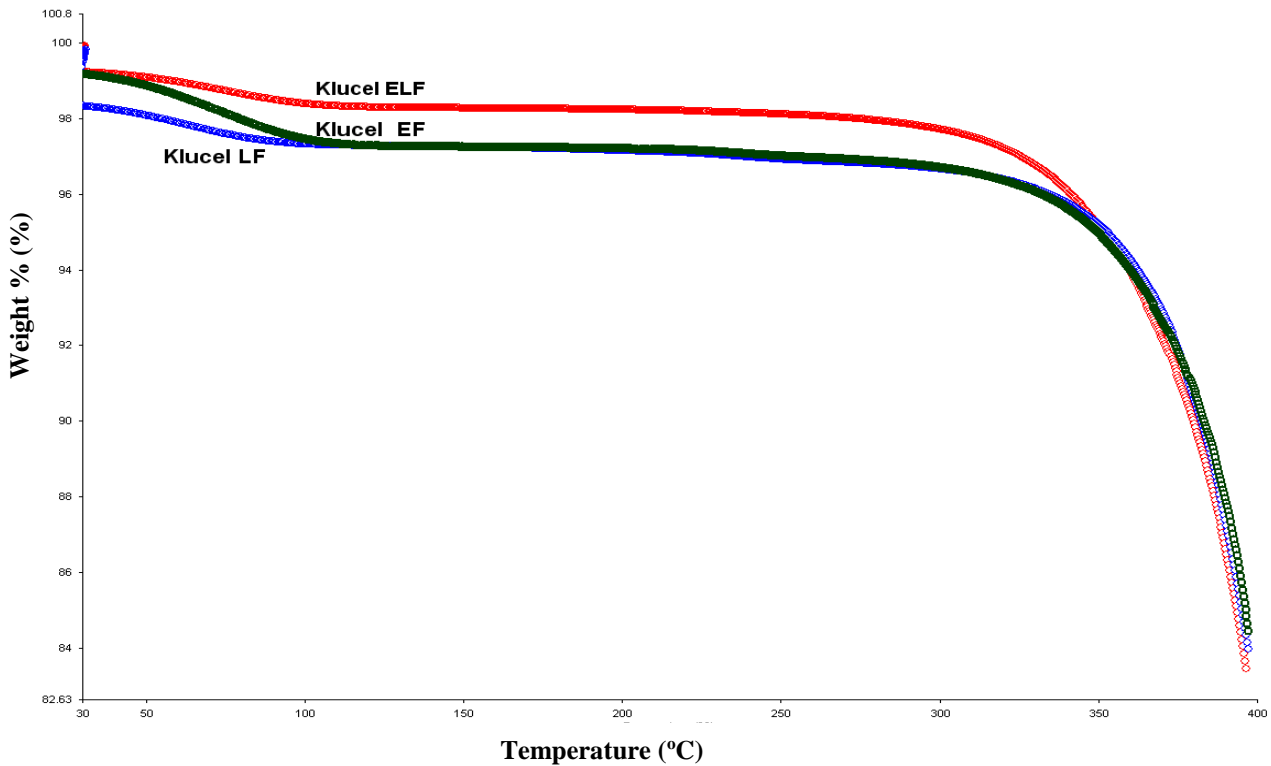
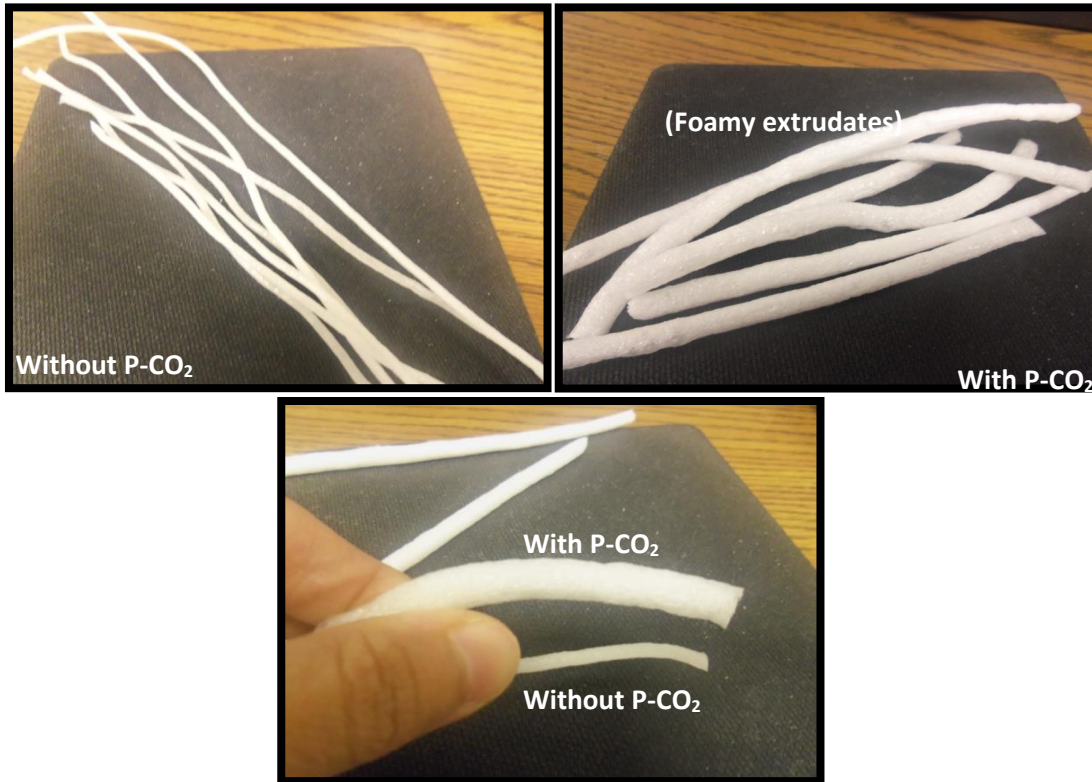


Figure 3-4: TGA thermogram of that Klucel™ ELF, EF and LF.

### 3.4.2. Hot Melt Extrusion

During extrusion with P-CO<sub>2</sub> injection, metering of CO<sub>2</sub> was controlled using the regulator until the reading on the pressure gauge located at the 4-way connector was maintained between 75-150 psi. CO<sub>2</sub> was provided in a liquid form from a CO<sub>2</sub> gas cylinder (pure clean). The back pressure from the injection port maintained the CO<sub>2</sub> in a liquid state that further dropped the temperature at the injection port as low as 2°C. The injection zone should be completely filled with the physical mixture for the formation of the melt seals to prevent any leakage of gas from the extruder and allow good mixing between the materials and CO<sub>2</sub>. As described by Verreck *et al.*, 2007d, diffusion and dissolution of the injected P-CO<sub>2</sub> in the polymers manifested as extremely foamy extrudates with the increment of die swelling accompanied by CO<sub>2</sub> expansion at the terminal end of the die (Figure 3-5).





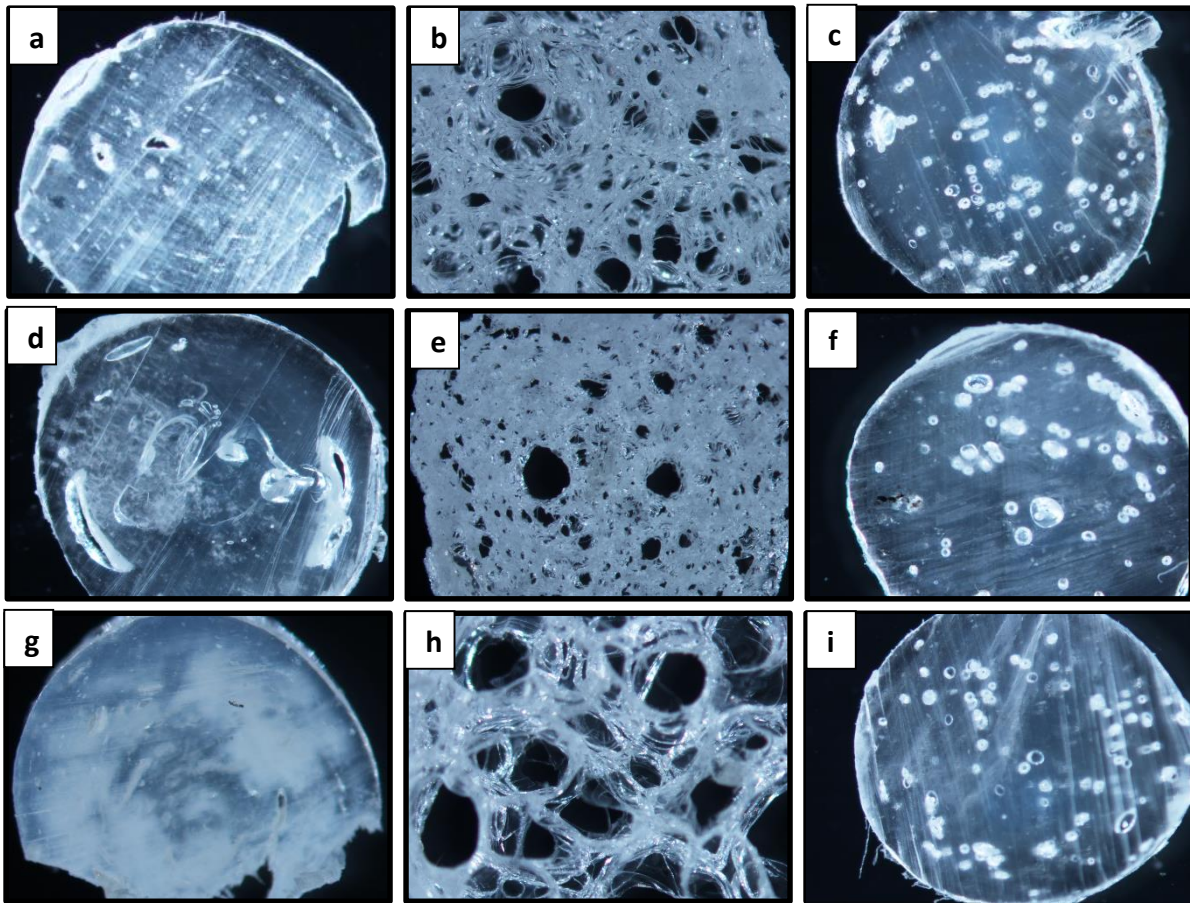
**Figure 3-5: HME extrudates processed with and without P-CO<sub>2</sub> injection.**

As investigated by Repka *et al.*, HPC extrudates were more dense, flexible and hygroscopic [37]. While, upon injection of PG in zone 4, the extrudates were sticky and elastic. Injection of PG as a plasticizer reduced the extrusion processing temperature by about 30°C. However, the P-CO<sub>2</sub> can also act as a plasticizer which has been previously mentioned by Lyons *et al.* [33]. In formulations of k<sub>4</sub>, k<sub>5</sub> and k<sub>6</sub> when P-CO<sub>2</sub> was injected in zone 4, the processing temperature decreased by about 20°C as compared to the processing temperature without injecting P-CO<sub>2</sub> (Table 3-3).

**Table 3-3: Processing parameters for hot melt extrusion process of K<sub>1</sub>- K<sub>9</sub>**

<b>Formulation</b>	<b>Extrusion Temp. (°C)</b>	<b>Screw Speed (rpm)</b>	<b>Torque (Nm)</b>
<b>K<sub>1</sub></b>	140	100	21-22
<b>K<sub>2</sub></b>	140	100	22
<b>K<sub>3</sub></b>	140	100	20-22
<b>K<sub>4</sub></b>	Zone 2-4 (140 °C) Rest of the zones (120 °C)	100	18-18.5
<b>K<sub>5</sub></b>	Zone 2-4 (140 °C) Rest of the zones (120 °C)	100	18
<b>K<sub>6</sub></b>	Zone 2-4 (140 °C) Rest of the zones (120°C)	100	17-19
<b>K<sub>7</sub></b>	90	100	12-16
<b>K<sub>8</sub></b>	90	100	12-17
<b>K<sub>9</sub></b>	90	100	14-18

These findings confirmed that CO<sub>2</sub> acts as a reversible plasticizer and escapes from the formulation at the end of HME processing and no more weight will be added to the formulation as shown by Verreck *et al.* [31]. Furthermore, CO<sub>2</sub> is chemically inert, so the compatibility issue of other plasticizers with the polymers used in the study was avoided. The microscopical images of the extrudates processed with P-CO<sub>2</sub> injection demonstrated higher surface area and porosity as compared to the extrudates processed without P-CO<sub>2</sub> injection and, the one with PG injection (Figure 3-6).



**Figure 3-6: Microscopy photographs of Klucel™ (ELF, EF, and LF) extrudates with and without P-CO<sub>2</sub> injection, or with PG injection (Magnification 3X). (a) ELF without P-CO<sub>2</sub>, (b) ELF with P-CO<sub>2</sub>, (c) ELF with PG injection, (d) EF without P-CO<sub>2</sub>, (e) EF with P-CO<sub>2</sub>, (f) EF with PG injection, (g) LF without P-CO<sub>2</sub>, (h) LF with P-CO<sub>2</sub>, (i) LF with PG injection.**

HPC extrudates typically are very difficult to be milled and a freezing process is required before the milling procedure [38]. Because of the high flexibility and hygroscopicity of the extrudates with PG injection, milling failing occurs due to the shutdown of the Fitzmill as a result of generation of maximum torque (Figure 3-7).



**Figure 3-7: Failed milling of Klucel™ (ELF, EF, and LF) extrudates with PG injection.**

The phenomenon of milling failing on these extrudates with PG injection could not be improved even when the freezing process is used before the milling. Milling process is an essential step in the pharmaceutical industries and failing of this step will prevent any further processing into suitable dosage forms. A significant enhancement of the milling efficiency of extrudates with P-CO<sub>2</sub> injection was observed. The milling efficiency was determined by the torque value of the

Fitzmill. As mentioned by Verreck *et al.*[30] these processing properties of the materials would provide numerous benefits during manufacturing of various solid dosage forms such as tablets and capsules.

Jeong *et al.* has shown that there is a lowering in bulk density of extrudates in the presence of P-CO<sub>2</sub> injection [39]. Our results showed that foamed milled extrudates exhibited lower bulk density and tap density as compared to the extrudates without P-CO<sub>2</sub> injection, due to an increase in porosity and surface area of the extrudates (Table 3-4).

**Table 3-4: Bulk and tap density of milled extrudates with and without P-CO<sub>2</sub> injection (g/mL) ±SD (n=3)**

Sample name	Without P-CO <sub>2</sub> injection		With P-CO <sub>2</sub> injection	
	Bulk density	Tap density	Bulk density	Tap density
<b>Klucel™ ELF</b>	0.265± 0.009	0.366± 0.011	0.154± 0.003	0.241± 0.002
<b>Klucel™ EF</b>	0.294± 0.007	0.441± 0.008	0.131± 0.002	0.213± 0.005
<b>Klucel™ LF</b>	0.304± 0.013	0.435± 0.004	0.191± 0.004	0.227± 0.007

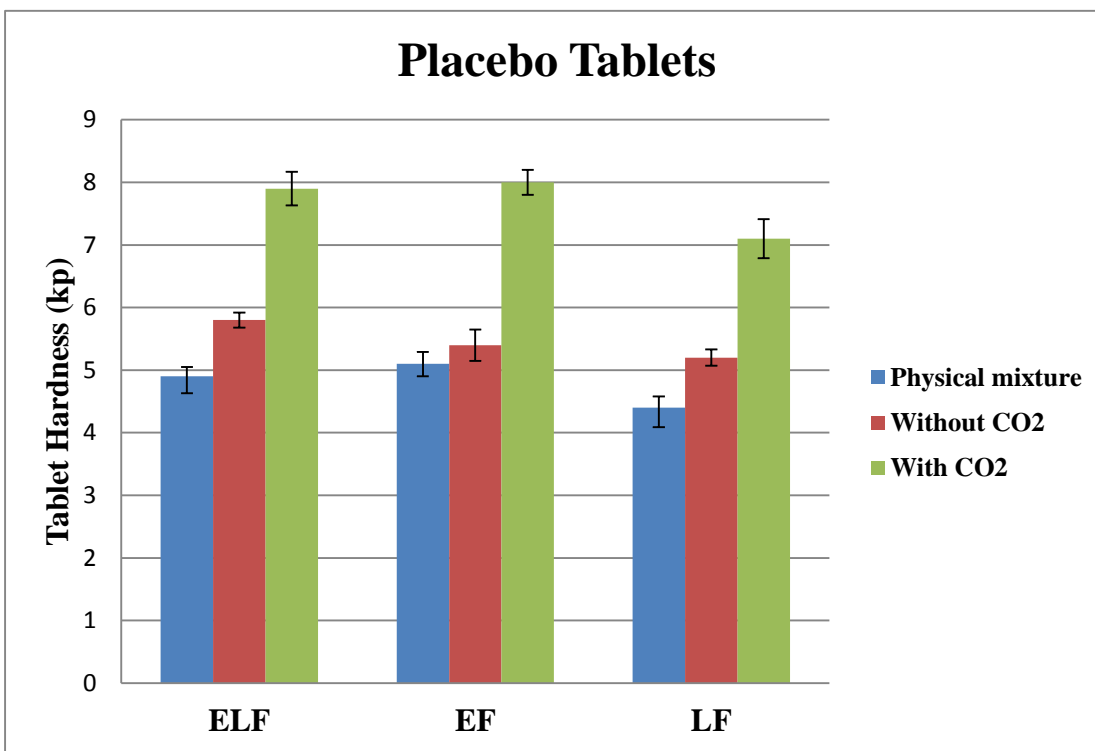
### 3.4.3. Tablets evaluation

The bulk density and tap density of the tablet blends prepared with extrudates processed with P-CO<sub>2</sub> injection was lower as compared to the other blends without P-CO<sub>2</sub> injection and unprocessed physical mixtures, as a result of the foam extrudates (Table 3-5).

**Table 3-5: Bulk and Tap density of placebo tablet blends (g/mL)**

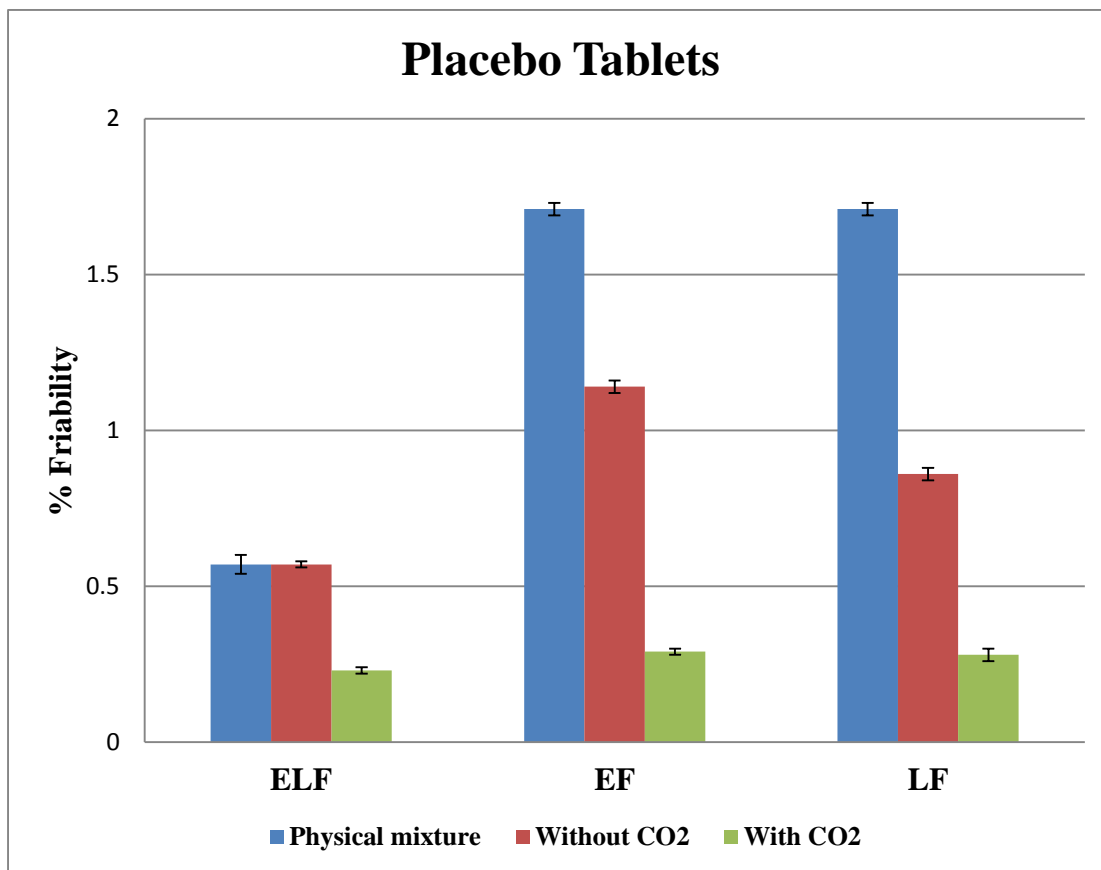
Sample name	Physical mixture		Without P-CO <sub>2</sub> injection		With P-CO <sub>2</sub> injection	
	Bulk Density	Tap Density	Bulk Density	Tap Density	Bulk Density	Tap Density
<b>Klucel™ELF</b>	0.393	0.492	0.366	0.473	0.303	0.419
<b>Klucel™EF</b>	0.395	0.510	0.385	0.485	0.303	0.413
<b>Klucel™LF</b>	0.407	0.516	0.393	0.492	0.354	0.462

The evaluation of all Klucel™ ELF, EF and LF placebo tablets showed that the tablet weight variations of all the formulations were acceptable with very low standard deviations ( $SD < 1.0$ ). In case of the tablets prepared with foamed extrudates, tablet hardness was enhanced by 22%-33% compared to those prepared by extrudates without P-CO<sub>2</sub> injection and unprocessed physical mixtures (Figure 3-8). Tablet friability was evaluated for all of the formulations and the results showed lowering in the % friability of tablets prepared with foamy extrudates (less than 0.3%) as compared to the other tablet formulations (0.6%-1.7%) (Figure 3-9). These results indicated good binding properties and compressibility of foamy extrudates.



**Figure 3-8: Hardness in (kp) of Klucel™ ELF/EF/LF placebo tablets.**





**Figure 3-9: % Friability of Klucel™ ELF/EF/LF placebo tablets.**

### **3.5. Conclusion**

P-CO<sub>2</sub> acted as a temporary plasticizer for Klucel™ ELF, EF, and LF when injected in zone 4 during HME processing, allowing reduction in extrusion temperatures. Whereas, when the P-CO<sub>2</sub> was injected in zone 6 the reduction in extrusion temperature was not feasible. Thus, the zone in which P-CO<sub>2</sub> is injected plays a significant role in melt extrusion processing. The microscopic morphology of the extrudates with P-CO<sub>2</sub> injection was changed to a foam-like structure, which increases their surface area and porosity. Moreover, the milling efficiency of all extrudates processed with P-CO<sub>2</sub> was enhanced, which may be beneficial for optimizing the manufacturing of solid dosage forms. A combination of P-CO<sub>2</sub> and HME improved the tablet properties (higher hardness & lower friability) indicating good binding properties and compressibility of the blends.

### **Acknowledgement**

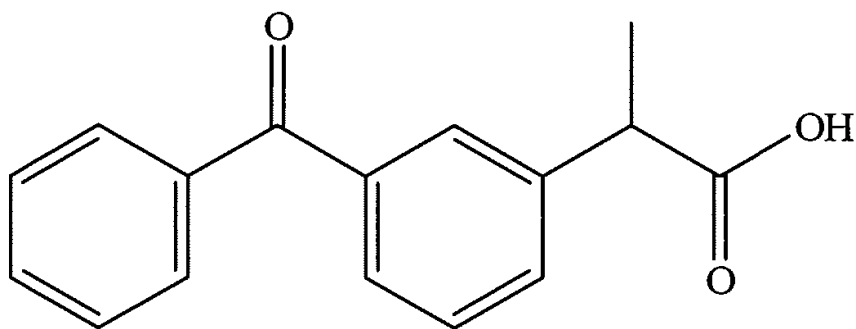
This work is the authors accepted manuscript of an article published as the version of record in Drug Development and Industrial Pharmacy 2015 [58].

## CHAPTER IV

### **Influence of Pressurized Carbon Dioxide on Ketoprofen-Incorporated Hot-Melt Extruded Low Molecular Weight Hydroxypropylcellulose**

#### **4.1. Introduction:**

HME is commonly used in the pharmaceutical industry for solubility enhancement applications. Carbon dioxide is non-toxic, non-flammable, and chemically inert [26, 27]. It was observed in earlier study that hot-melt extrusion processing assisted with P-CO<sub>2</sub> increased porosity and the surface area of the extrudates and changed the macroscopic morphology to a foam-like structure and furthermore enhanced the milling efficiency. Additionally, the drug dissolution rates increased significantly up on foaming extrudates structures. In this current research study, the main objective was to evaluate the effect of P-CO<sub>2</sub> on ketoprofen (KTP) and HPC polymers using HME techniques. The model drug KTP (Figure 4-1) is a non-steroidal anti-inflammatory agent[40] and, it is crystalline in nature with poor water solubility [41]. It is conventionally formulated as an oral dosage form [42]. It is thermally stable with a melting point of approximately 95°C and “burns out” over a temperature range of 235-400°C [43]. Indeed the literature has recently reported that hot melt extrudates of KTP and HPC has demonstrated poor milling efficiency [38]. In order to solve these underlining issues, in the present study we investigated the effect of P-CO<sub>2</sub> on the physico-mechanical properties as well as the release profiles of KTP and HPC extrudates produced using HME techniques.



**Figure 4-1: Chemical structure of Ketoprofen (KTP)**

#### **4.2. Material**

Klucel™ LF, EF and ELF hydroxypropylcellulose (HPC) and polyplasdone XL™ were obtained as gift samples from Ashland Inc. (Wilmington, DW 19808 USA). Ketoprofen was purchased from Parchem-Fine & specialty chemicals (415 Huguenot St, New Rochelle, NY 10801 USA). CO<sub>2</sub> was supplied in gas cylinders (pure clean) from Airgas (902 Rockefeller St, Tupelo, MS 38801 USA), Avicel®102 was received as a gift samples from FMC biopolymers (1735 Market Street, Philadelphia PA 19103 USA). Flow lac® 90 was received as a gift samples from Meggle USA Inc. (50 Main street, White Plains, NY 10606 USA). Syloid® was received from W. R. Grace & Co.- Conn (7500 Grace Drive, Columbia, MD 21044 USA). Magnesium Stearate was purchased from Spectrum Chemicals (14422 S. San Pedro Street Gardena, CA 90248 USA). All other chemicals and reagents used in the present study were of analytical grade and obtained from Fisher scientific (Fair Lawn, NJ 07410 USA).

### **4.3. Method**

#### **4.3.1. Thermal Analysis**

##### **4.3.1.1. Thermogravimetric Analysis (TGA)**

TGA studies were performed for KTP and polymers used in this study to determine their stability at the extrusion temperatures using a Perkin Elmer Pyris 1 TGA equipped with Pyris manager software (PerkinElmer Life and Analytical Sciences, 710 Bridgeport Ave., Connecticut, USA).

##### **4.3.1.2. Differential Scanning Calorimetry (DSC)**

DSC was obtained using Perkin Elmer Pyris 1 DSC equipped with Pyris manager software (PerkinElmer Life and Analytical Sciences, 710 Bridgeport Ave., Connecticut, USA). Approximately 2-4 mg of KTP, physical mixtures or extrudates were heated from 30°C to 200 °C at heating rate of 10°C/min.

#### **4.3.2. Physical mixture**

KTP and Klucel™ LF, EF and ELF hydroxypropylcellulose (HPC) polymers were sieved using ASTM #35 mesh. Physical mixture of 15% w/w KTP with each polymer were mixed using a V-Shell blender for 10 minutes. Three samples from each physical mixture were analyzed for blend drug content and uniformity.

#### **4.3.3. Hot Melt Extrusion**

The physical mixture blends (Table 4-1) were extruded with or without P-CO<sub>2</sub> injection using a twin-screw extruder (16 mm Prism EuroLab, ThermoFisher Scientific) (Figure 4-2) at screw speeds of 100 rpm (temp range: 90–140°C) (Table 4-2) P-CO<sub>2</sub> was injected into the extruder as

described previously in chapter I using a high-pressure regulator connected with flexible stainless steel armor-cased hosing. The other end of the hose was connected to the injection port seating on segment 6 of the extruder barrel (Figure 4-3).

**Table 4-1: Formulation composition of HME**

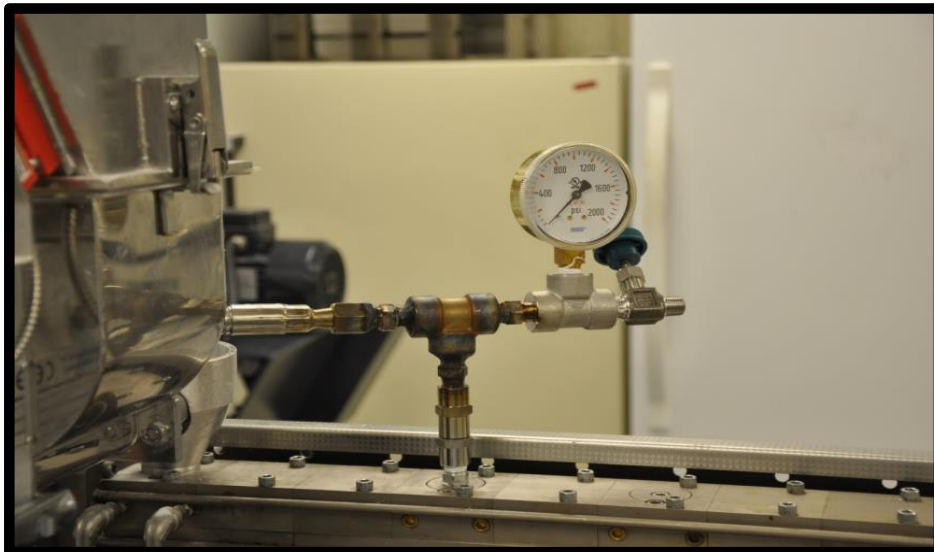
<b>Formulation</b>	<b>KTP (%)</b>	<b>Klucel™ ELF (%)</b>	<b>Klucel™ EF (%)</b>	<b>Klucel™ LF (%)</b>	<b>CO<sub>2</sub> injection zone</b>
<b>K<sub>10</sub></b>	15	85	-	-	-
<b>K<sub>11</sub></b>	15	-	85	-	-
<b>K<sub>12</sub></b>	15	-	-	85	-
<b>K<sub>13</sub></b>	15	85	-	-	Zone 6
<b>K<sub>14</sub></b>	15	-	85	-	Zone 6
<b>K<sub>15</sub></b>	15	-	-	85	Zone 6

**Table 4-2: Processing parameters for hot melt extrusion process of K<sub>10</sub>-K<sub>15</sub>**

<b>Formulation</b>	<b>Extrusion Temp. (°C)</b>	<b>Screw Speed (rpm)</b>	<b>Torque (Nm)</b>
<b>K<sub>10</sub></b>	110	75	9-14
<b>K<sub>11</sub></b>	110	75	9-12
<b>K<sub>12</sub></b>	110	75	11-13
<b>K<sub>13</sub></b>	100	75	8-9
<b>K<sub>14</sub></b>	100	75	9-10
<b>K<sub>15</sub></b>	100	75	9-12



**Figure 4-2: 16 mm Prism EuroLab, ThermoFisher Scientific.**



**Figure 4-3: P-CO<sub>2</sub> injection port.**



#### **4.3.4. Microscopical images**

Microscopy photographs were performed for thin transverse section (TS) of all extrudates using light microscope with camera (Nikon SMZ-U). Photographs of TS samples were taken with zoom power 3x.

#### **4.3.5. Milling**

All the extrudates were milled and sieved through ASTM #35 mesh using a comminuting mill (Fitzpatrick, Model L1A).

#### **4.3.6. High-Performance Liquid Chromatography (HPLC)**

All samples were analyzed using a Waters HPLC equipped with Empower software to analyze the data. HPLC consisted of a Water 600 binary pump, Waters 2489 UV/detector, and Waters 717 plus autosampler (Waters Technologies Corporation, 34 Maple St., Milford, MA 0157). The column used was phenomenex luna C18 (5 $\mu$ , 250 mm  $\times$  4.6 mm). The mobile phase constituted of acetonitrile/20 mMol phosphate buffer, 55:45 (%v/v) at pH 4 [38, 44] at a flow rate of 1 mL/min and injection volume of 20  $\mu$ l. The UV detector wavelength for KTP detection was set at 256 nm.

#### **4.3.7. In Vitro Drug Release**

Extrudates equivalent to 25 mg KTP were filled in HPMC capsules and in vitro drug release profiles were performed using a USP type II dissolution apparatus. The dissolution media was 1000 mL 0.05 M phosphate buffer pH 7.4 and, was maintained at 37 °C. A sample volume of 2 mL were taken at time points 10, 20, 30, 45, 60 min. [45], filtered and analyzed using HPLC and

2 mL of fresh dissolution media were added back to the dissolution vessel at each time point. The release profiles of 25 mg KTP tablets were obtained in the same conditions.

#### 4.3.8. Tableting

##### 4.3.8.1. Tablet preparation

The milled extrudates were used to prepare the tablet blends using microcrystalline cellulose (Avicel®102) or lactose (flow lac® 90) as diluent, silicon dioxide (Syloid®) as flowability enhancer, polyplasedone XL™ as a disintegrant and magnesium stearate as a lubricant (Table 4-3). The 25 mg strength tablets were compressed with the same compression force (1.5-1.6 kN) on a manual tablet press using 10 mm biconcave punch to a final tablet weight of 350 mg.

**Table 4-3: KTP tablet composition of extrudates with and without P-CO<sub>2</sub> injection**

<b>Excipients</b>	<b>% (w/w)</b>	<b>Weight (mg/tablet)</b>
<b>KTP</b>	7.14	25.00
<b>Klucel™ (ELF/EF/LF)</b>	40.46	141.66
<b>Avicel® 102</b>	24.60	86.10
<b>Flowlac 90</b>	12.30	43.05
<b>Syloid®</b>	10.00	35.00
<b>Polyplasdone™ XL</b>	5.00	17.5
<b>Magnesium stearate</b>	0.50	1.75

#### **4.3.8.2. Tablet Evaluation**

Tablets were evaluated for thickness, hardness, friability, and disintegration time as well as release profiles.

#### **4.3.9. Moisture Analysis**

To evaluate the moisture content of the extrudates , OHOUS MB45 moisture analyzer was used. 6-7 gm. of the extrudates placed in the sample pan and inserted in the sample chamber and then heated to 110 °C for 15 minutes. Samples weight loss of drying was recorded as well as the % of the moisture.

#### **4.3.10. Stability Study**

All KTP/Klucel™ ELF, EF and LF extrudates with and without P-CO<sub>2</sub> injection were sealed in glass bottles and stored at 25°C/60% RH for three months. Recrystallization assessments were determined by DSC.

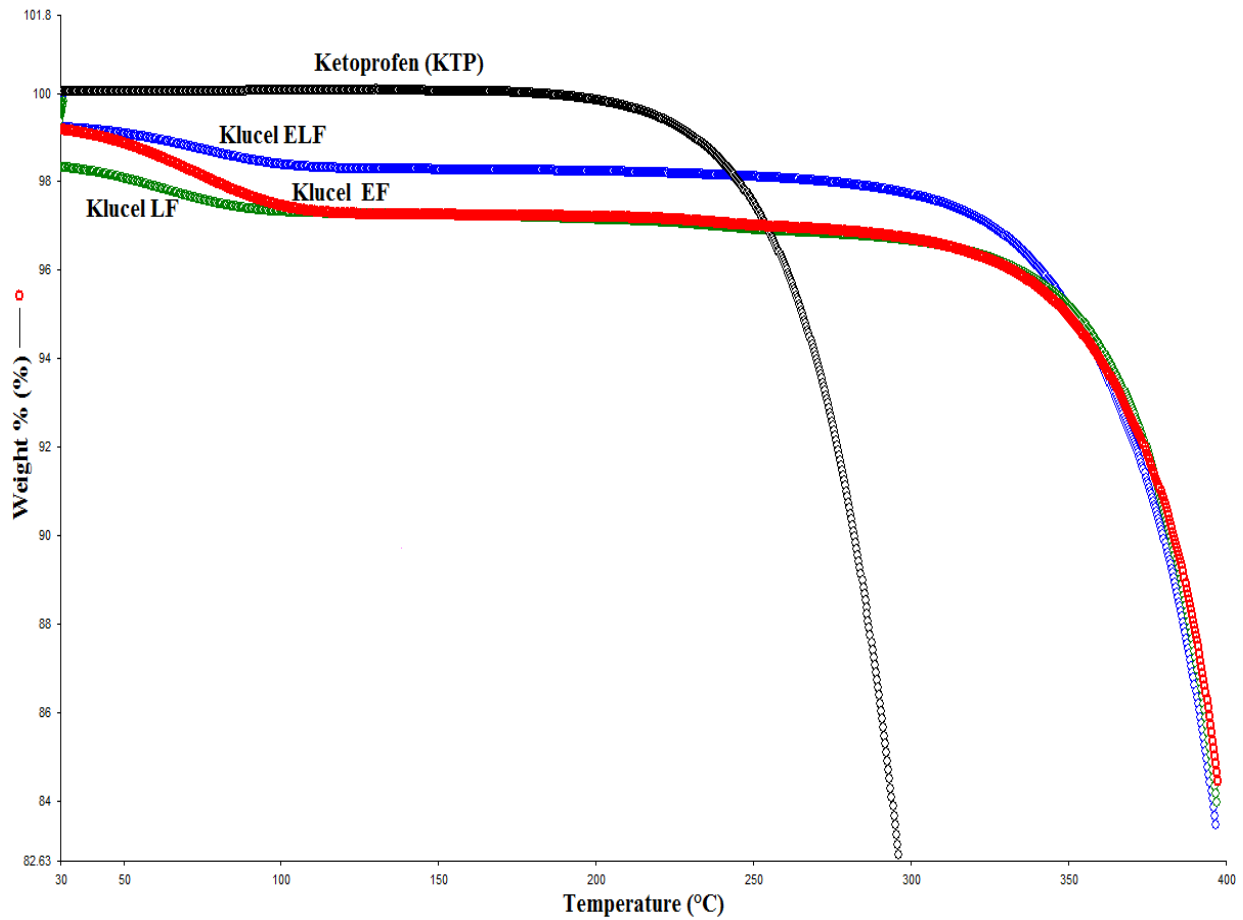
### **4.4. Results and discussion**

#### **4.4.1. Thermal Analysis**

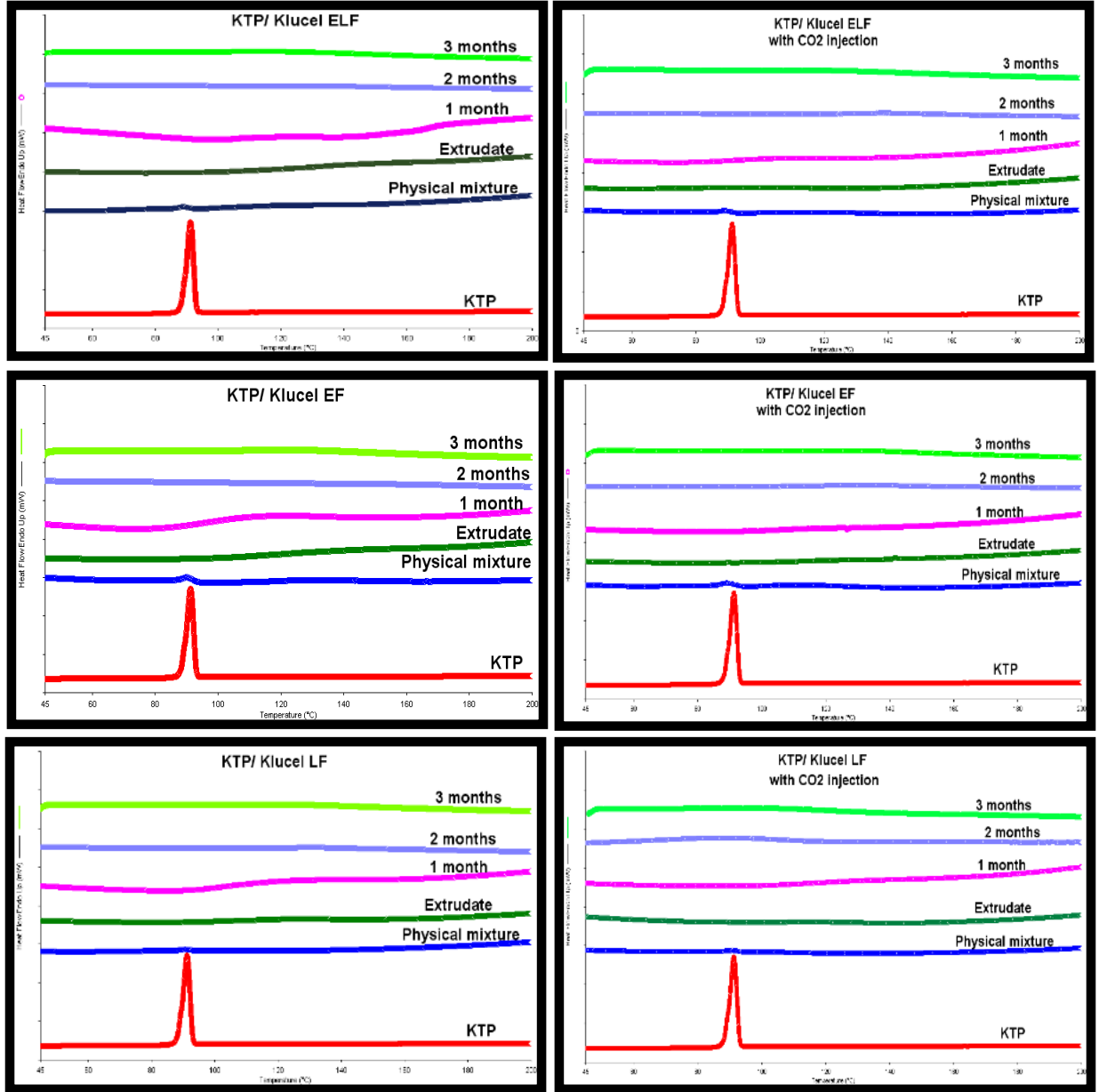
TGA data demonstrated that all formulations utilized in this study were stable under the employed processing temperature (Figure 4-4).

Differential Scanning Calorimetry, or DSC, is a thermal analysis technique evaluates how a material's heat capacity (Cp) is changed by temperature. The information generate by DSC is used to understand amorphous and crystalline behavior of the polymer and drug in the pharmaceutical industries. The DSC data showed that ketoprofen melting peaks at 90°C

disappeared for all of the milled extrudates with and without P-CO<sub>2</sub> injection, which indicated the conversion of the crystalline form into the amorphous form. All milled extrudates remained in an amorphous form at the end of the last time point after 3 months of storage at 25°C/60% RH (Figure 4-5).



**Figure 4-4: TGA thermogram of that Ketoprofen and Klucel™ ELF, EF and LF.**



**Figure 4-5: DSC thermogram of Ketoprofen, physical mixture and extrudates with and without P-CO<sub>2</sub> injection at 0, 1, 2, 3 months.**

#### 4.4.2. Hot Melt Extrusion

Hot melt extrusion processes were performed using 16 mm Prism Euro Lab, Thermo Fisher Scientific) with Thermo Fisher Scientific standard screw configuration. The injections were made through the injection port at the conveying zone of the screw configuration. The resulted extrudates processed without P-CO<sub>2</sub> injection were dense, opaque, elastic and sticky extrudates with all polymeric matrices. While other extrudates which processed with P-CO<sub>2</sub> were foamy and porous extrudates (Figure 4-6).

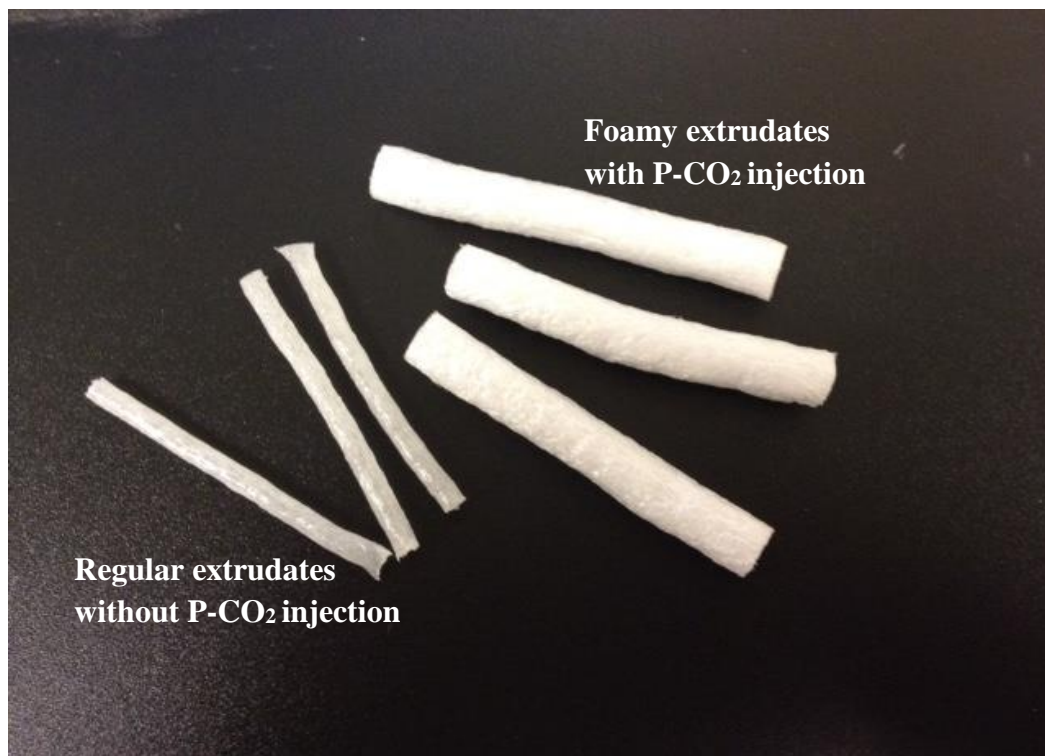


Figure 4-6: KTP/ Klucel<sup>TM</sup> extrudates with and without P-CO<sub>2</sub> injection.

The microscopical images of the TS sections of different extrudates showed that the porosity of the extrudates processed with P-CO<sub>2</sub> was increased (Figure 4-7). This change in the extrudates morphological properties was due to the expansion of the carbon dioxide at the extrusion die.

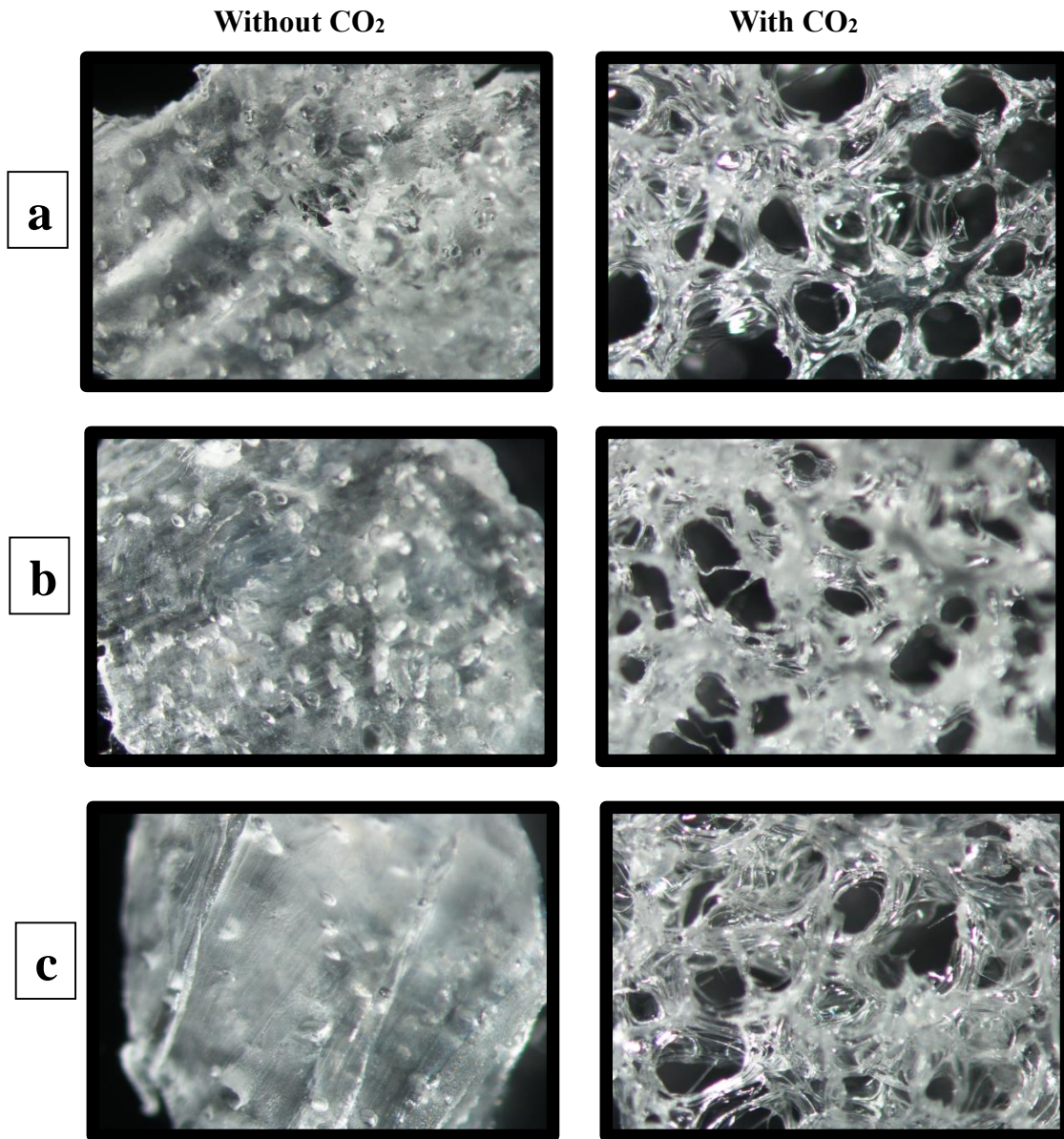
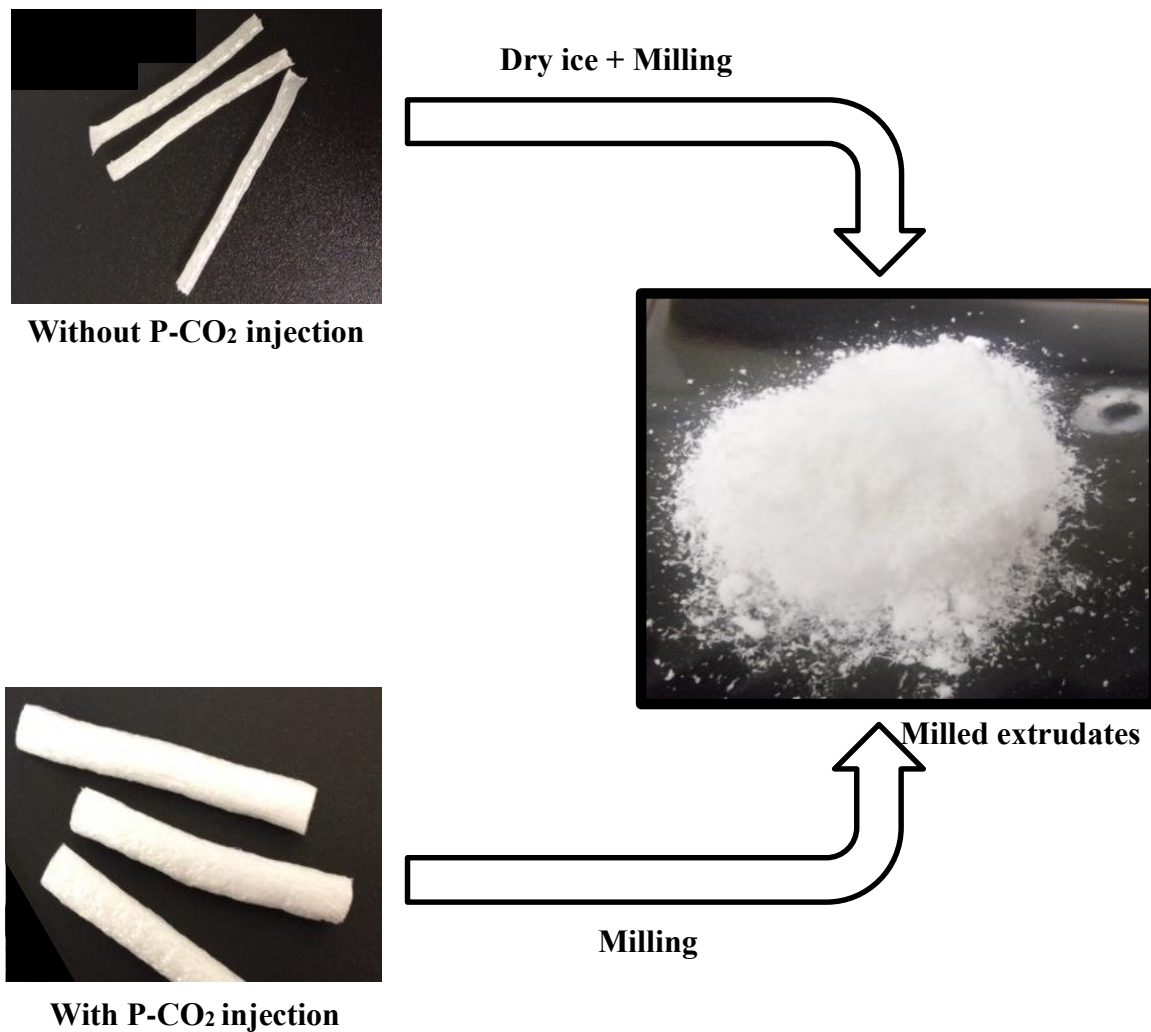


Figure 4-7: Microscopy photographs of TS sections of a) 15% KTP& Klucel<sup>TM</sup> ELF b) 15% KTP& Klucel<sup>TM</sup> EF, and c) 15% KTP& Klucel<sup>TM</sup> EF extrudates with and without P-CO<sub>2</sub> injections (Magnification 3X).

As observed previously, the milling efficiency of the extrudates processed with P-CO<sub>2</sub> was enhanced compared with extrudates processed without P-CO<sub>2</sub> (Figure 4-8). The foamed milled extrudates exhibited lower bulk density and tap density as compared to the extrudates processed without P-CO<sub>2</sub> injection, due to an increase in porosity and surface area of the extrudates (Table 4-4).



**Figure 4-8: Milling processing and milled extrudates.**



**Table 4-4: Bulk and tap density of milled extrudates with and without P-CO<sub>2</sub> injection (g/mL)**

Sample name	Without P-CO <sub>2</sub> injection		With P-CO <sub>2</sub> injection	
	Bulk density	Tap density	Bulk density	Tap density
<b>KTP/ Klucel™ ELF</b>	0.382± 0.012	0.434± 0.008	0.175± 0.001	0.270± 0.003
<b>KTP/ Klucel™ EF</b>	0.286± 0.009	0.373± 0.007	0.150± 0.001	0.235± 0.005
<b>KTP/ Klucel™ LF</b>	0.325± 0.013	0.415±0.011	0.145± 0.002	0.240± 0.006

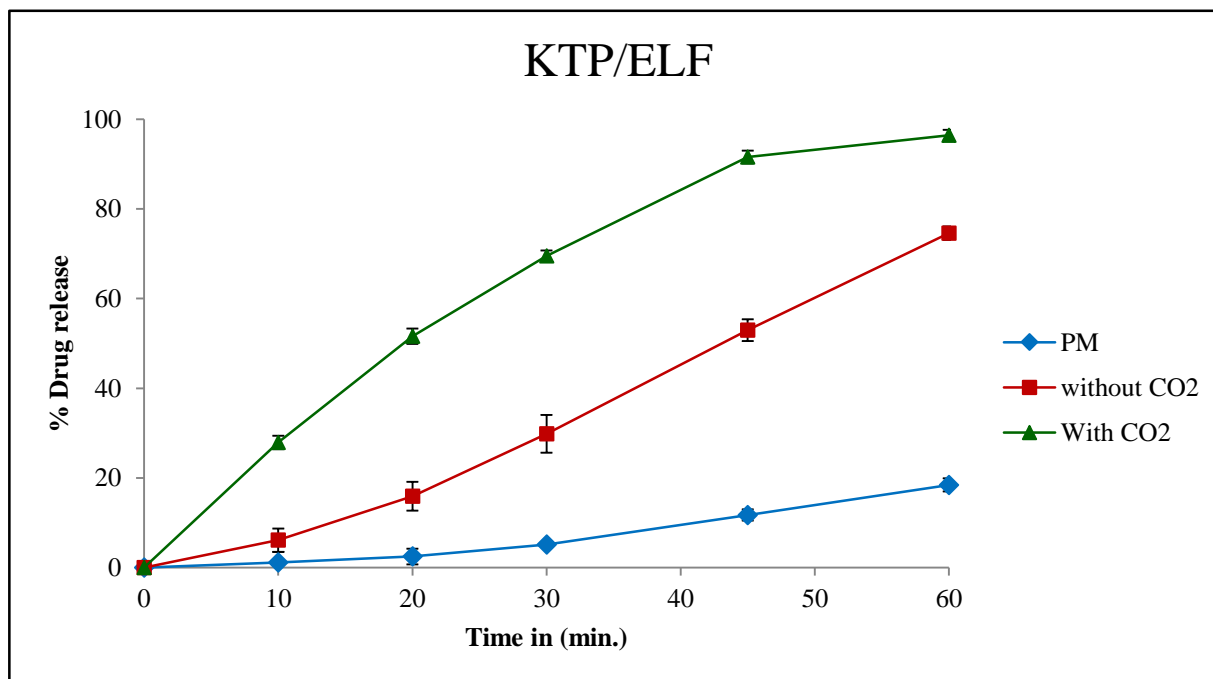
#### 4.4.3. Drug Content

HPLC analysis confirmed that the drug content uniformity of KTP in all formulations were acceptable and within the range of 98-105%. These results indicated good homogeneity of all formulations.

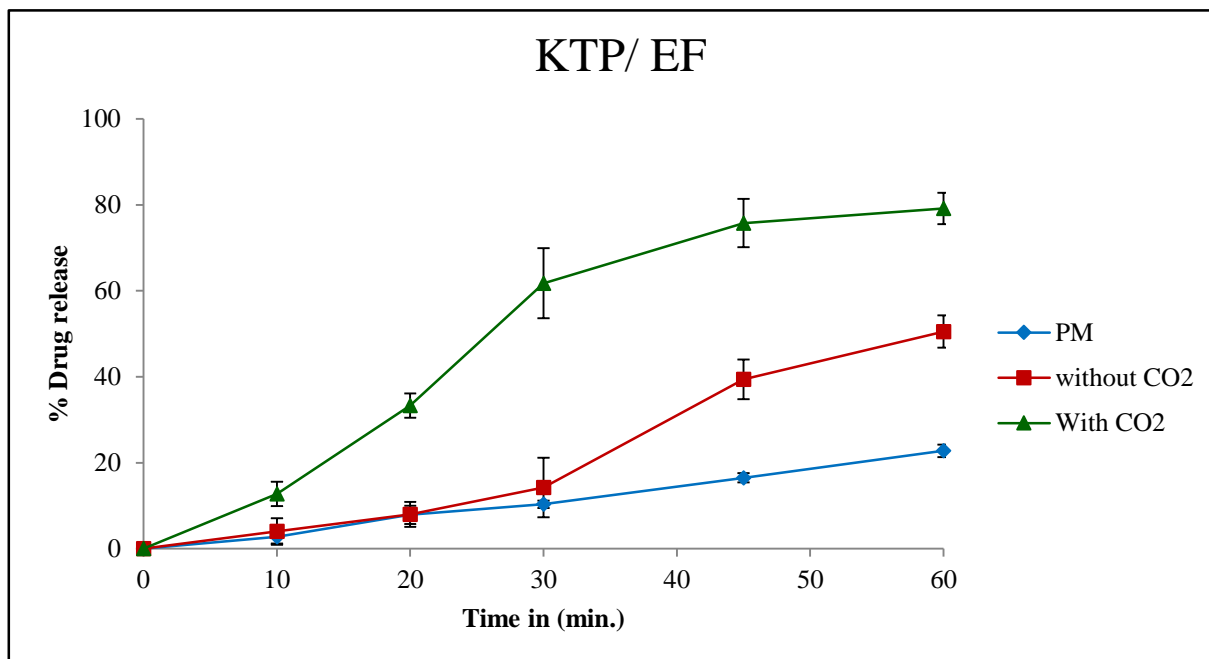
#### 4.4.4. *In-vitro* Drug Release

The *in vitro* drug release concedes as an important aspect in drug development that reflect drug *in vivo* performance [46]. The *in vitro* dissolution profiles were performed to evaluate the KTP/ Klucel™ ELF, EF and LF release behavior of milled extrudates with or without P-CO<sub>2</sub> injection as well as unprocessed physical mixtures. Plots of time vs. % drug release, which is the average of three replicates, were used as dissolution profiles for different formulations (Figures 4-9, 4-10, and 4-11). These profiles demonstrated a significant improvement of KTP release in the presence

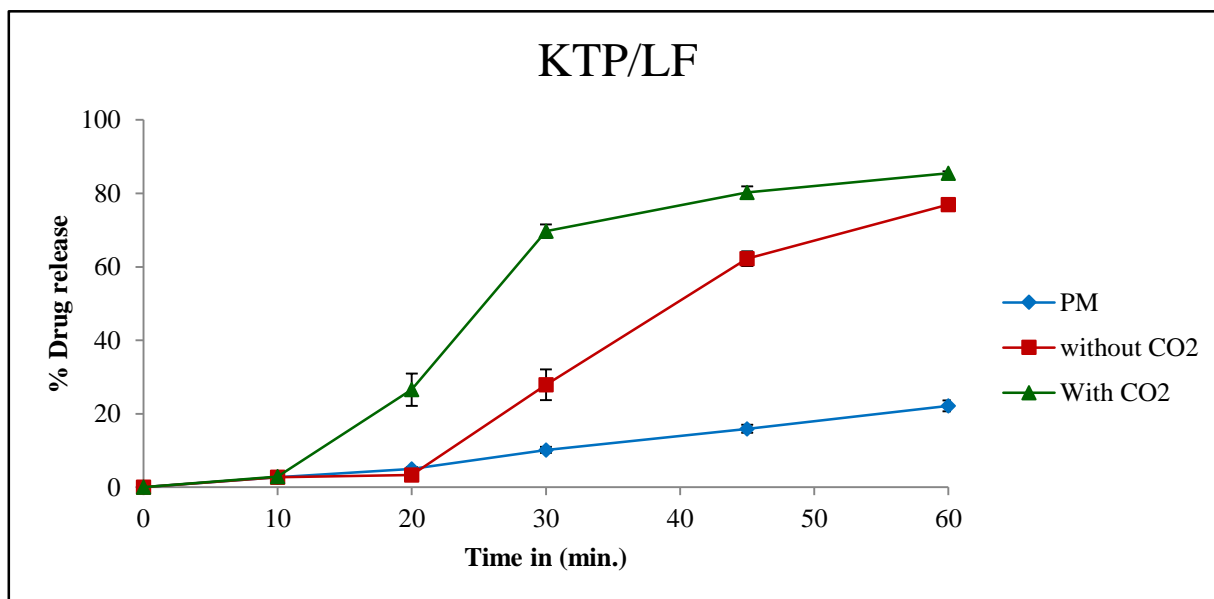
of P-CO<sub>2</sub> injection as compared to the other formulations. The release enhancement was observed as a direct result of the foam-like structure and high surface area of those extrudates with P-CO<sub>2</sub> injection[47-50].



**Figure 4-9: Dissolution profiles of KTP/Klucel™ ELF extrudates with and without P-CO<sub>2</sub> injection and physical mixture (pH 7.4 phosphate buffers, USP App II, 50 rpm/37°C).**



**Figure 4-10: Dissolution profiles of KTP/Klucel™ EF extrudates with and without P-CO<sub>2</sub> injection and physical mixture (pH 7.4 phosphate buffers, USP App II, 50 rpm/37°C).**



**Figure 4-11: Dissolution profiles of KTP/Klucel™ LF extrudates with and without P-CO<sub>2</sub> injection and physical mixture (pH 7.4 phosphate buffers, USP App II, 50 rpm/37°C).**

#### 4.4.5. Tablet Evaluation

The tablet blends prepared with extrudates processed with P-CO<sub>2</sub> injection showed lower bulk and tap density compared to other tablet blends due to formation of foam like structure as well as increase porosity and surface area of these extrudates (Table 4-5).

**Table 4-5: Bulk and Tap density of KTP tablet blends (g/mL)**

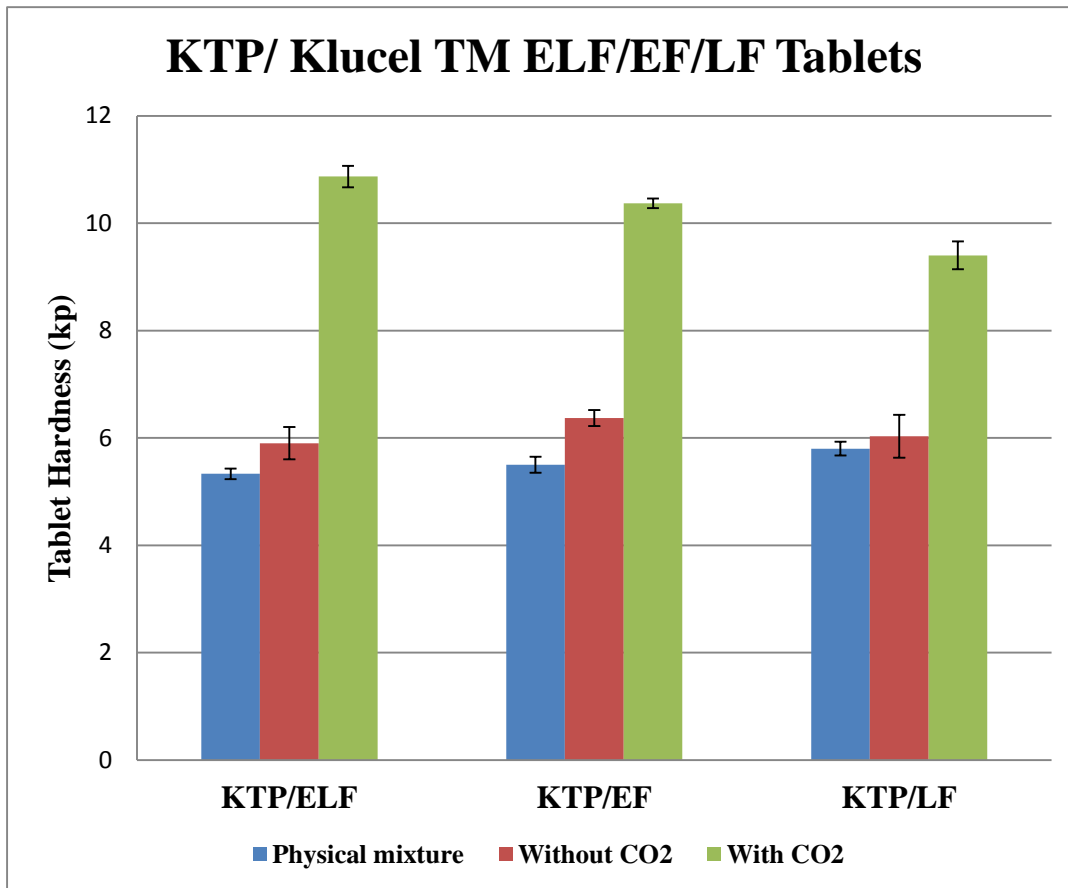
Sample Name	Physical mixture		Without P-CO <sub>2</sub> injection		With P-CO <sub>2</sub> injection	
	Bulk Density	Tap Density	Bulk Density	Tap Density	Bulk Density	Tap Density
<b>KTP/ Klucel™ ELF</b>	0.40	0.61	0.46	0.66	0.35	0.49
<b>KTP/ Klucel™ EF</b>	0.39	0.57	0.44	0.59	0.33	0.47
<b>KTP/ Klucel™ LF</b>	0.39	0.57	0.44	0.59	0.33	0.47

Tablets were successfully prepared (Figure 4-12) and showed that the drug content of all formulations ranged from 96-110% indicating good drug uniformity of all formulations. Furthermore, tablet weight variations of all the formulations were very low with standard deviations ( $SD < 1.0$ ).

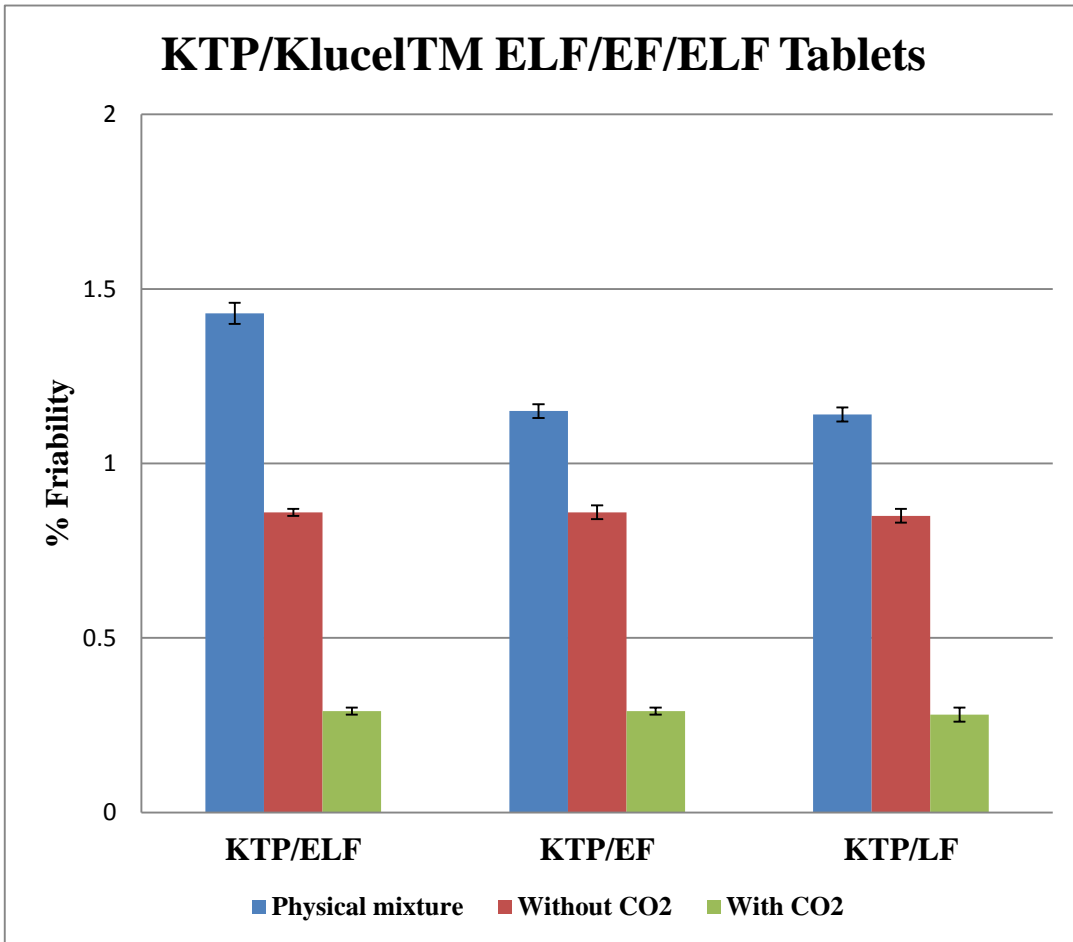


**Figure 4-12: Ketoprofen tablets.**

Tablets processed using P-CO<sub>2</sub> assisted extrudates exhibited higher hardness (Figure 4-13) and lower % friability (Figure 4-14) due to good binding properties and compressibility of the extrudates, as compared to those not processed with P-CO<sub>2</sub>. To understand this phenomenon, moisture content of the extrudates was performed. Table 4-6 showed the moisture content of the extrudates with and without P-CO<sub>2</sub> injection. The results clearly demonstrated that extrudates processed with P-CO<sub>2</sub> having more moisture than extrudates processed without P-CO<sub>2</sub>. This observation explained the increases of the tablet hardness in case of using blends of extrudates processed with P-CO<sub>2</sub>.



**Figure 4-13: Hardness in (kp) of KTP/Klucel <sup>TM</sup> ELF/EF/LF tablets, with and without P-CO2 injection and physical mixture.**



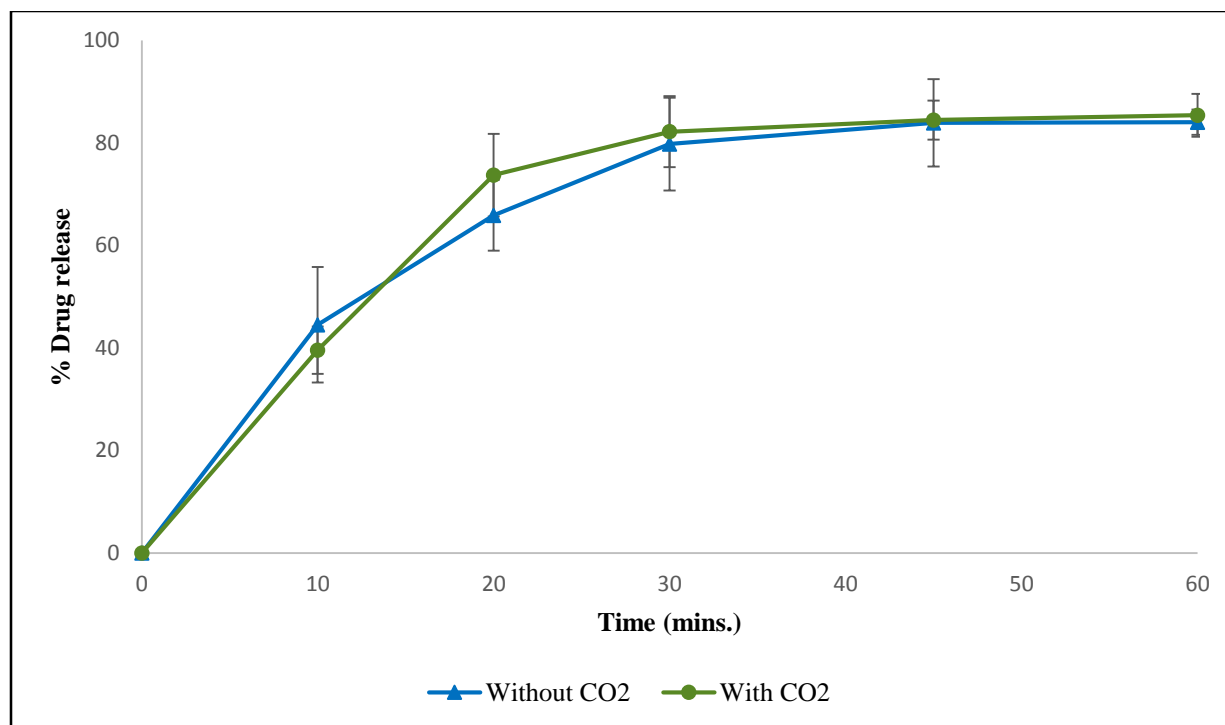
**Figure 4-14: % Friability of KTP/Klucel™ ELF/EF/LF tablets, with and without P-CO2 injection and physical mixture.**

**Table 4-6: Moisture content of KTP/ Klucel™ ELF, EF, and LF**

<b>Sample Name</b>	<b>LOD%</b>	
	<b>Without P-CO<sub>2</sub></b>	<b>With P-CO<sub>2</sub></b>
<b>KTP/ Klucel™ ELF</b>	0.53	0.88
<b>KTP/ Klucel™ EF</b>	0.69	0.91
<b>KTP/ Klucel™ LF</b>	0.56	1.54

The tablets were also subjected to *in vitro* dissolution studies of KTP/ Klucel™ EF tablets with and without P-CO<sub>2</sub> injection. No significant differences were observed in the drug release profiles of tablets with and without P-CO<sub>2</sub> extrudates (Figure 4-15). These results indicate that the dissolution improvement of extrudates processed with P-CO<sub>2</sub> was due to the high surface area and porosity, as compared to the extrudates without P-CO<sub>2</sub> injection. Whereas, when these extrudates were compressed into tablets, the compression force reduced the surface area of the foamy extrudates which eliminates the dissolution improvements utilizing P-CO<sub>2</sub> injections. Therefore, there was no effect of P-CO<sub>2</sub> injection on the tablet release profile.





**Figure 4-15: Dissolution profiles of KTP/Klucel™ EF tablets with and without P-CO<sub>2</sub> injection (pH 7.4 phosphate buffers, USP App II, 50 rpm and 37°C).**

#### **4.5. Conclusion**

It has been observed that Hot-melt extrusion processing assisted with P-CO<sub>2</sub> increased porosity of the KTP/ KluCEL™ ELF, EF and LF extrudates and changed the macroscopic morphology to a foam-like structure due to expansion of the carbon dioxide at the extrusion die. These properties allowed enhancement of the milling efficiency of the extrudates assisted with P-CO<sub>2</sub>. Furthermore, the extrudates processed with P-CO<sub>2</sub> injection demonstrated an enhancement of KTP release as compared to the physical mixtures and the extrudates processed without P-CO<sub>2</sub> injection, due to the increase in the surface area and porosity. However, there was no significant difference in the drug release profiles of tablets prepared with or without CO<sub>2</sub> extrudates after the compression process, which indicates that P-CO<sub>2</sub> injection does not alter the drug release profiles of tablets. Alternatively, it instead improves the processing properties of the tablets. P-CO<sub>2</sub> utilized in HME processing may exhibit similar benefits of supercritical CO<sub>2</sub> while avoiding some of the disadvantages experienced when utilized at the supercritical fluid level.

#### **Acknowledgement**

Part of this work is the authors accepted manuscript of an article published as the version of record in Drug Development and Industrial Pharmacy 2015 [58].

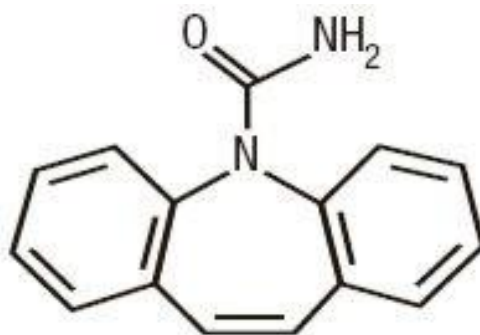
## CHAPTER V

### **Influence of Pressurized Carbon Dioxide on drug loading of High Melting Point Carbamazepine and Low Molecular Weight Hydroxypropylcellulose Matrices Using Hot Melt Extrusion**

#### **5.1. Introduction**

Carbamazepine (CBZ) (Figure 5-1) is an anticonvulsant drug used in the treatment of epilepsy, bipolar disorder and specific analgesic for trigeminal neuralgia [51, 52]. Biopharmaceutics Classification System categorized CBZ as class II with poor water solubility and good permeability [53]. It has prolonged absorption rate due to its lower dissolution rate [54]. However, CBZ crystallizes under at least four polymorphic crystal forms which include; Triclinic (Form I), Trigonal (Form II), P-Monoclinic (Form III), C-Monoclinic (Form IV). Variations in dissolution rate and absorption rate of CBZ have been reported due to the presence of the drug in different crystalline forms [55]. To overcome this issue, CBZ solid dispersion formulations were prepared by different methods to produce uniform and stable CBZ solid dispersion and to minimize the absorption variability. Zerrouk *et al* used fusion and crystallization to prepare the solid dispersion of CBZ with PEG 6000 and observed the ability of PEG 6000 to enhance the CBZ solubility [56]. Soluplus and polyvinylpyrrolidone (PVP/ VA 64) were used as polymeric carriers to prepare CBZ solid dispersion via HME process [53, 57]. However, a concern of HME is the limitation of the drug loading due to drug-polymer miscibility. In a previous study, we investigated the effect of P-CO<sub>2</sub> on the physico-mechanical properties as well as the drug release

profile using HME process. Successfully, foamed extrudates were prepared with high surface area and enhanced drug release profiles [58]. Elizondo *et al* observed that P-CO<sub>2</sub> can be used to prepare highly loaded antibiotic nanostructured PVM/MA matrices [59]. Considering these observations, it would be interesting to investigate the effect of P-CO<sub>2</sub> on the drug loading and the dissolution profiles of CBZ processed by HME.



**Figure 5-1: Chemical structure of Carbamazepine (CBZ).**

## 5.2. Material

Klucel™ ELF hydroxypropylcellulose (HPC) was received as gift samples from Ashland Inc (Wilmington, DW 19808 USA). CBZ was purchased from AFINE Chemicals Limited (Sandun Town, Hangzhou 310030 China). CO<sub>2</sub> was supplied in gas cylinders (pure clean) from Airgas (902 Rockefeller St, Tupelo, MS 38801 USA). All other chemicals and reagents used in the present study were of analytical grade and obtained from Fisher scientific (Fair Lawn, NJ 07410 USA).

### **5.3. Method**

#### **5.3.1. Thermal Analysis**

##### **5.3.1.1. Thermogravimetric Analysis (TGA)**

TGA studies were performed for CBZ and Klucel™ ELF to determine their stability at the extrusion temperatures using a Perkin Elmer Pyris 1 TGA equipped with Pyris manager software (PerkinElmer Life and Analytical Sciences, 710 Bridgeport Ave., Connecticut, USA). 7-10 mg. of the sample was weighed and heated from 30°C to 400 °C at heating rate of 20°C/min under nitrogen purging.

##### **5.3.1.2. Differential Scanning Calorimetry (DSC)**

DSC was performed to evaluate the drug polymer miscibility at different drug loading as well as the physical state of the all extrudates using Perkin Elmer Pyris 1 DSC equipped with Pyris manager software (PerkinElmer Life and Analytical Sciences, 710 Bridgeport Ave., Connecticut, USA). Approximately 2-4 mg of CBZ, physical mixtures or extrudates were heated from 30°C to 230°C at heating rate of 10°C/min. DSC data are also used to evaluate the % crystallinity of CBZ in the extruded formulation.

#### **5.3.2. Hot Melt Extrusion (HME)**

CBZ and Klucel™ ELF hydroxypropylcellulose (HPC) polymers were sieved using ASTM #35 mesh. Physical mixtures of 20-50% w/w CBZ with Klucel™ ELF (Table 5-1) were mixed using a V-Shell blender for 10 minutes. Three samples from each physical mixture were analyzed for blend drug content and uniformity. The resulting blends were extruded with or without P-CO<sub>2</sub> injection using a twin-screw extruder (16 mm Prism EuroLab, ThermoFisher Scientific) at screw speeds of 100-120 rpm and temperature range 110–130°C. P-CO<sub>2</sub> was injected at 125-175 psi into the extruder using a high-pressure regulator connected with flexible

stainless steel, armor-cased hosing. The other end of the hose was connected to the injection port seating on segment 6 of the extruder barrel. All of the extrudates were milled and sieved through ASTM #35 mesh using a comminuting mill (Fitzpatrick, Model L1A).

**Table 5-1: CBZ formulation composition of HME**

<b>Formulation</b>	<b>CBZ (%)</b>	<b>Klucel™ ELF(%)</b>	<b>CO<sub>2</sub> injection Zone</b>	<b>CO<sub>2</sub> Pressure (PSI)</b>
<b>C<sub>1</sub></b>	20	80	-	-
<b>C<sub>2</sub></b>	20	80	Zone 6	175
<b>C<sub>3</sub></b>	30	70	-	-
<b>C<sub>4</sub></b>	30	70	Zone 6	150
<b>C<sub>5</sub></b>	40	60	-	-
<b>C<sub>6</sub></b>	40	60	Zone 6	150
<b>C<sub>7</sub></b>	50	50	-	-
<b>C<sub>8</sub></b>	50	50	Zone 6	125

### **5.3.3. Density**

Bulk and tap density were performed for all extrudates as well as for physical mixtures. True density was measured using Micromeritics AccuPyc II1340 Gas Pycnometer, where the samples were measured by helium displacement methods. The principle of this operation is to seal the known volume sample in the instrument compartment then the helium as an inert gas is inserted, and then helium molecules rapidly fill the pores; only the solid phase of the sample displaces the gas. Dividing this volume into the sample weight gives the gas displacement density.

### **5.3.4. Surface Area**

Surface areas of all milled extrudates with and without CO<sub>2</sub> injection were evaluated using Micromeritics, Gemini VII. 2-3 gm. of milled extrudates were placed in the sampling tube and the reference sample was used to calibrate the analysis to produce continued accuracy of results. Before analysis start, each sample was placed under vacuum to remove the moisture. The nitrogen adsorption-desorption isotherms of the samples were obtained at liquid nitrogen temperature (-195 C°). The specific surface area of the samples was obtained by means of the standard method of Brunauer Emmett-Teller (BET).

### **5.3.5. Scanning Electron Microscopy (SEM)**

Scanning Electron Microscopy (SEM) was used to evaluate the morphology of the extrudates with and without P-CO<sub>2</sub> injection. Samples were mounted on adhesive carbon pads placed on aluminum then they sputter coated with gold using a Hummer<sup>®</sup> 6.2 sputtering system (Anatech LTD, Springfield, VA) in a high vacuum evaporator. A JEOL JSM-5600 scanning electron microscope operating at an accelerating voltage of 10kV was used for imaging.

### 5.3.6. High-Performance Liquid Chromatography (HPLC)

All samples analyses were performed on a Waters HPLC and Empower software was used to analyze the data. HPLC system consists of Waters e2695 separation Module and Waters 2489 UV/Visible detector (Waters Technologies Corporation, 34 Maple St., Milford, MA 0157). A Phenomenex luna C18 (250 mm × 4.6 mm, 5 $\mu$ ) coulumn was used. The mobile phase constituted of 65:35:0.1 (%v/v) Methanol: Water: Acetic acid at flow rate of 1 mL/ min and injection volume of 20  $\mu$ l. The UV detector wavelength for CBZ detection was set at 285 nm.

### 5.3.7. *In-Vitro* Drug Release

Extrudates equivalent to 50 mg CBZ were filled in HPMC capsules. The *in vitro* drug release profiles were performed using a USP type II dissolution apparatus. The dissolution medium was 900 mL water and, was maintained at 37 °C with paddle rotation speed of 100 rpm. A sample volume of 2 mL was taken at time points 10, 20, 30, 45, 60, 90 and 120 min., filtered and analyzed using HPLC and 2 mL of fresh dissolution medium were added back to the dissolution vessel at each time point to maintain the dissolution medium volume.

To understand the CBZ release results, data observed from *in-vitro* release study were used to calculate Dissolution Efficiency (DE) and Mean Dissolution Time (MDT) of the all formulation as a model independent method to compare the drug release profile of the extrudates with and without P-CO<sub>2</sub> injection. KinetDS 3.0 software was used to calculate DE and MDT [60] using the following equations.



$$DE = \frac{\int_0^t Q dt}{Q_{100} \times 100} \times 100 \quad \text{(Equation 5-1)}$$

Where:

Q – amount (%) of drug substance released at the time t

t- time

Q100 – maximum amount of drug released (= 100%)

$$MDT = \frac{\sum_{j=1}^n t_j^{AV} \times \Delta Q_j}{\sum_{j=1}^n \Delta Q_j} \quad \text{(Equation 5-2)}$$

Where:

$\Delta Q = Q(t) - Q(t-1)$

$t_j^{AV} = (t_i + t_{i-1})/2$

n – amount of time points

Similarity factors ( $f_2$ ) were also calculated using (equation 5-3) to evaluate the effect of P-CO<sub>2</sub> on the drug release.

$$f_2 = 50 \times \log \left\{ \left[ 1 + (1/n) \sum_{j=1}^n W_j |R_j - T_j|^2 \right]^{-0.5} \times 100 \right\} \quad \text{(Equation 5-3)}$$

## 5.4. Results and Discussion

### 5.4.1. Thermal Analysis

TGA data of CBZ, Klucel<sup>TM</sup> ELF and physical mixture did not show any sign of degradation until reaching approximately 250 °C and 300 °C for CBZ and Klucel<sup>TM</sup> ELF respectively. At those temperatures, the samples weight decreased by elevation the temperature. These results indicate that all prepared formulations were stable under the utilized processing temperatures (Figure 5-2). Additionally, TGA data also showed that Klucel<sup>TM</sup> ELF exhibited around 3% moisture uptake.

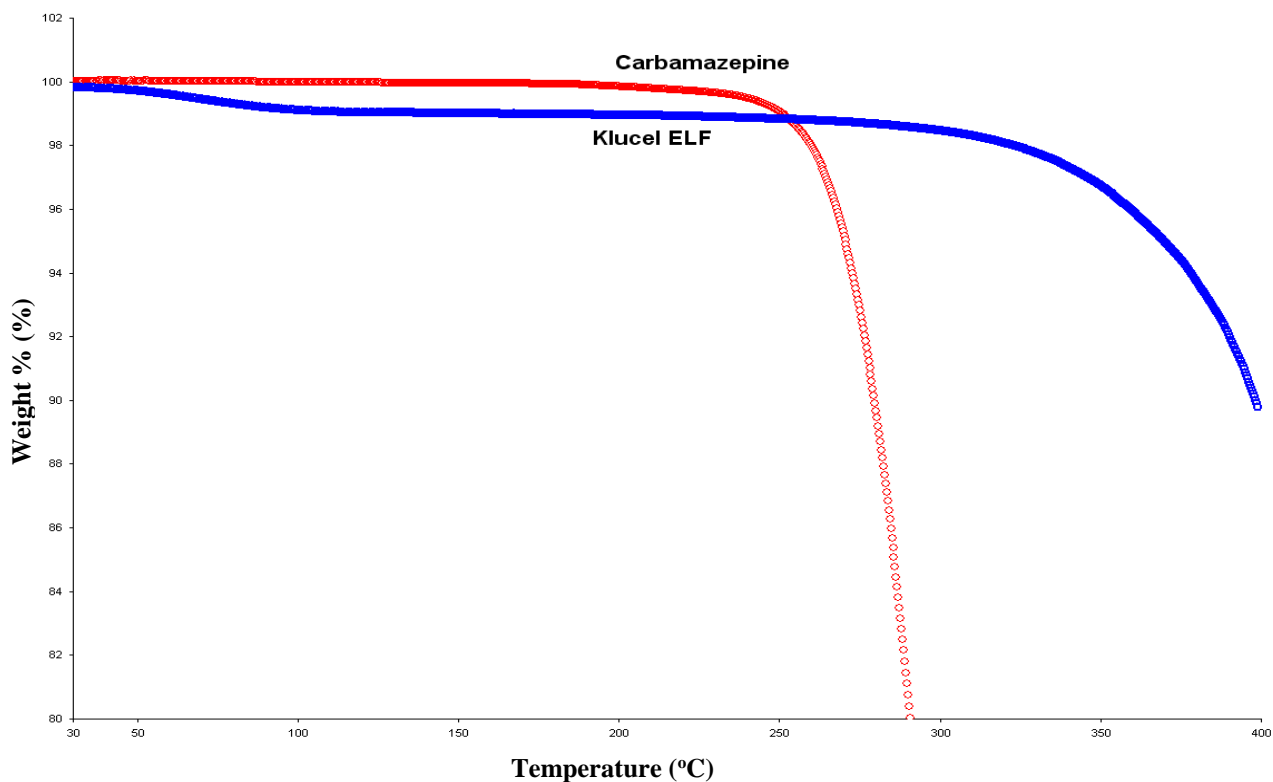
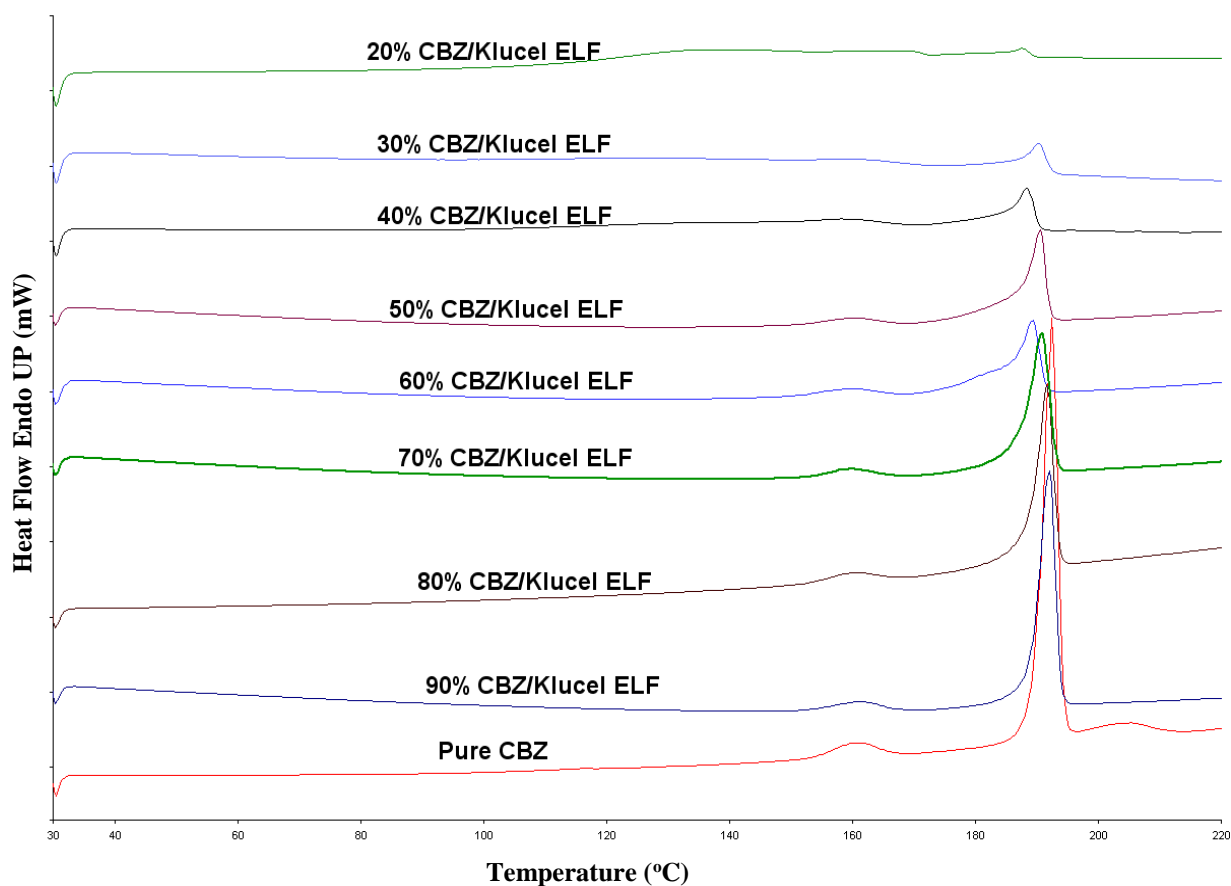
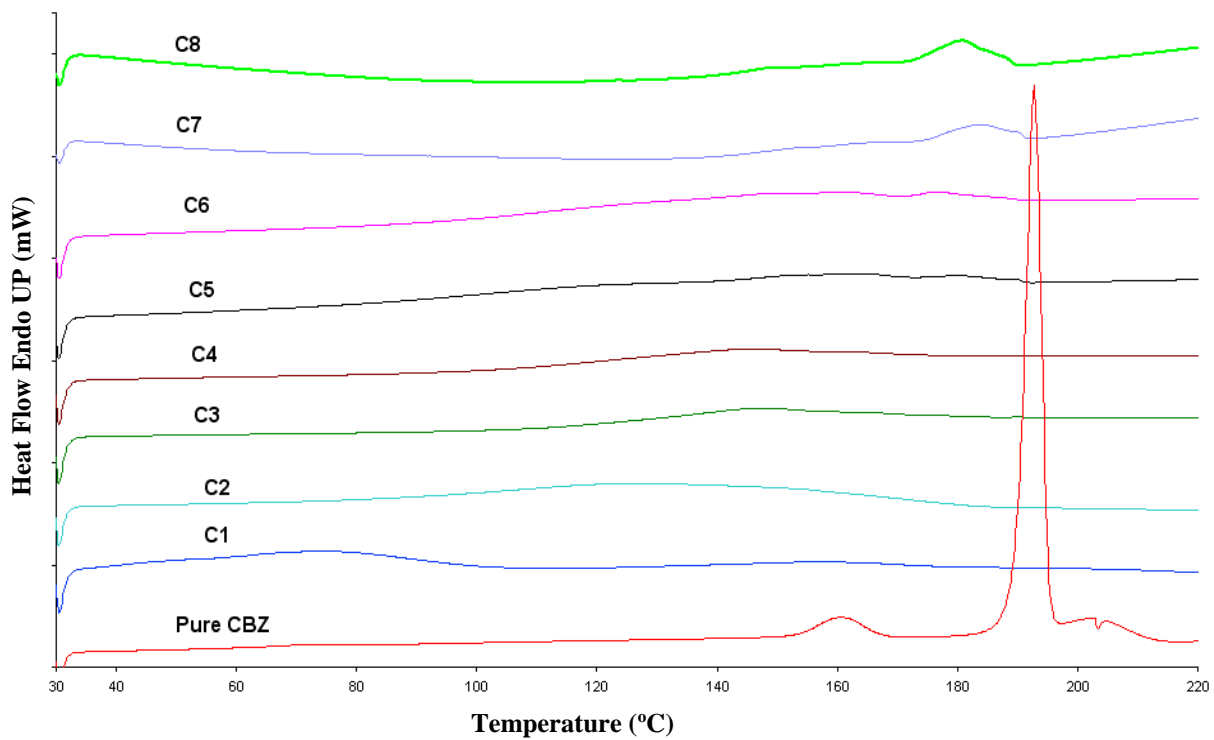


Figure 5-2: TGA thermogram of carbamazepine (CBZ) and Klucel<sup>TM</sup> ELF.

DSC analysis was performed to determine the miscibility of CBZ/Klucel™ ELF in different drug load as well as evaluate the physical state of the CBZ in all extrudates prepared in this study. The DSC thermogram showed the CBZ endotherm melting peaks at 190°C. On the other hand, the physical mixtures showed a slight melting point depression of CBZ in the presence of the Klucel™ ELF, indicating its miscibility in the polymeric matrix (Figure 5-3). DSC data of the extrudates exhibit the disappearance of the endothermic melting peak of CBZ for all extrudates with and without P-CO<sub>2</sub> injection except for C<sub>7</sub> and C<sub>8</sub>. The absence of the CBZ endothermic melting peak indicates the formation of amorphous solid dispersion (Figure 5-4).



**Figure 5-3: DSC thermogram of CBZ/ Klucel™ ELF physical mixtures showing the drug- polymer miscibility at different drug loading.**

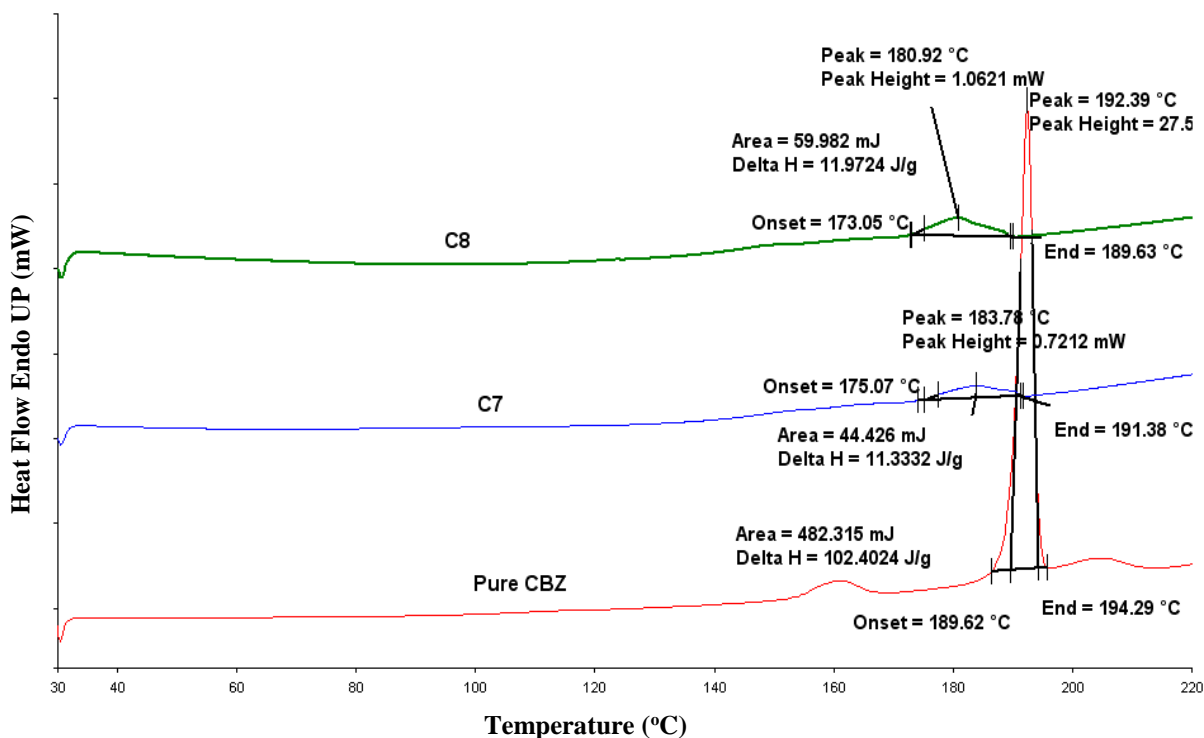


**Figure 5-4: DSC thermogram of 20%, 30%, 40% and 50% of CBZ/ Klucel™ ELF extrudates with and without P-CO<sub>2</sub> injection as well as pure CBZ.**

DSC data are also used to determine the % crystallinity of CBZ in C<sub>7</sub> and C<sub>8</sub> formulation using the following equation

$$\text{Crystallinity (\%)} = [\Delta H_{\text{Extrudate}} / (\Delta H_{\text{CBZ}} \times w \%) ] \times 100 \quad \text{(Equation 5-4)}$$

The DSC thermogram (Figure 5-5) showed that  $\Delta H$  of the CBZ is 102.402 J/g and the w% of the formulations were calculated depending on the drug content results. There was no significant different between the % crystallinity of C<sub>7</sub> and C<sub>8</sub> (approximately 23%).



**Figure 5-5: DSC thermogram showing the  $\Delta H$  values of 50% CBZ/ Klucel™ ELF extrudates with and without P-CO<sub>2</sub> injection as well as pure CBZ.**

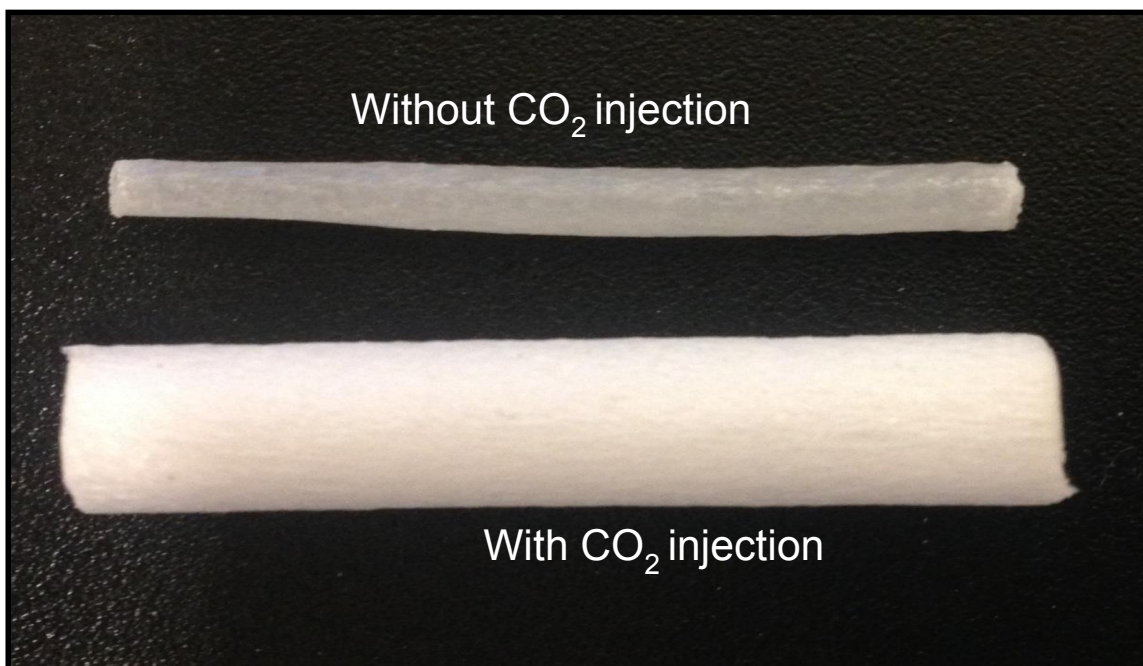
#### **5.4.2. Hot Melt Extrusion (HME)**

The extrusion processing parameters were set depending on the TGA results and the feasibility and processability of the physical mixtures used in this study (Table 5-2). The twin-screw extruder (16 mm Prism EuroLab, ThermoFisher Scientific) consists of ten segments and an extrusion die. The screw configuration used in this study was Thermo Fisher Scientific standard configuration which consists of four conveying segments and three mixing zones and all of the injections were made through the injection port at the conveying zones of the screw configuration. The carbon dioxide was injected in the extruder using a high-pressure regulator connected with flexible stainless steel hose with armor casing. The other end of the hose was connected to the four-way connection, fitted with a pressure gauge, bleed valve, check valve (ball type for unidirectional flow of gas), with the later being connected to the injection port seating on the extruder in barrel segment 6. Before the injection of P-CO<sub>2</sub>, all the extruder barrel segments were filled with melted physical mixture to form melt seal and prevent the escaping of CO<sub>2</sub> from the feeding zone.

**Table 5-2: Processing parameters for hot melt extrusion process of C<sub>1</sub>-C<sub>8</sub>**

<b>Formulation</b>	<b>Extrusion Temp. (°C)</b>	<b>Screw Speed (rpm)</b>	<b>Torque (Nm)</b>
<b>C<sub>1</sub></b>	130	100	9
<b>C<sub>2</sub></b>	130	100	7
<b>C<sub>3</sub></b>	110	100	8-9
<b>C<sub>4</sub></b>	110	100	6-8
<b>C<sub>5</sub></b>	110	100	9-12
<b>C<sub>6</sub></b>	110	100	9-10
<b>C<sub>7</sub></b>	120	100	14-18
<b>C<sub>8</sub></b>	120	100	8

The extrudates without P-CO<sub>2</sub> were dense and opaque, also having plastic morphology. On the other hand, the morphology of all extrudates processed with P-CO<sub>2</sub> were changed to a foam like structure (Figure 5-6) due to the carbon dioxide expansion exiting at the terminal end of the die. The torque values of the extruder were decreased with the formulations processed with P-CO<sub>2</sub> injection compared with the formulations without P-CO<sub>2</sub> injection. This observation indicating the plasticization effect of carbon dioxide and prove the decrease in the glass transition temperature (T<sub>g</sub>) of the blends processed with P-CO<sub>2</sub>.



**Figure 5-6: Photographic picture of CBZ /Klucel<sup>TM</sup> ELF extrudates with and without P-CO<sub>2</sub> injection.**



The milling efficiency of formulations C<sub>2</sub>, C<sub>4</sub>, C<sub>6</sub> and C<sub>8</sub> were higher than the milling efficiency of formulations C<sub>1</sub>, C<sub>3</sub>, C<sub>5</sub> and C<sub>7</sub>. This result was concluded by the torque values of the comminuting mill (Fitzpatrick, Model L1A).

### **5.4.3. Density**

True density was evaluated using AccuPyc II1340, Micromeritics to all formulations, C<sub>1</sub>-C<sub>8</sub>. There are negligible differences in the true density values of the extrudates with and without CO<sub>2</sub> injection indicating no chemical change in the nature of the CBZ/Klucel™. This result confirmed that CO<sub>2</sub> is an inert material and there is no interaction between CO<sub>2</sub> and CBZ/Klucel™ formulations. On the other hand, there was a decrease in the bulk and tap densities of the formulations processed with CO<sub>2</sub> injection (C<sub>2</sub>, C<sub>4</sub>, C<sub>6</sub>, C<sub>8</sub>) than those processed without CO<sub>2</sub> (C<sub>1</sub>, C<sub>3</sub>, C<sub>5</sub>, C<sub>7</sub>) as a direct result of the formation of foamy like structure extrudates in case of CO<sub>2</sub> injection as well as increase in the pore size of those extrudates. Table 5-3 displayed that the bulk density of formulations (C<sub>2</sub>, C<sub>4</sub>, C<sub>6</sub>, C<sub>8</sub>) are lower than formulations (C<sub>1</sub>, C<sub>3</sub>, C<sub>5</sub>, C<sub>7</sub>) by 23-43%, While, the tap density lowered by 16- 35%.

**Table 5-3: Bulk and tap density of CBZ /Klucel™ ELF with and without P-CO<sub>2</sub> injection ± Standard deviation n=3**

<b>Sample Name</b>	<b>Bulk Density</b>	<b>Tap Density</b>
<b>20% CBZ/ELF PM</b>	0.436 ± 0.013	0.578 ± 0.008
<b>C1</b>	0.356 ± 0.009	0.470 ± 0.006
<b>C2</b>	0.205 ± 0.008	0.307 ± 0.005
<b>30% CBZ/ELF PM</b>	0.335 ± 0.001	0.554 ± 0.032
<b>C3</b>	0.377 ± 0.011	0.490 ± 0.002
<b>C4</b>	0.262 ± .001	0.367 ± 0.001
<b>40% CBZ/ELF PM</b>	0.452 ± 0.003	0.637 ± 0.004
<b>C5</b>	0.469 ± 0.003	0.616 ± 0.011
<b>C6</b>	0.325 ± 0.006	0.449 ± 0.010
<b>50% CBZ/ELF PM</b>	0.484 ± 0.008	0.715 ± 0.016
<b>C7</b>	0.507 ± 0.011	0.638 ± 0.017
<b>C8</b>	0.391± 0.006	0.537 ± .016

#### 5.4.4. Surface area

Surface area is considered as one of the important factors that affect the dissolution profiles of any drug. It was observed that increasing the surface area of any formulation will result in more contact with the dissolution medium and hence increase the *in-vitro* drug release. Moreover, the drug absorption will increase which enhance the drug bioavailability. Gemini VII, Micromeritics was used to measure the surface area of C<sub>1</sub>-C<sub>8</sub>. Table 5-4 shows the surface area and the calculated % porosity for C<sub>1</sub>-C<sub>8</sub> formulations. The % porosity was calculated using the following equation:

$$\% \text{ Porosity} = \left(1 - \frac{\text{Bulk Density}}{\text{True Density}}\right) \times 100 \quad \text{(Equation 5-5)}$$

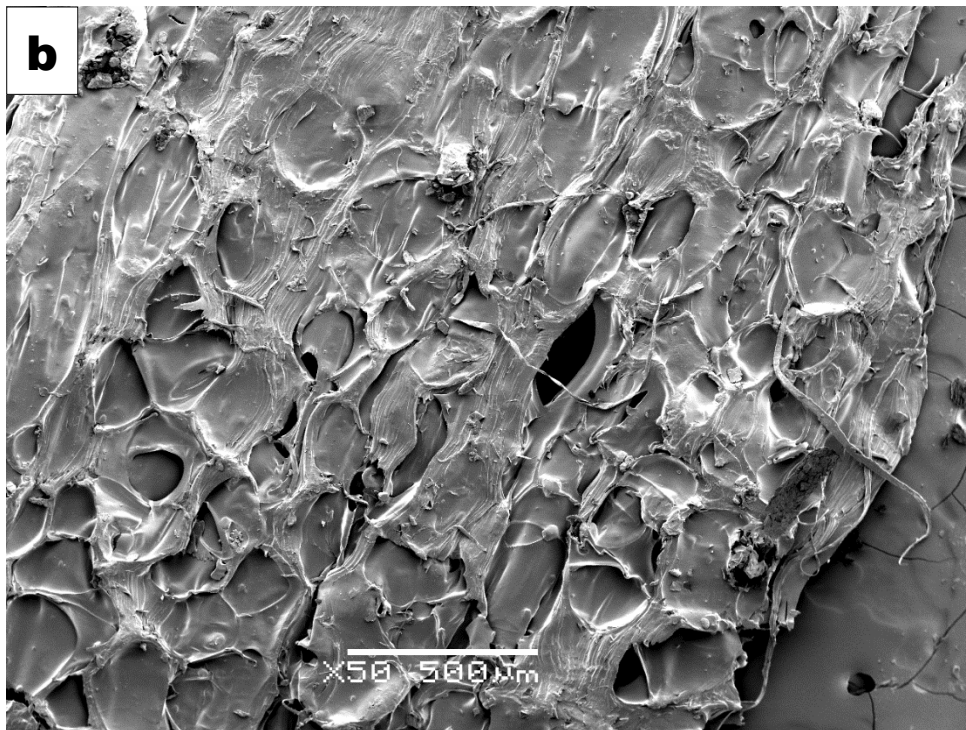
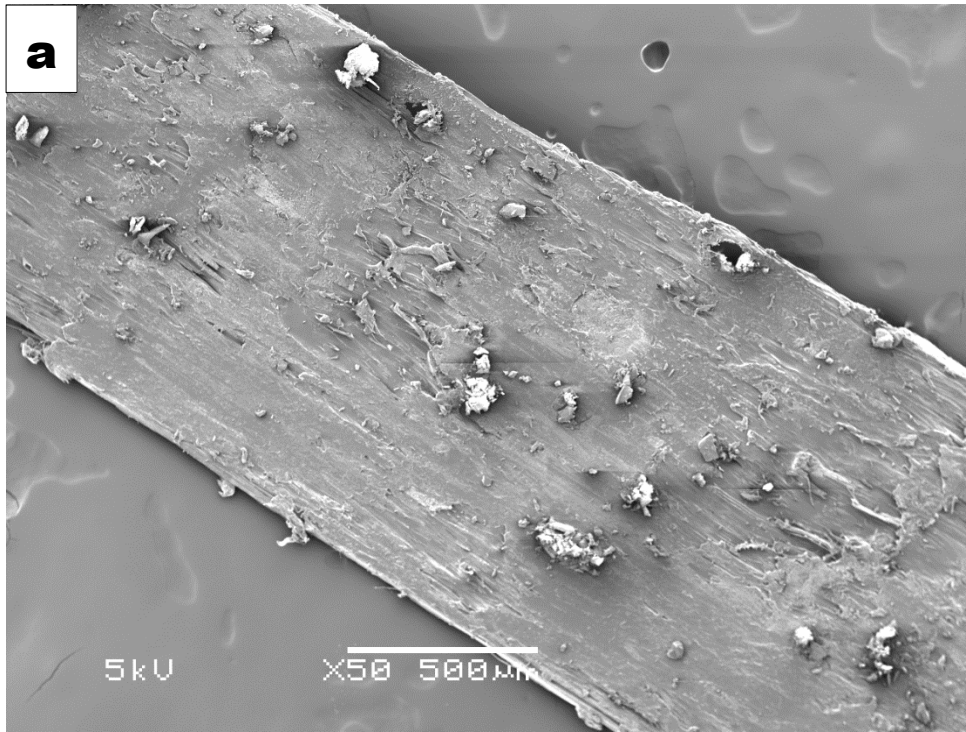
Formulations C<sub>2</sub>, C<sub>4</sub>, C<sub>6</sub> and C<sub>8</sub> exhibited higher surface area as well as higher % porosity compared to formulations C<sub>1</sub>, C<sub>3</sub>, C<sub>5</sub> and C<sub>7</sub>. This is considered as a direct result of morphological change of C<sub>2</sub>, C<sub>4</sub>, C<sub>6</sub> and C<sub>8</sub> due to the injection of P-CO<sub>2</sub> during the HME process.

**Table 5-4: Surface area and % porosity of different drug loading CBZ /Klucel™ ELF with and without P-CO<sub>2</sub>**

<b>Sample Name</b>	<b>Surface Area (m<sup>2</sup>/gm)</b>	<b>% Porosity</b>
<b>C<sub>1</sub></b>	0.261	71
<b>C<sub>2</sub></b>	0.394	84
<b>C<sub>3</sub></b>	0.350	70
<b>C<sub>4</sub></b>	0.493	79
<b>C<sub>5</sub></b>	0.412	62
<b>C<sub>6</sub></b>	0.489	74
<b>C<sub>7</sub></b>	0.445	59
<b>C<sub>8</sub></b>	0.523	68

#### **5.4.5. Scanning electron microscopy (SEM)**

SEM images were used to evaluate the morphological surface of the extrudates C<sub>1</sub>-C<sub>8</sub>. Figure 5-7 presented the differences in the morphological characterization of formulations C<sub>1</sub>, C<sub>3</sub>, C<sub>5</sub>, C<sub>7</sub> (without P-CO<sub>2</sub> injection) and formulations C<sub>2</sub>, C<sub>4</sub>, C<sub>6</sub>, C<sub>8</sub> (with P-CO<sub>2</sub> injection) by using longitudinal section (LS) of the extrudate samples. The images confirmed that all formulations processed with P-CO<sub>2</sub> were porous that is one of the foam like structure characterization. While, the other extrudates formulated without P-CO<sub>2</sub> were dense and no evidence of any pores in their extrudates structure was observed.



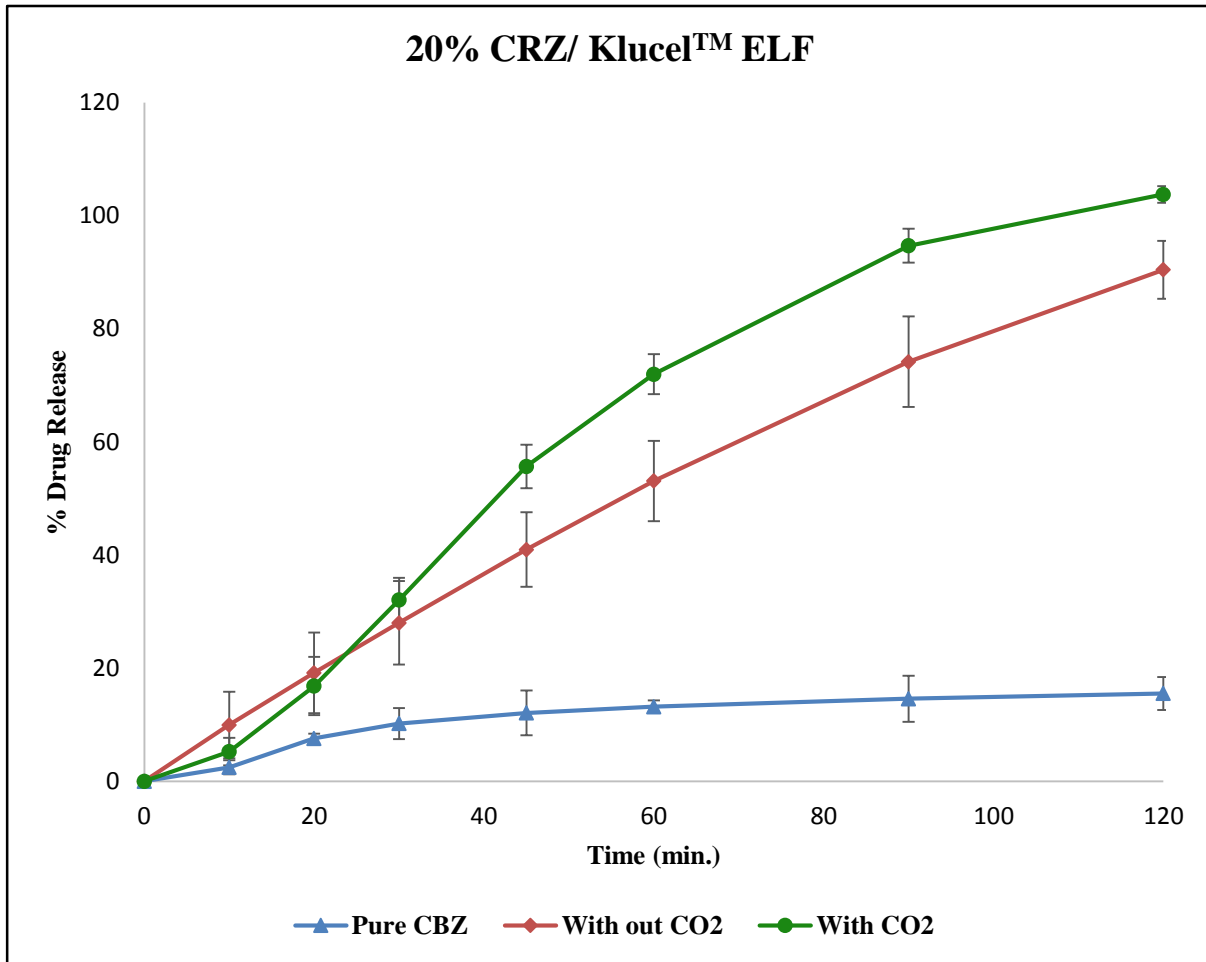
**Figure 5-7: SEM image of LS of CBZ /Klucel™ ELF extrudates a) without P-CO<sub>2</sub> injection, b) with P-CO<sub>2</sub> injection.**

#### **5.4.6. CBZ Drug Content and Uniformity**

HPLC analysis was used to evaluate the drug content uniformity of all CBZ/Klucel™ ELF extrudates and physical mixtures with different drug loading that were used in this study. The results showed that, all physical mixture blends and extrudates were in an acceptable range of (93%-101%). With more focus on the formulations processed with P-CO<sub>2</sub>, the drug content results indicating more precision and uniformity of the drug in the polymer carrier (97%-101%). These results may give more additional advantage of the carbon dioxide as a drug content uniformity enhancer.

#### **5.4.7. In-Vitro Drug Release**

As mentioned earlier, the *in-vitro* drug release profile is important for the prediction of the absorption and the bioavailability of any API. In many published reports, changing the morphology of the hot melt extrudates as well as increasing the surface area will enhance the release profile of the API. In this study, all the formulations processed with P-CO<sub>2</sub> exerted an enhancement of CBZ release in water at 37°C compared to other formulations without P-CO<sub>2</sub> and the pure CBZ (Figure 5-8). Moreover, the CBZ release profile of the 50% drug load formulations processed with P-CO<sub>2</sub> injection was less than 20%, 30% and 40% drug loading which have a complete drug release within 2 hours. While, the drug release profile of different drug loading formulations processed without P-CO<sub>2</sub> injection results showed that 20% , 30%, 40% and 50% having 90%, 86%, 80% and 73% CBZ drug release respectively. From these results, it can be concluded that 40% drug load is the saturation point of the CBZ/ Klucel™. Because of reaching this point, 50% drug loading formulations C<sub>7</sub> and C<sub>8</sub> the CBZ dispersed as a mixture of amorphous and crystalline state.



**Figure 5-8-a: Dissolution profiles of 20% CBZ/Klucel™ ELF extrudates with and without P-CO<sub>2</sub> injection and pure CBZ (Water, USP App II, 100 rpm and 37°C).**



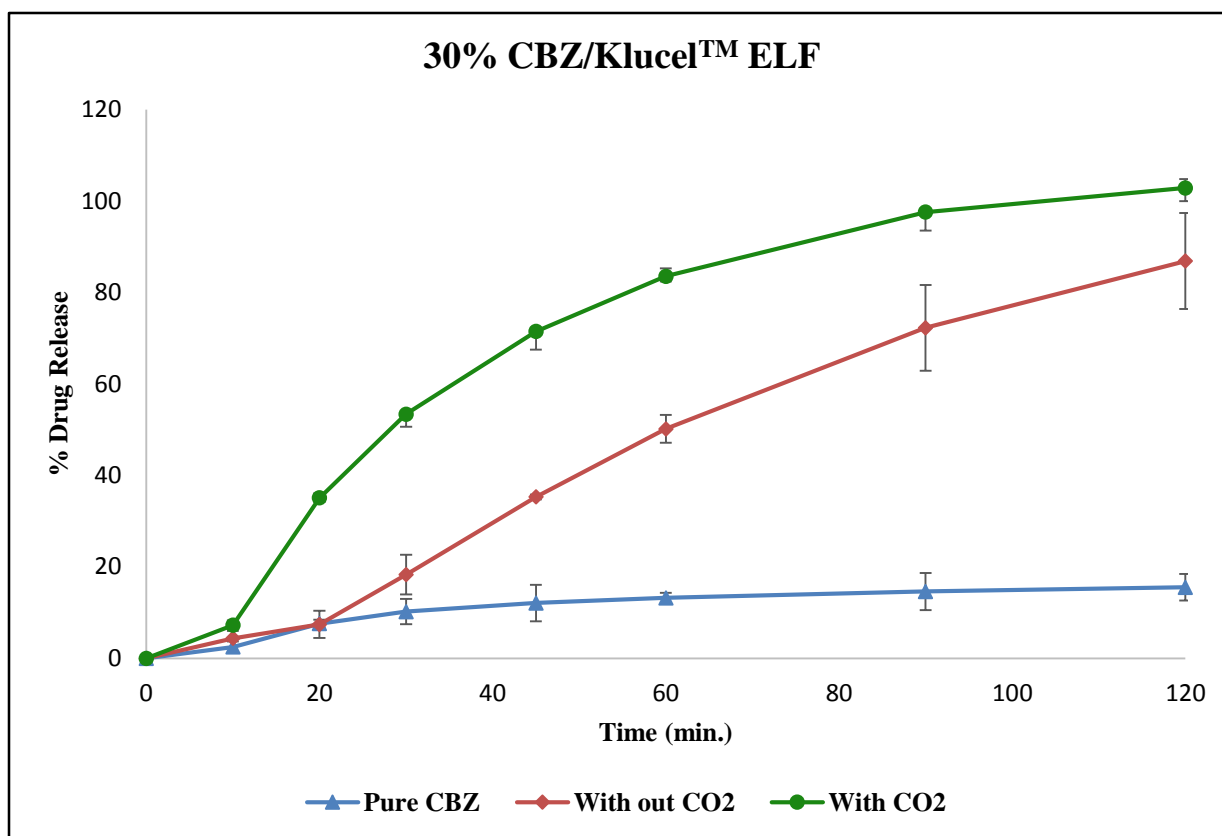
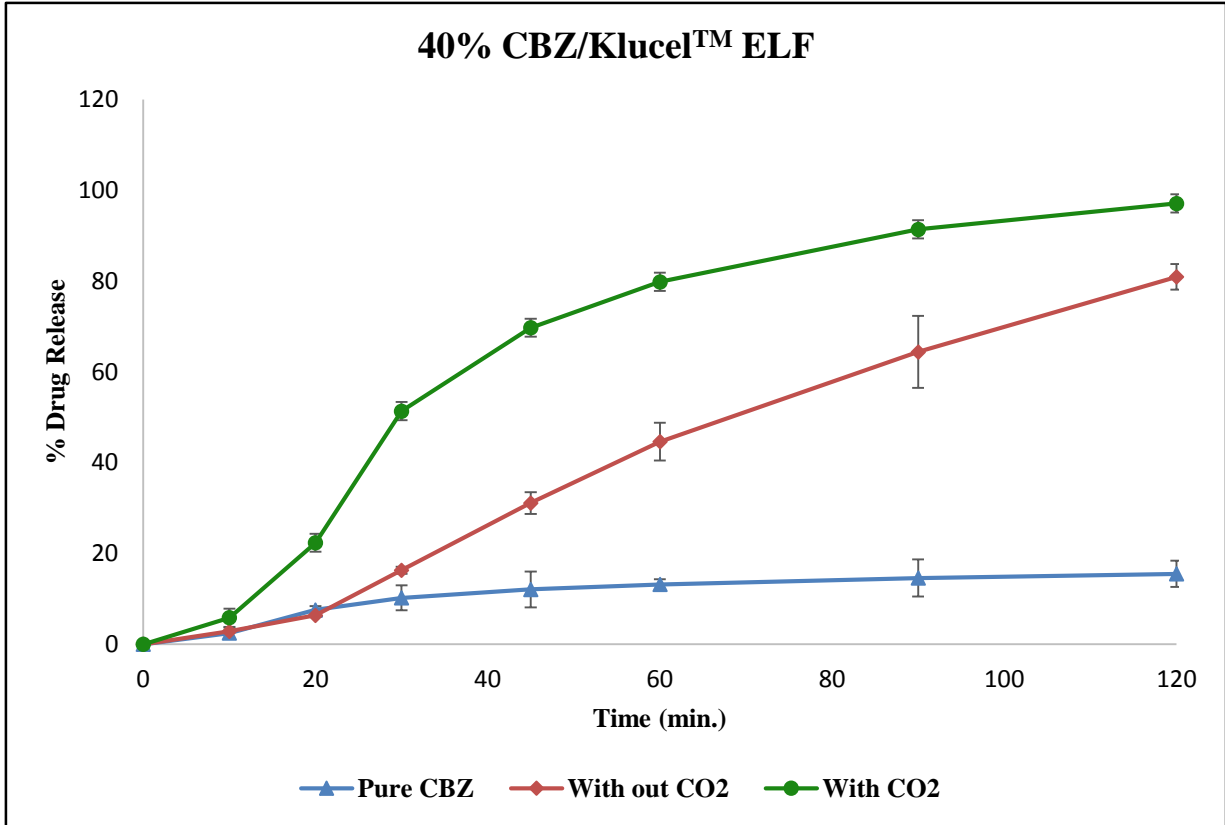
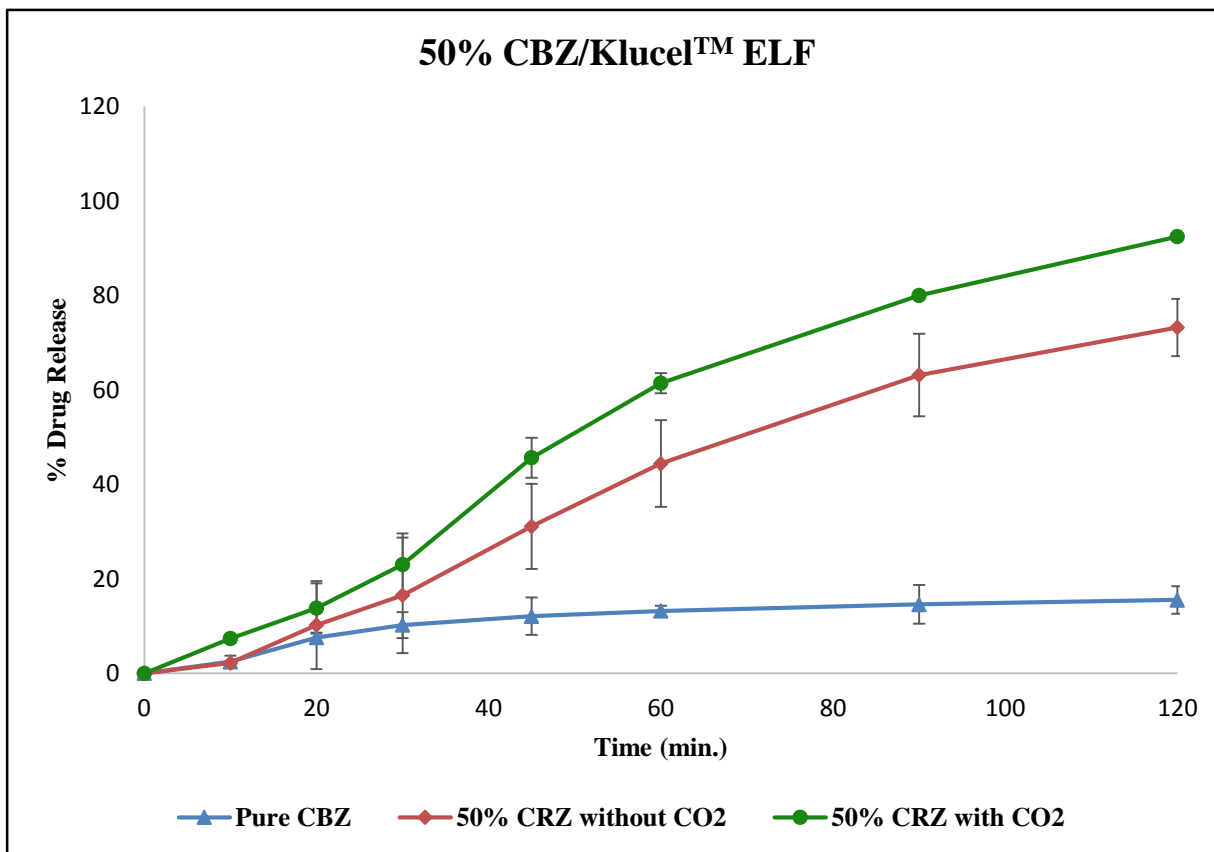


Figure 5-8-b: Dissolution profiles of 30% CBZ/Klucel™ ELF extrudates with and without P-CO<sub>2</sub> injection and pure CBZ (Water, USP App II, 100 rpm and 37°C).



**Figure 5-8-c: Dissolution profiles of 40% CBZ/Klucel™ ELF extrudates with and without P-CO<sub>2</sub> injection and pure CBZ (Water, USP App II, 100 rpm and 37°C).**



**Figure 5-8-d: Dissolution profiles of 50% CBZ/Klucel™ ELF extrudates with and without P-CO<sub>2</sub> injection and pure CBZ (Water, USP App II, 100 rpm and 37°C).**

$f_2$  values were calculated to compare the formulations of the same drug loading with and without P-CO<sub>2</sub> injection. The results showed that all  $f_2$  values were less than 50 (Table 5-5) indicating that dissolution profiles were not similar. Furthermore, 30% and 40% drug loading formulation exhibited significant dissimilarity with  $f_2$  values of 27.96 and 28.18 respectively.

Models independent approaches were used to understand and compare the drug dissolution profile of the same drug loading formulation with and without P-CO<sub>2</sub> injection. The dissolution efficiency of all formulations processed with P-CO<sub>2</sub> were increased compared with the same drug loading formulation processed without P-CO<sub>2</sub> (Table 5-6). On the other hand, the mean dissolution time of all formulations processed with P-CO<sub>2</sub> were decreased compared with the same drug loading formulation processed without P-CO<sub>2</sub> (Table 5-6). C<sub>4</sub> and C<sub>6</sub> formulation observed the maximum DE value of 70.577 % and 66.374% and the lowest MDT of 35.308 and 37.987 minutes respectively. Based on  $f_2$ , DE and MDT results it was confirmed that the injection of P-CO<sub>2</sub> through HME process increased the CBZ/klucel<sup>TM</sup> ELF solid dispersion drug load capacity up to 20% more than the regular HME process.

**Table 5-5: Similarity factor of 20%, 30%, 40% and 50% CBZ /Klucel™ ELF formulations with and without P-CO<sub>2</sub>**

Formulation	$f_2$	Similarity Status
C <sub>1</sub> and C <sub>2</sub>	43.967	Dissimilar
C <sub>3</sub> and C <sub>4</sub>	27.960	Dissimilar
C <sub>5</sub> and C <sub>6</sub>	28.183	Dissimilar
C <sub>7</sub> and C <sub>8</sub>	43.744	Dissimilar

**Table 5-6: Dissolution efficiency and the mean dissolution time of 20%, 30%, 40% and 50% CBZ /Klucel™ ELF formulations with and without P-CO<sub>2</sub>**

	Without P-CO <sub>2</sub> injection		With P-CO <sub>2</sub> injection	
	DE*	MDT**	DE*	MDT**
20% CRZ /Klucel™ ELF	50.276	53.291	61.800	45.837
30% CRZ /Klucel™ ELF	45.626	56.968	70.577	35.308
40% CRZ /Klucel™ ELF	40.941	59.296	66..374	37.987
50% CRZ /Klucel™ ELF	39.907	54.600	52.950	51.292

DE\* Dissolution efficiency

MDT\*\* Mean Dissolution Time

## **5.5. Conclusion**

Carbamazepine (CBZ) polymeric dispersions can be prepared using the novel technique of linking HME with P-CO<sub>2</sub> injection. The resulted extrudates showed an increase in porosity and changed the macroscopic morphology to a foam-like structure due to expansion of the carbon dioxide at the extrusion die. HME processing assisted with P-CO<sub>2</sub> increased the drug loading capability of CBZ in Klucel™ ELF polymeric matrix as well as optimized CBZ drug- release profiles. These processed properties of materials would provide numerous benefits during manufacturing of various solid dosage forms.

## **CHAPTER VI**

### **Dissolution Enhancement of the Psychoactive Natural Product- Piperine Using Hot Melt**

#### **Extrusion Techniques**

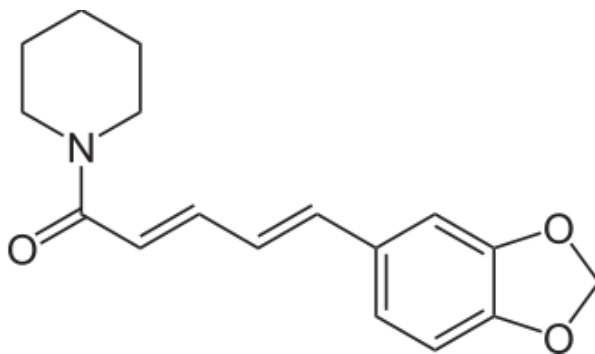
##### **6.1. Introduction**

Oral drug delivery is considered as the simplest and easiest route of the drug administration [61, 62]. Oral bioavailability is mainly affected by drug solubility, permeability [63-66] and first pass metabolism [67]. In fact, most of the new APIs have low water solubility with low release profiles after oral administration. The biggest challenge in the pharmaceutical industry was to enhance the solubility, and the permeability of those drugs as key factors to improve their bioavailability. There are many techniques which have been used to improve the drug water solubility and release profile, and solid dispersions are considered to be the most successful techniques. There are two main solid dispersions manufacturing methods ; the melting methods such as hot melt extrusion; and solvent evaporation methods such as spray drying [15]. Hot melt extrusion (HME) is one of the most commonly used techniques to enhance the solubility and oral bioavailability of poorly soluble drugs as a beneficial technique for solid dispersion. It involves simple dispersion of poorly water soluble API in an inert carrier (polymer), where the drug could exist in amorphous or crystalline state. . There are many advantages of using HME due to the speed and the continuous manufacturing process. Moreover, since no solvent is required, it is considered to be a green method for enhancement of the solubility and oral bioavailability of poorly soluble drugs. Depending on the polymeric carrier; hot melt extrusion can be also used for

other purposes such as taste masking, controlling or modifying drug release and stabilizing the active pharmaceutical ingredient.

Piperine (1-piperoylpiperidine) (Figure 6-1) is a crystalline pungent alkaloid isolated from black pepper (*Piper nigrum*), long pepper (*Piper longum*) and other pepper species (family: Piperaceae) [68-70]. Piperine is a poorly water soluble compound with a melting point at 135 °C. It has been extensively used in folk medicine in many Asian countries [69] and various studies have focused on investigating the pharmacological effects of piperine. Recently, it was reported as an anti-inflammatory, analgesic [71] [72], anti-depressant [73], cytoprotective, anti-leukemic and anti-oxidant agent [68, 74]. Furthermore, piperine significantly improves spatial memory and neurodegeneration in an Alzheimer's disease animal model [75]. Furthermore, piperine was reported to be a bioavailability enhancer [76]. Pattanaik *et al* investigated that 20 mg oral piperine can enhance the bioavailability of phenytoin and carbamazepine by increasing their plasma drug concentration [77, 78]. Atal *et al* proved that piperine is a potent inhibitor of the drug metabolism [79]. Literatures reports show that piperine acts as a metabolic inhibitor which inhibits the drug metabolizing enzyme such as CYP3A4, CYP1B1, CYP1B2 and CYP2E1. [76] [80] [81]. This finding gave the interest to incorporate the piperine with the anti-cancer acetyl-11-keto- $\beta$ -boswellic acid to increase its bioavailability and therapeutic efficacy [82]. Additionally, piperine modulate the permeability characteristics to increase the drug absorption through the cell membrane by increasing the vasodilation of the GIT membrane [70, 83]. Being a natural product, piperine had many advantages compared to other chemical entities such as low cost due to availability from plant material using easy and well known extraction and isolation methods [84]. Moreover, it is safe to use.





**Figure 6-1: Chemical structure of piperine.**

In the current study, the main goals were to enhance the solubility and the permeability of piperine in order to enhance its bioavailability and therapeutic efficacy. Three polymeric carriers Soluplus<sup>®</sup>, polyvinylpyrrolidone-co-vinylacetate 64 (Kollidon<sup>®</sup> VA 64) and Eudragit<sup>®</sup> EPO were used via the hot melt extrusion process to accomplish these goals.

## **6.2. Materials**

Piperine was purchased from Sigma-Aldrich (Milwaukee, WI 53233, USA), while Soluplus<sup>®</sup> and Kollidon<sup>®</sup> VA 64 were obtained from BASF- SE (Ludwigshafen, Germany), Eudragit<sup>®</sup> EPO was received as a gift sample from Evonik Industries (Parsippany, NJ 07045, USA). All other chemicals and reagents used in the present study were of analytical grade and obtained from Fisher Scientific (Fair Lawn, NJ 07410 USA).

## **6.3. Methods**

### **6.3.1. Thermogravimetric Analysis (TGA)**

TGA analysis were performed for piperine, Soluplus<sup>®</sup>, Kollidon<sup>®</sup> VA 64 and Eudragit<sup>®</sup> EPO to evaluate their stability at the extrusion temperatures using a Perkin Elmer Pyris 1 TGA equipped with Pyris manager software (PerkinElmer Life and Analytical Sciences, 710 Bridgeport Ave., Connecticut, USA). Approximately 10-15 mg of piperine, polymers as well as physical mixtures were heated from 30°C to 300 °C at heating rate of 20°C/min.

### **6.3.2. Differential Scanning Calorimetry (DSC)**

DSC studies were obtained using Perkin Elmer Pyris 1 DSC equipped with Pyris Manager Software (PerkinElmer Life and Analytical Sciences, 710 Bridgeport Ave., Connecticut, USA). Approximately 2-4 mg of piperine, physical mixtures or extrudates were heated from 30°C to 200°C at a heating rate of 10°C/min.

### **6.3.3. Hot Melt Extrusion (HME)**

Piperine 10–40% w/w and Eudragit<sup>®</sup> EPO, Kollidon<sup>®</sup> VA 64 or Soluplus<sup>®</sup> (Table 6-1) were mixed using a V-shell blender (Patrtreson-Kelley Twin Shell Dry Blender) for 10 minutes. The resulting physical mixture blends were extruded using a twin-screw extruder (Process 11 Twin Screw Extruder, ThermoFisher Scientific) at the screw speed of 150 rpm at a temperature range of 100–130°C. All extrudates were milled and sieved through an ASTM #35 mesh to obtain a uniform particle size.

**Table 6-1: Piperine formulation composition of HME**

<b>Formulation</b>	<b>Piperine (PIP) (%)</b>	<b>Eudragit<sup>®</sup> PE (%)</b>	<b>Soluplus<sup>®</sup> (%)</b>	<b>Kollidon<sup>®</sup> VA (%)</b>
<b>P<sub>1</sub></b>	10	90	-	-
<b>P<sub>2</sub></b>	20	80	-	-
<b>P<sub>3</sub></b>	40	60	-	-
<b>P<sub>4</sub></b>	10	-	90	-
<b>P<sub>5</sub></b>	20	-	80	-
<b>P<sub>6</sub></b>	40	-	60	-
<b>P<sub>7</sub></b>	10	-	-	90
<b>P<sub>8</sub></b>	20	-	-	80
<b>P<sub>9</sub></b>	40	-	-	60

#### **6.3.4. Scanning Electron Microscopy (SEM)**

The morphology and physical state of the extrudates were evaluated using SEM analysis. Samples were mounted on adhesive carbon pads placed on aluminum and were sputter coated with gold using a Hummer<sup>®</sup> 6.2 sputtering system (Anatech LTD, Springfield, VA) in a high vacuum evaporator. A JEOL JSM-5600 scanning electron microscope (SEM) operating at an accelerating voltage of 10kV was used for imaging.

#### **6.3.5. Fourier transforms infrared spectroscopy (FTIR)**

FTIR spectra of piperine, polymeric carriers, physical mixtures as well as extrudates were performed using Agilent Cary 630 FTIR spectrometer equipped with a DTGS detector. 2-4 mg sample was placed directly on ATR and the scanning range was 400 - 4000  $\text{cm}^{-1}$  and the resolution was 1  $\text{cm}^{-1}$ .

#### **6.3.6. High Performance Liquid Chromatography (HPLC)**

HPLC analyses were performed on all samples for piperine content using a Waters HPLC equipped with Empower software to analyze the data. HPLC consisted of a Waters e2695 separation Module and Waters 2489 UV/Visible detector, (Waters Technologies Corporation, 34 Maple St., Milford, MA 0157). The column used was Phenomenex Luna C18 (5 $\mu$ , 250 mm  $\times$  4.6 mm). The mobile phase consisted of a mixture of 0.1% ortho phosphoric acid and acetonitrile (45:55 v/v) with a flow rate of 1.2 mL/min and 20 $\mu$ L injection volume. The column temperature was 35°C ( $\pm$ 2). The UV detector wavelength for piperine detection was set at  $\lambda_{\text{max}}$  262 nm [85].

### **6.3.7. Solubility test**

The solubility was determined at pH 1.2, 5 (water), and 6.8 for formulations P<sub>4</sub> - P<sub>9</sub> as well as pure piperine. Sample equivalents to approximately 100 mg of piperine based on the drug load of each formulation were shaken in 20 mL scintillation vials containing 10 mL of tested pH solution. The samples were shaken at 80 rpm and at 25°C using Thermo Scientific Precision Reciprocal Shaking Bath. A sample volume of 1 mL was collected at time points 4, 10, 20 and 24 h. The samples were filtered and analyzed by HPLC, and 1 mL of the same pH solution was added back to the scintillation vials to maintain the volume.

### **6.3.8. *In-vitro* Drug Release**

A sample equivalent to 40 mg piperine of each extrudate as well as pure piperine were filled in gelatin capsules and the *in-vitro* drug release profiles were run using a USP type II dissolution apparatus. The used dissolution medium was 900 mL 0.1 N HCl maintained at 37 °C. A sample volume of 2 mL was taken at time points 10, 20, 30, 45, 60, 90, and 120 min. and was filtered and analyzed using HPLC; then 2 mL of fresh dissolution medium was added back to the dissolution vessel at each time point to maintain the volume.

### **6.3.9. Ex vivo permeability model (non-everted intestinal sac)**

The permeability studies were performed for the most promising formulation (P<sub>4</sub>) and pure piperine was used as the control. Non-everted intestinal sacs of male Sprague- Dawley rats, weighing approximately 200 -250 g, were provided from Charles river (Wilmington MA 01887, USA). Sacs of 4-5 cm in length were prepared. Each sac was filled with 0.5 mL of incubated Krebs-Ringer bicarbonate phosphate buffer, pH 7.4 with piperine 5mg/ml. Each non-everted sac was placed in 25mL beaker containing 5mL of Krebs-Ringer bicarbonate phosphate buffer, pH

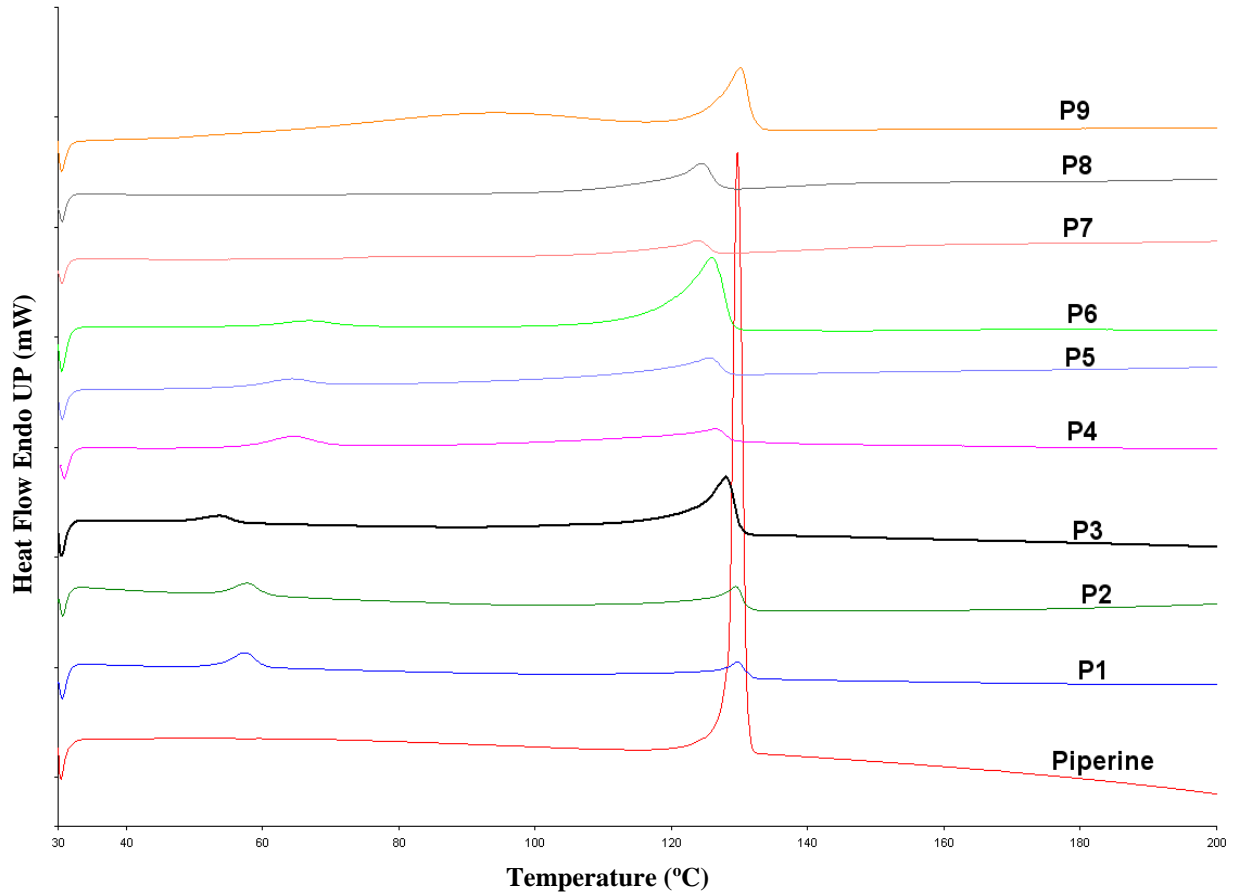
7.4. A sample volume of 1 ml was taken from the solution outside the sac at time points of 0, 20, 50, 80 and 120 minutes. The samples were filtered and analyzed for the content using HPLC. Fresh Krebs-Ringer buffer (1 mL) was added back to the beaker at each time point to maintain the volume. Cumulative dissolution profiles were calculated.

## **6.4. Results and discussion:**

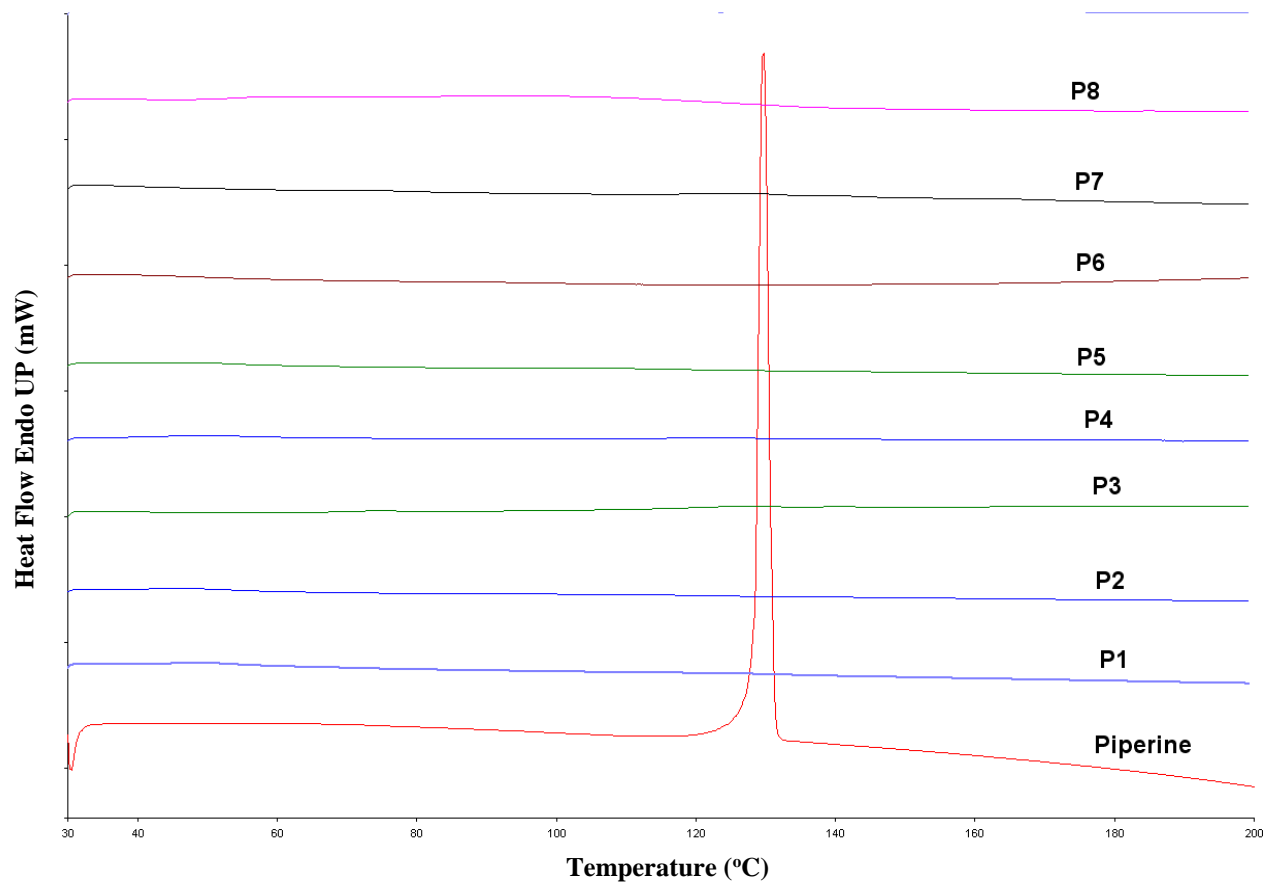
### **6.4.1. Pre-formulation Studies**

Under all utilized processing temperatures, TGA data showed no decrease in sample weight which indicate that all formulations in the study were stable under all applied extrusion temperatures.

DSC data showed the endothermic crystalline melting peak at 135°C for pure piperine and all the physical mixture samples (Figure 6-2). Alternatively, all the extrudates showed absence of crystalline melting peaks in DSC data (Figure 6-3).



**Figure 6-2: DSC thermogram of 10%, 20% and 40% of PIP/ Eudragit<sup>®</sup> PEO, PIP/ Soluplus<sup>®</sup> and PIP/ Kollidon<sup>®</sup> VA 64 physical mixtures.**



**Figure 6-3: DSC thermogram of 10%, 20% and 40% of Piperine/ Eudragit<sup>®</sup> PEO, Piperine/ Soluplus<sup>®</sup> and PIP/ Kollidon<sup>®</sup> VA 64 extrudates.**



#### **6.4.2. Hot Melt Extrusion (HME)**

HME process was carried out using (Process 11 Twin Screw Extruder, from Thermo Fisher Scientific). The Thermo Fisher standard screw configuration was used in this study. The screw configuration consists of four conveying zones and three mixing zones (Figure 6-4). The hot melt extrusion processing conditions such as extrusion temperature, screw speed and the torque values are shown in (Table 6-2). The resulting extrudates were transparent, greenish yellow and brittle extrudates except for P<sub>3</sub> (40% piperine/ Eudragit<sup>®</sup> EPO) which was opaque. This observation can be explained by the fact that 40% of drug load exceeded the Eudragit<sup>®</sup> EPO carrier capacity allowing the extrudate to mimic the appearance of the piperine only. All extrudates were milled using coffee grinder and sieved through an ASTM #35 mesh to obtain a uniform particle size.

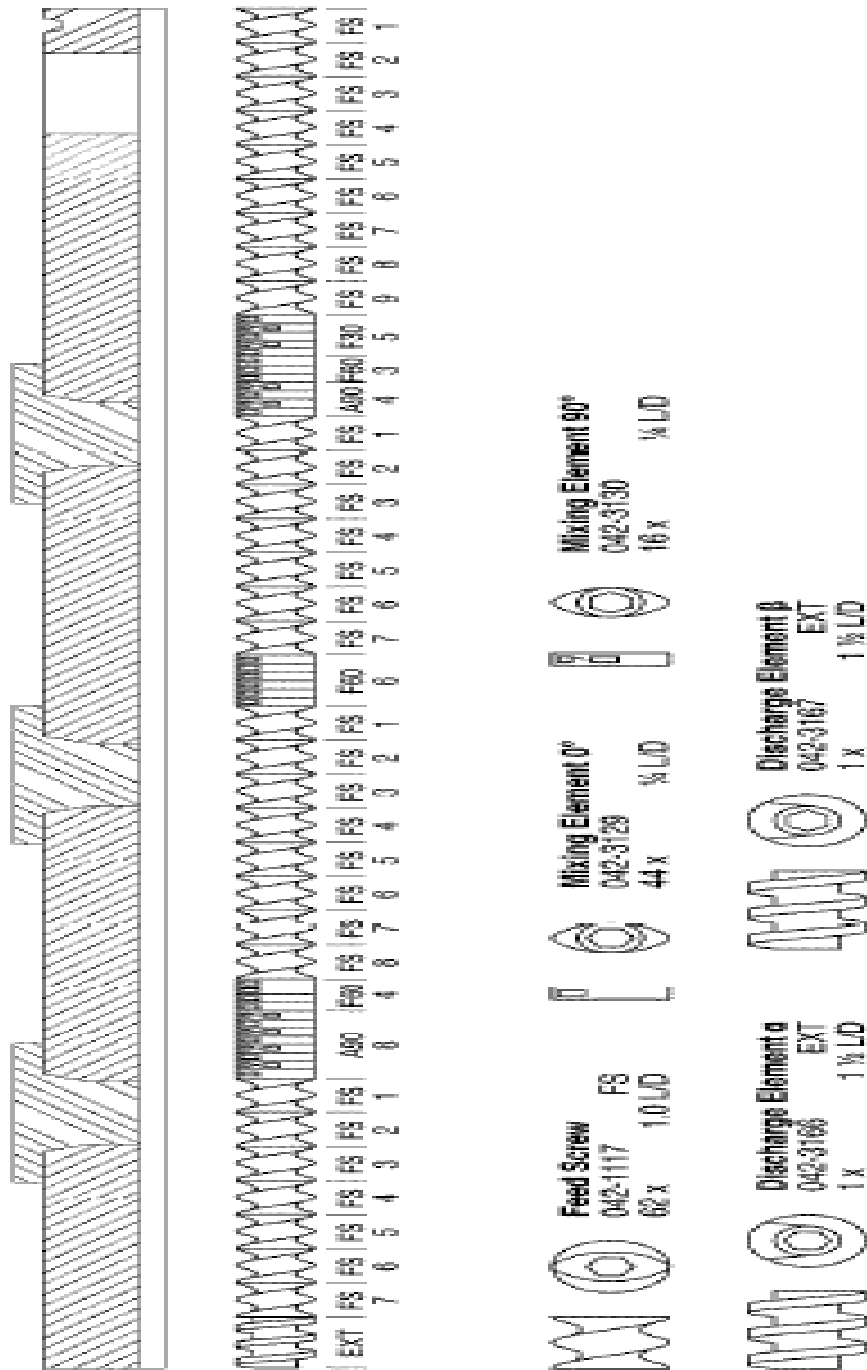






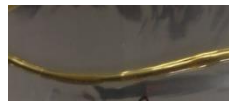
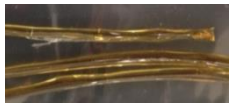



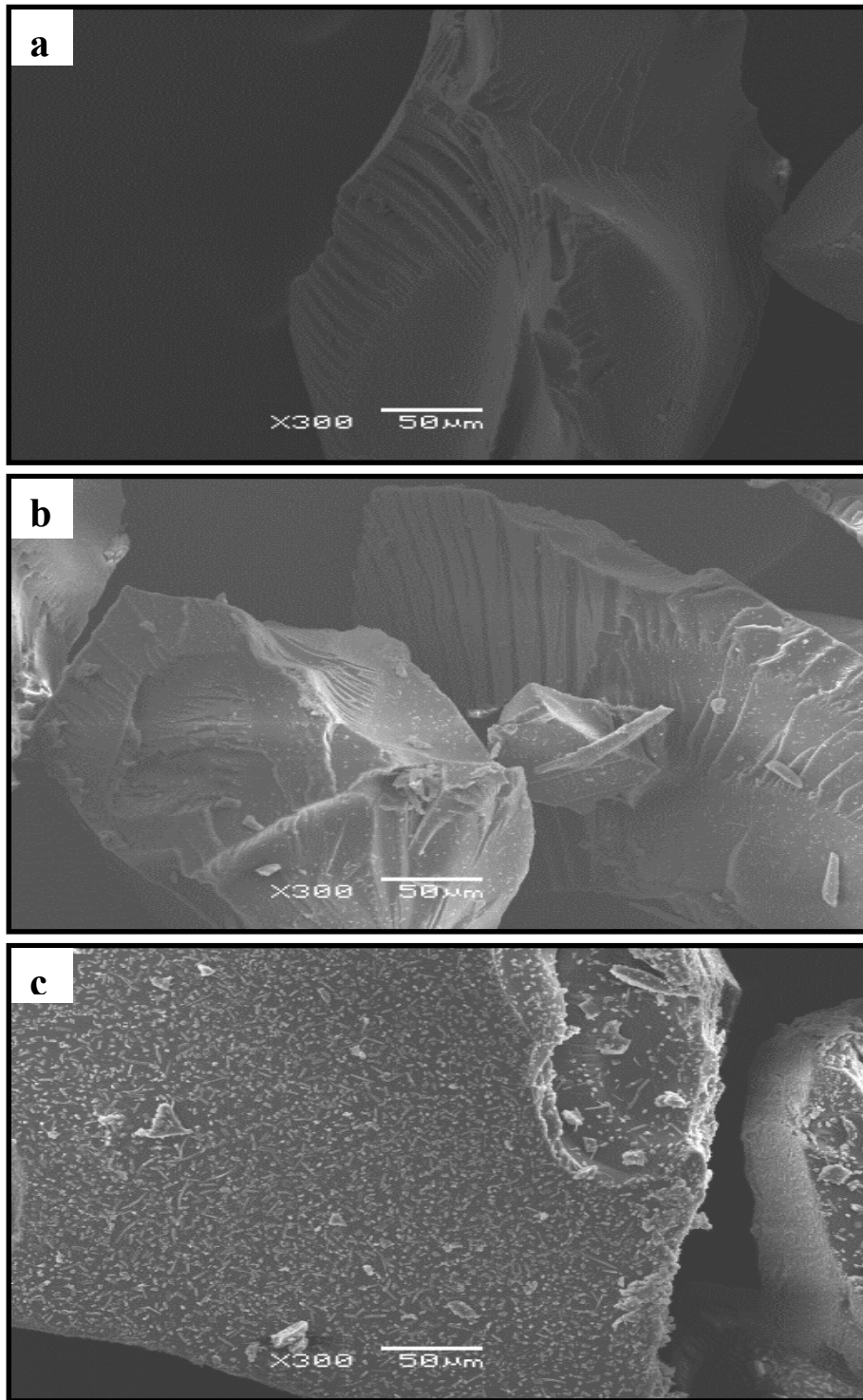
Figure 6-4: Standard screw configuration of Process 11 Twin Screw Extruder, Thermo Fisher Scientific.

**Table 6-2: Processing parameters for hot melt extrusion of PIP/ Eudragit<sup>®</sup> PEO, PIP/ Soluplus<sup>®</sup> and PIP/ Kollidon<sup>®</sup> VA formulations**

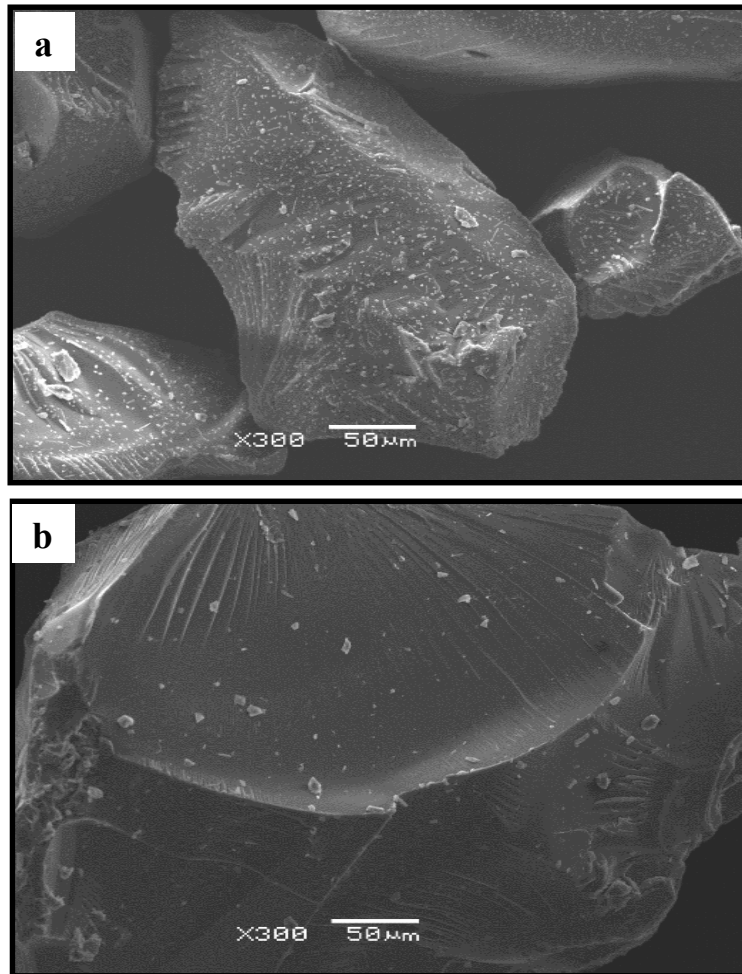
<b>Formulation</b>	<b>Processing Temperature (°C)</b>	<b>Screw Speed (rpm)</b>	<b>Torque (Nm)</b>	<b>Extrudate Image</b>
<b>P<sub>1</sub></b>	110	150	6-7	
<b>P<sub>2</sub></b>	110	150	4-5	
<b>P<sub>3</sub></b>	110	150	3	
<b>P<sub>4</sub></b>	120	150	7-8	
<b>P<sub>5</sub></b>	120	150	4-5	
<b>P<sub>6</sub></b>	120	150	3-4	
<b>P<sub>7</sub></b>	130	150	7-8	
<b>P<sub>8</sub></b>	130	150	3-4	
<b>P<sub>9</sub></b>	130	150	3-4	

### 6.4.3. Scanning electron microscopy (SEM)

SEM images showed absence of crystals in 10% w/w piperine/Soluplus<sup>®</sup> indicating that piperine was dispersed in the Soluplus<sup>®</sup> polymer carrier as an amorphous form. This may help to enhance the solubility and the bioavailability of this formulation. However, crystals were evident in the other piperine/ Soluplus<sup>®</sup> formulations with different ratios (Figure 6-5). In addition, SEM images demonstrated crystals in Kollidon<sup>®</sup> VA 64 and Eudragit<sup>®</sup> EPO formulation (Figure 6-6). These results are not consistent with the DSC results that showed absence of the piperine crystalline peak in the resulting extrudates. This observation be explained the fact that all polymers used in this study i.e., Eudragit<sup>®</sup> EPO, Kollidon<sup>®</sup> VA 64, and Soluplus<sup>®</sup> had a T<sub>g</sub> temperature of 45 °C, 101 °C and 70 °C respectively which are lower than the piperine melting point. Due to this; the polymers used will soften before the melting temperature of piperine allowing the piperine to solubilize in the polymer matrix and prevent the melting peak appearance.



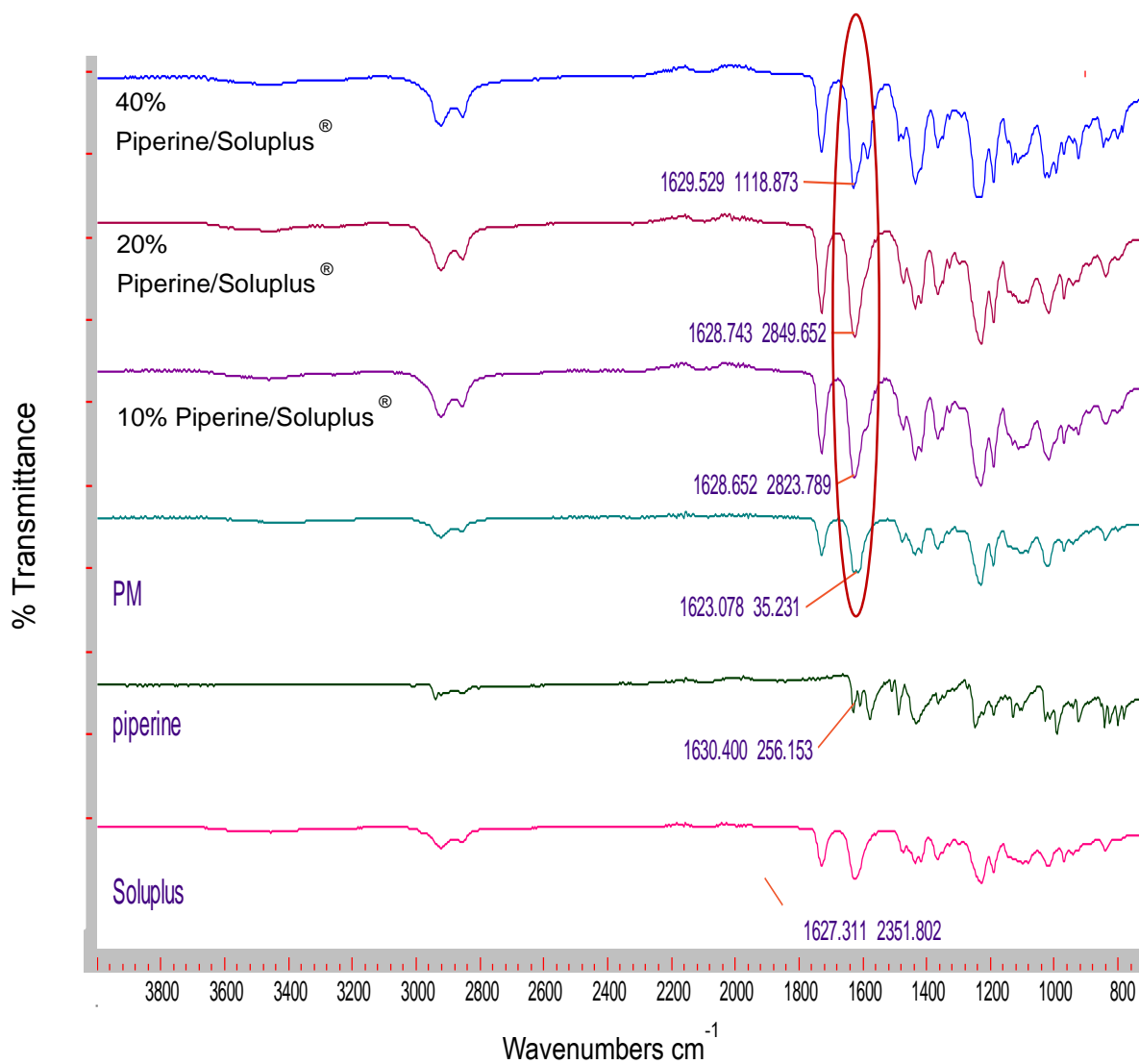
**Figure 6-5: SEM of extrudates: a) 10% w/w piperine/Soluplus<sup>®</sup>, b) 20% w/w piperine/Soluplus<sup>®</sup>, c) 40% w/w piperine/Soluplus<sup>®</sup>.**



**Figure 6-6: SEM of extrudates: a) 20% piperine/Eudragit<sup>®</sup> EPO, b) 20% piperine/Kollidon<sup>®</sup> VA64.**

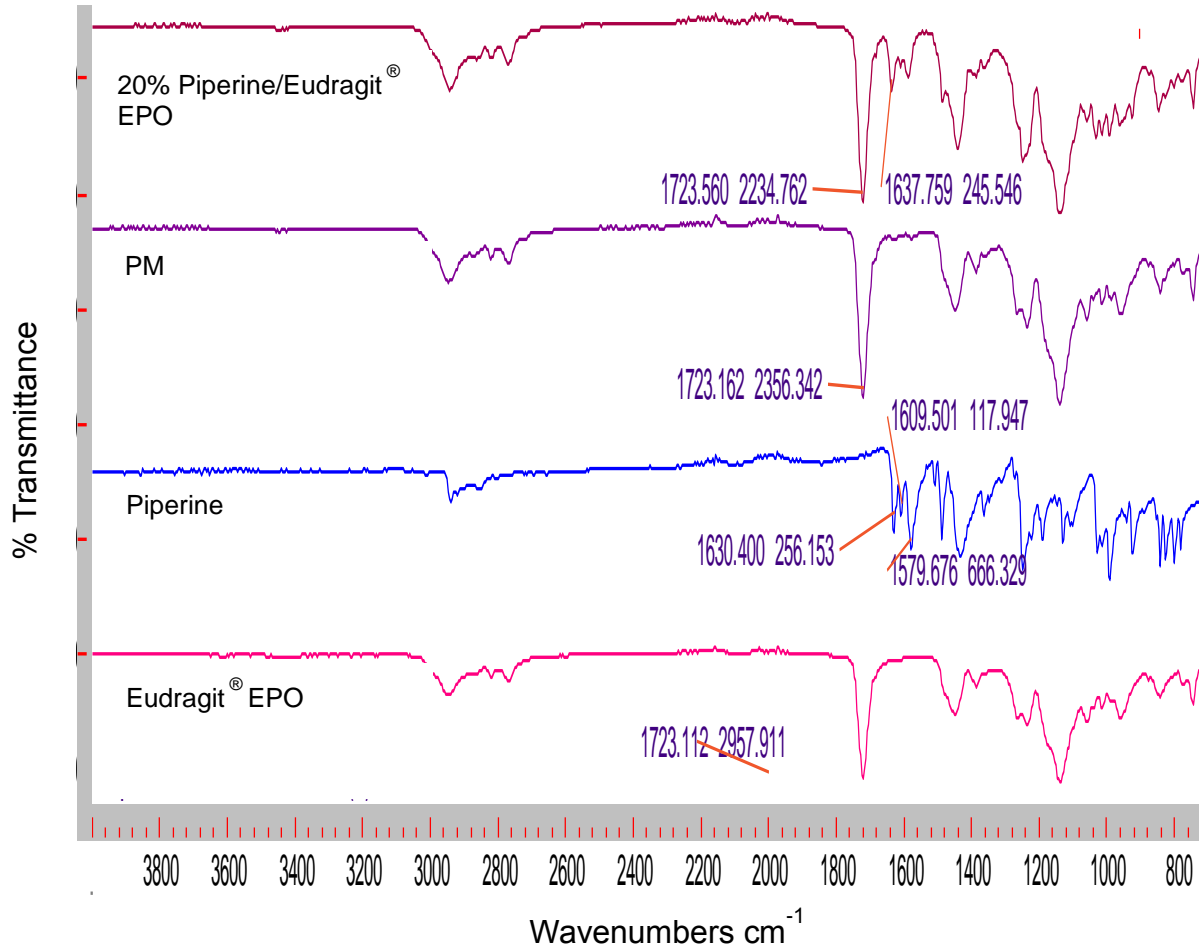
#### **6.4.4. Fourier transforms infrared spectroscopy (FTIR)**

FTIR analysis was performed to evaluate any chemical or physical interaction between piperine and the different polymeric carriers. Figure 6-7 shows the FTIR spectra of Soluplus and their formulations, the physical mixture displays a sharp peak at  $1623\text{ cm}^{-1}$ , and this peak shifts to approximately  $1629\text{ cm}^{-1}$  for all Soluplus formulations confirmed the presence of hydrogen bonding between piperine and Soluplus<sup>®</sup>. While, there were no shift observed in Eudragit<sup>®</sup> EPO (Figure 6-8), and Kollidon<sup>®</sup> VA 64 formulations (Figure 6-9). The formation of hydrogen bonding will increase the stability of the Soluplus solid dispersion formulations and prevent recrystallization of piperine [15, 86, 87].

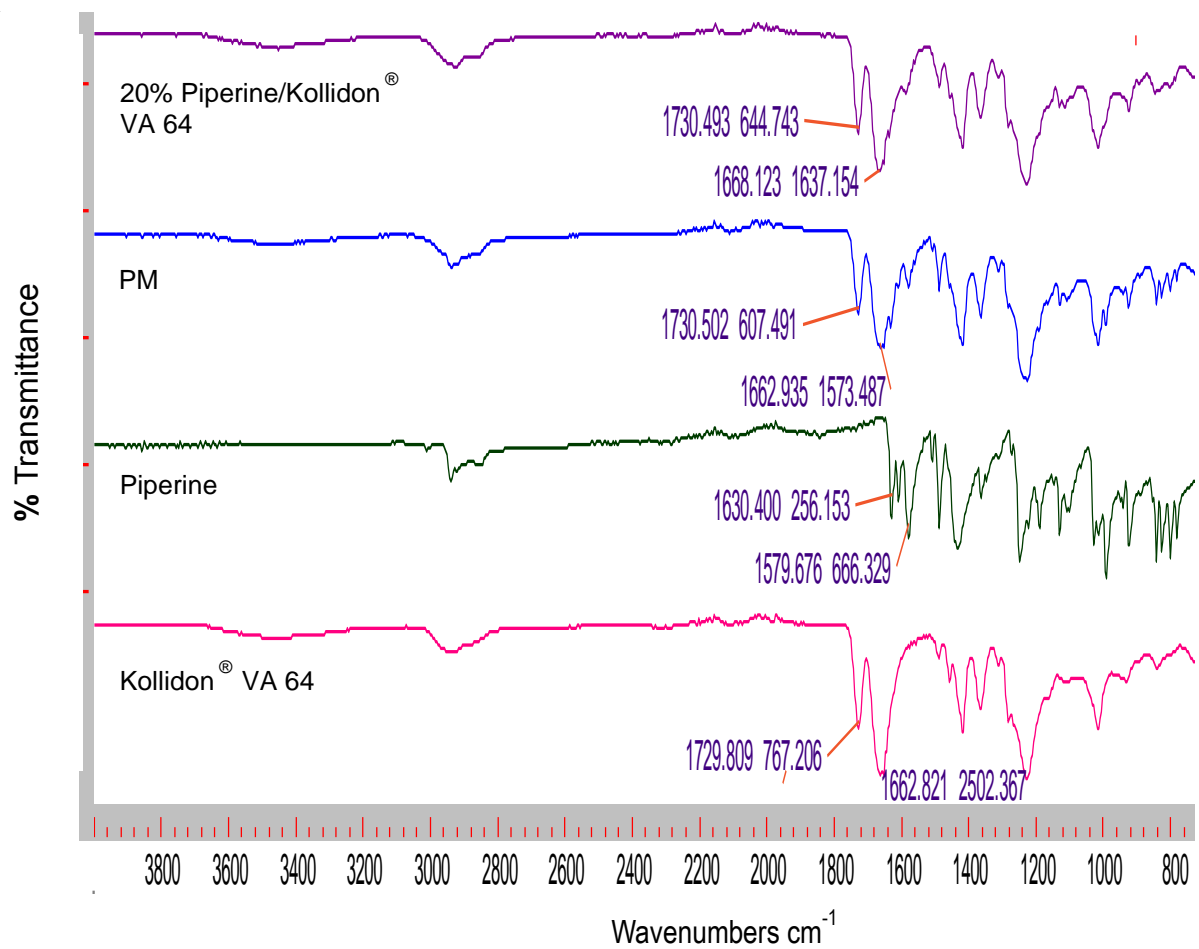


**Figure 6-7: FTIR spectra of Soluplus<sup>®</sup>, piperine, 10% piperine /Soluplus<sup>®</sup>, 20% piperine /Soluplus<sup>®</sup>, and 40% piperine /Soluplus<sup>®</sup> extrudates.**





**Figure 6-8: FTIR spectra of Eudragit<sup>®</sup> EPO, piperine, 20% piperine / Eudragit<sup>®</sup> EPO physical mixture and extrudates.**



**Figure 6-9: FTIR spectra of Kollidon<sup>®</sup> VA 64, piperine, 20% piperine / Kollidon<sup>®</sup> VA 64 physical mixture and extrudates.**

#### 6.4.5. Solubility Evaluation

The shake- flask method was used to determine the piperine solubility at pH value at equilibrium state [88]. Solubility study was performed for formulations P<sub>4</sub>, P<sub>5</sub>, P<sub>6</sub>, P<sub>7</sub>, P<sub>8</sub> and P<sub>9</sub> using three different solvents pH (1.2, 5 [(water)], and 6.8) to evaluate whether piperine solubility is pH dependent or not. The pH did not have any effect on the solubility of piperine as there were slight changes in the solubility values at pH 1.2 and 6.8 (Table 4-3). Furthermore, in formulations P<sub>4</sub> P<sub>5</sub>, P<sub>6</sub>, P<sub>7</sub>, P<sub>8</sub> and P<sub>9</sub> water solubility of piperine increased more than 160, 45, 25, 20, 5 and 3 folds respectively compared to pure piperine solubility in water (Table 6-3). This significant enhancement in the water solubility of piperine in P<sub>4</sub> was due to the dispersion of piperine in its amorphous state. Amorphous solid dispersion play a significant role in increasing the solubility and the dissolution rate of poorly water soluble APIs [89-92]. In general, amorphous API is more soluble than crystalline ones because of its higher effective surface area than the crystalline form [93-95]. However, the main problem associated with amorphous API is its instability, which can lead to recrystallization during storage as well as during dissolution [96]. In contrast, amorphous solid dispersions are stable as the polymeric carrier prevent the API recrystallization [97].

**Table 6-3: Solubility of piperine and piperine formulation in water, pH 1.2 and 6.8**

<b>Formulation</b>	<b>Solubility in Water (mg/L)</b>	<b>Solubility in pH 1.2 (mg/L)</b>	<b>Solubility in pH 6.8 (mg/L)</b>
<b>Piperine</b>	1	0.9	0.9
<b>P<sub>4</sub></b>	163	117	117
<b>P<sub>5</sub></b>	47	39	45
<b>P<sub>6</sub></b>	27	21	27
<b>P<sub>7</sub></b>	20	18	17
<b>P<sub>8</sub></b>	6	6	6
<b>P<sub>9</sub></b>	3	3	3

#### **6.4.6. *In-vitro* Release Profiles**

Dissolution studies demonstrated improvement in piperine drug release of 10% and 20% w/w piperine/Soluplus<sup>®</sup> extrudates up to 95% and 74%, respectively (Figure 6-10). However, no effect on piperine drug release profiles for other formulations was noted due to remaining of piperine in the crystalline state. These results confirmed that the dispersion of piperine in amorphous state plays a big role in enhancing the solubility [98] and drug release. Additionally, it can be concluded that the maximum drug loading capacity of piperine in Soluplus to form stabilized amorphous solid dispersion is approximately 10%. Soluplus<sup>®</sup> (Polyvinyl caprolactam-polyvinyl acetate-polyethylene glycol graft copolymer) is a relatively new polymer designed mainly for use in solid dispersion preparation APIs [99]. It acts as a polymeric stabilizer and solubilizing agent to improve the solubility and bioavailability of poor water soluble APIs [100-102]. It is a good polymeric carrier candidate to prepare amorphous solid dispersions of many poor water soluble APIs such as clotrimazole, carbamazepine, griseofulvine, and itraconazole by improving their dissolution profiles as well as their intestinal absorption and bioavailability [100]. In the recent study, Soluplus<sup>®</sup> was successfully used to prepare 10% piperine amorphous solid dispersion with a significant increase in the piperine release profile.

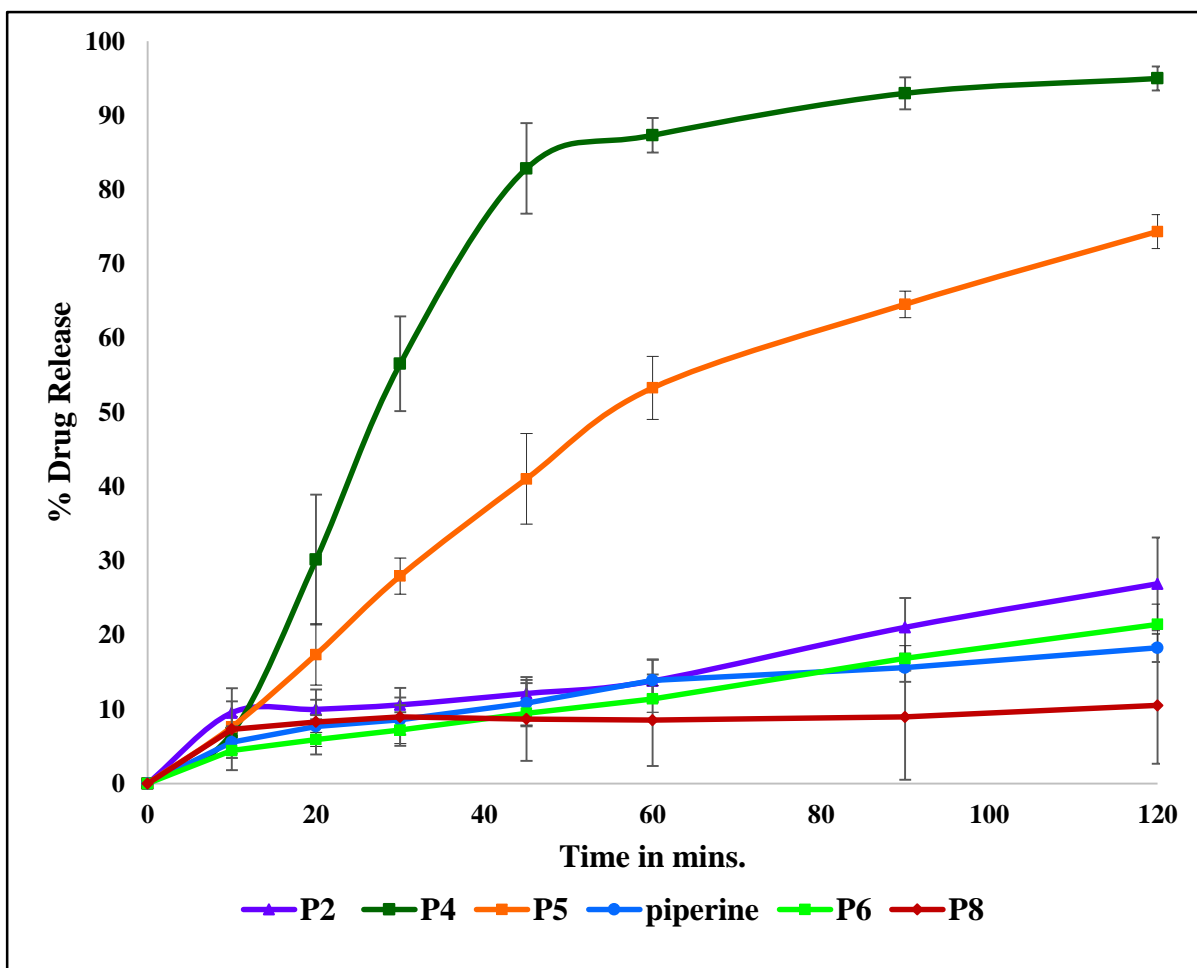
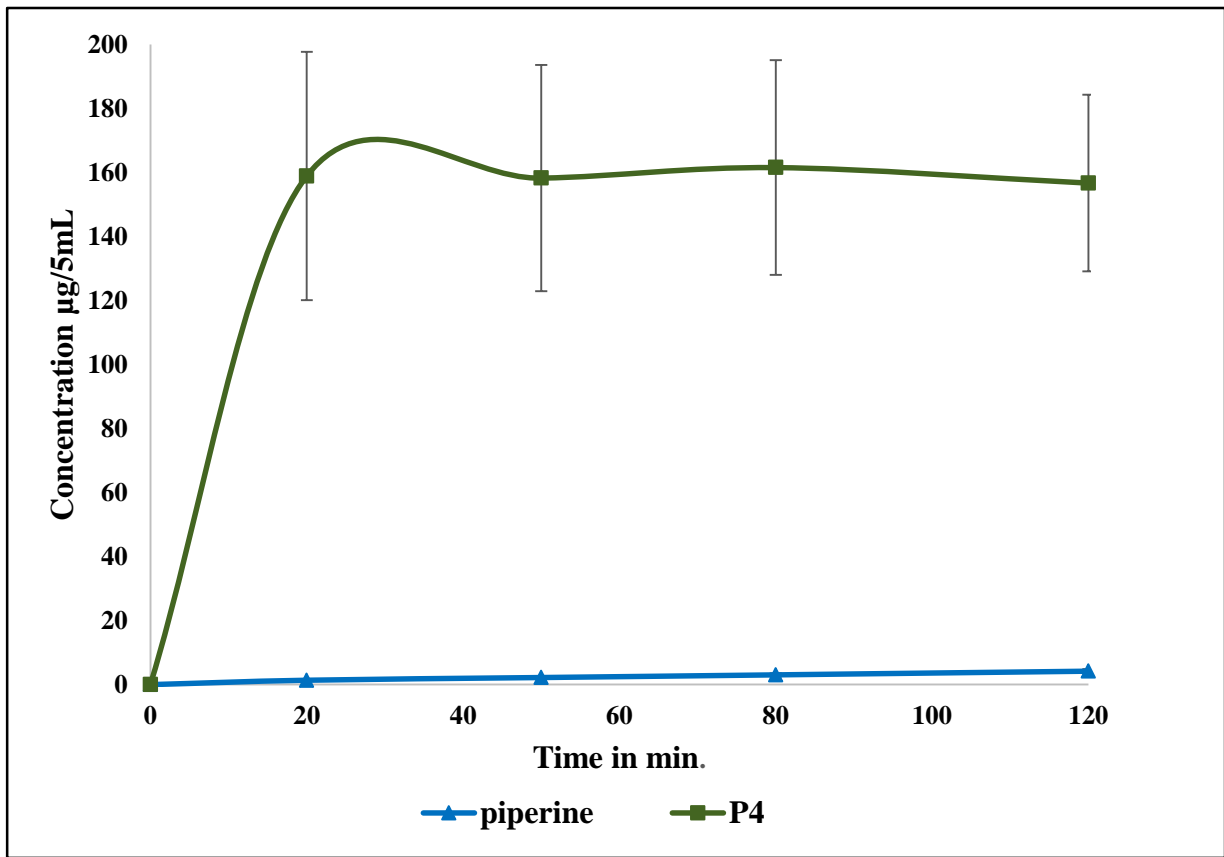


Figure 6-10: *In-vitro* release profiles of 10% w/w piperine/Soluplus<sup>®</sup>, 20% w/w piperine/Soluplus<sup>®</sup>, 40% w/w piperine/Soluplus<sup>®</sup>, 20% piperine/Eudragit<sup>®</sup> EPO, 20% piperine/Kollidon<sup>®</sup> VA64 and pure piperine.

#### **6.4.7. Ex vivo permeability model (non-everted intestinal sac)**

There are many in vivo, ex-vivo and in vitro assays used to evaluate the intestinal drug permeability [103, 104]. These assays include perfusion, diffusion chambers, gut sac, cultured cell and artificial membran [105]. The results of a research investigation showed that there was a good correlation between rat and human oral absorption. There are two types of rat intestinal sac models which are used to evaluate the drug permeability, everted and non-everted sacs. Some studies have been done to compare the permeability values of some APIs through both everted and non-everted sacs and no significant difference was observed in the permeability results. In this study, non everted rat intestinal sac model have been used to give an idea about the piperine absorption in humans. The permeability study results (Figure 6-11) demonstrated the enhancement in piperine absorption of 10% w/w piperine/Soluplus<sup>®</sup> up to 158.9 µg/5mL compared to 1.4 µg/5mL in the case of pure piperine within 20 min. as a direct result of the solubility improvement.



**Figure 6-11: Piperine absorption characteristics using jejunum non-everted sac under normal physiological conditions (Krebs Ringer bicarbonate phosphate buffer, pH 7.4).**



## **6.5. Conclusion**

HME was successfully used to enhance the solubility of the psychoactive natural product piperine. The drug release profiles of 10% and 20% w/w piperine/Soluplus<sup>®</sup> hot melt extrudates were significantly enhanced due to piperine in its amorphous state. In addition, the formation of hydrogen bond between piperine and Soluplus<sup>®</sup> may inhibit drug recrystallization and assist in the maintenance of the drug in its amorphous form thereby enabling good formulation stability. Furthermore, a significant improvement in piperine permeability has been confirmed using a non-everted rat intestinal sac. These results demonstrate that increase the absorption and bioavailability of piperine are possibilities.

## **BIBLIOGRAPHY**

1. Ghebre-Selassie, I. and C. Martin, *Pharmaceutical extrusion technology*2003: CRC Press.
2. Yang, M., et al., *Solid dispersion of acetaminophen and poly (ethylene oxide) prepared by hot-melt mixing*. International journal of pharmaceutics, 2010. **395**(1): p. 53-61.
3. Verreck, G., et al., *The effect of supercritical CO<sub>2</sub> as a reversible plasticizer and foaming agent on the hot stage extrusion of itraconazole with EC 20cps*. The Journal of supercritical fluids, 2007. **40**(1): p. 153-162.
4. <https://maritzaperez6270.wordpress.com/2010/09/20/first-post-year-2010-2011/>.
5. Sekhon, B.S., *Supercritical fluid technology: an overview of pharmaceutical applications*. Int J Pharm Tech Res, 2010. **2**(1): p. 810-826.
6. Delattre, L. [*Pharmaceutical applications of supercritical carbon dioxide*]. in *Annales pharmaceutiques francaises*. 2007.
7. Lee, S.-T. and N.S. Ramesh, *Polymeric foams: mechanisms and materials*2004: CRC press.
8. Terife, G., *Foaming of amorphous drug delivery systems prepared by hot melt mixing and extrusion*, 2013, NEW JERSEY INSTITUTE OF TECHNOLOGY.
9. Shugarts, S. and L.Z. Benet, *The role of transporters in the pharmacokinetics of orally administered drugs*. Pharmaceutical research, 2009. **26**(9): p. 2039-2054.
10. Thakkar, F.M.V., T. Soni, and M. Gohel, *Supercritical fluid technology: a promising approach to enhance the drug solubility*. 2009. **1**(4): p. 1-14.
11. Vo, C.L.-N., C. Park, and B.-J. Lee, *Current trends and future perspectives of solid dispersions containing poorly water-soluble drugs*. European Journal of Pharmaceutics and Biopharmaceutics, 2013. **85**(3): p. 799-813.

12. Huang, Y. and W.-G. Dai, *Fundamental aspects of solid dispersion technology for poorly soluble drugs*. Acta Pharmaceutica Sinica B, 2014. **4**(1): p. 18-25.
13. Chiou, W.L. and S. Riegelman, *Preparation and dissolution characteristics of several fast release solid dispersions of griseofulvin*. Journal of pharmaceutical sciences, 1969. **58**(12): p. 1505-1510.
14. Gurunath, S., et al., *Amorphous solid dispersion method for improving oral bioavailability of poorly water-soluble drugs*. Journal of Pharmacy Research, 2013. **6**(4): p. 476-480.
15. Vasconcelos, T., B. Sarmiento, and P. Costa, *Solid dispersions as strategy to improve oral bioavailability of poor water soluble drugs*. Drug discovery today, 2007. **12**(23): p. 1068-1075.
16. Karolewicz, B., et al., *Solid dispersions in pharmaceutical technology. Part I. Classification and methods to obtain solid dispersions*. Polim. Med, 2012. **42**(1): p. 17-27.
17. Breitenbach, J., *Melt extrusion: from process to drug delivery technology*. European Journal of Pharmaceutics and Biopharmaceutics, 2002. **54**(2): p. 107-117.
18. Deng, W., et al., *Stabilization of fenofibrate in low molecular weight hydroxypropylcellulose matrices produced by hot-melt extrusion*. Drug development and industrial pharmacy, 2013. **39**(2): p. 290-298.
19. Chokshi, R.J., et al., *Characterization of physico-mechanical properties of indomethacin and polymers to assess their suitability for hot-melt extrusion process as a means to manufacture solid dispersion/solution*. Journal of pharmaceutical sciences, 2005. **94**(11): p. 2463-2474.

20. Terife, G., et al., *Hot melt mixing and foaming of soluplus® and indomethacin*. Polymer Engineering & Science, 2012. **52**(8): p. 1629-1639.
21. Repka, M.A., et al., *Pharmaceutical applications of hot-melt extrusion: Part II*. Drug development and industrial pharmacy, 2007. **33**(10): p. 1043-1057.
22. He, H., R. Yang, and X. Tang, *In vitro and in vivo evaluation of fenofibrate solid dispersion prepared by hot-melt extrusion*. Drug development and industrial pharmacy, 2010. **36**(6): p. 681-687.
23. Crowley, M.M., et al., *Pharmaceutical applications of hot-melt extrusion: part I*. Drug development and industrial pharmacy, 2007. **33**(9): p. 909-926.
24. Arwidsson, H., et al., *Properties of ethyl cellulose films for extended release. II: Influence of plasticizer content and coalescence conditions when using aqueous dispersions*. Acta pharmaceutica nordica, 1991. **3**(2): p. 65-70.
25. Elkovitch, M.D. and D.L. Tomasko, *Effect of supercritical carbon dioxide on morphology development during polymer blending*. Polymer Engineering & Science, 2000. **40**(8): p. 1850-1861.
26. Medina-Gonzalez, Y., S. Camy, and J.-S. Condoret, *Cellulosic materials as biopolymers and supercritical CO<sub>2</sub> as a green process: chemistry and applications*. International Journal of Sustainable Engineering, 2012. **5**(1): p. 47-65.
27. Subramaniam, B., R.A. Rajewski, and K. Snavely, *Pharmaceutical processing with supercritical carbon dioxide*. Journal of pharmaceutical sciences, 1997. **86**(8): p. 885-890.
28. Rizvi, S., S. Mulvaney, and A. Sokhey, *The combined application of supercritical fluid and extrusion technology*. Trends in Food Science & Technology, 1995. **6**(7): p. 232-240.

29. Kikic, I., et al., *Polymer plasticization using supercritical carbon dioxide: experiment and modeling*. Industrial & engineering chemistry research, 2003. **42**(13): p. 3022-3029.
30. Verreck, G., et al., *The effect of pressurized carbon dioxide as a temporary plasticizer and foaming agent on the hot stage extrusion process and extrudate properties of solid dispersions of itraconazole with PVP-VA 64*. European journal of pharmaceutical sciences, 2005. **26**(3): p. 349-358.
31. Verreck, G., et al., *Hot stage extrusion of p-amino salicylic acid with EC using CO<sub>2</sub> as a temporary plasticizer*. International journal of pharmaceutics, 2006. **327**(1): p. 45-50.
32. Verreck, G., et al., *The effect of pressurized carbon dioxide as a plasticizer and foaming agent on the hot melt extrusion process and extrudate properties of pharmaceutical polymers*. The Journal of supercritical fluids, 2006. **38**(3): p. 383-391.
33. Lyons, J.G., et al., *Preparation of monolithic matrices for oral drug delivery using a supercritical fluid assisted hot melt extrusion process*. International journal of pharmaceutics, 2007. **329**(1): p. 62-71.
34. Sauceau, M., et al., *New challenges in polymer foaming: a review of extrusion processes assisted by supercritical carbon dioxide*. Progress in Polymer Science, 2011. **36**(6): p. 749-766.
35. Nalawade, S.P., F. Picchioni, and L. Janssen, *Supercritical carbon dioxide as a green solvent for processing polymer melts: Processing aspects and applications*. Progress in Polymer Science, 2006. **31**(1): p. 19-43.
36. ingredients, A.s., *Klucel™ hydroxypropylcellulose physical and chemical properties*. 2012: p. 4.

37. Repka, M.A., et al., *Influence of plasticizers and drugs on the physical-mechanical properties of hydroxypropylcellulose films prepared by hot melt extrusion*. Drug development and industrial pharmacy, 1999. **25**(5): p. 625-633.
38. Mohammed, N.N., et al., *Klucel™ EF and ELF polymers for immediate-release oral dosage forms prepared by melt extrusion technology*. AAPS PharmSciTech, 2012. **13**(4): p. 1158-1169.
39. Jeong, H. and R. Toledo, *Twin-screw extrusion at low temperature with carbon dioxide injection to assist expansion: extrudate characteristics*. Journal of food engineering, 2004. **63**(4): p. 425-432.
40. Kantor, T.G., *Ketoprofen: a review of its pharmacologic and clinical properties*. Pharmacotherapy: The Journal of Human Pharmacology and Drug Therapy, 1986. **6**(3): p. 93-102.
41. Yadav, P.S., et al., *Physicochemical characterization and in vitro dissolution studies of solid dispersions of ketoprofen with PVP K30 and d-mannitol*. Saudi Pharmaceutical Journal, 2013. **21**(1): p. 77-84.
42. Vueba, M., et al., *Influence of cellulose ether polymers on ketoprofen release from hydrophilic matrix tablets*. European Journal of Pharmaceutics and Biopharmaceutics, 2004. **58**(1): p. 51-59.
43. Tița, D., A. Fuliaș, and B. Tița, *Thermal stability of ketoprofen—active substance and tablets*. Journal of thermal analysis and calorimetry, 2011. **105**(2): p. 501-508.
44. Crowley, M.M., et al., *The influence of guaifenesin and ketoprofen on the properties of hot-melt extruded polyethylene oxide films*. European journal of pharmaceutical sciences, 2004. **22**(5): p. 409-418.

45. [http://www.accessdata.fda.gov/scripts/cder/dissolution/dsp\\_SearchResults\\_Dissolutions.cfm](http://www.accessdata.fda.gov/scripts/cder/dissolution/dsp_SearchResults_Dissolutions.cfm).
46. Dressman, J.B., et al., *Dissolution testing as a prognostic tool for oral drug absorption: immediate release dosage forms*. Pharmaceutical research, 1998. **15**(1): p. 11-22.
47. Sprunk, A., S. Page, and P. Kleinebudde, *Influence of process parameters and equipment on dry foam formulation properties using indomethacin as model drug*. International journal of pharmaceutics, 2013. **455**(1): p. 189-196.
48. Andrews, G.P., et al., *Physicochemical characterization and drug release properties of celecoxib hot melt extruded glass solutions*. Journal of Pharmacy and Pharmacology, 2010. **62**(11): p. 1580-1590.
49. Ahern, R.J., A.M. Crean, and K.B. Ryan, *The influence of supercritical carbon dioxide (SC-CO<sub>2</sub>) processing conditions on drug loading and physicochemical properties*. International journal of pharmaceutics, 2012. **439**(1): p. 92-99.
50. Listro, T., *Foamed hot melt extrusion for solid molecular dispersions*. Innovation in Pharmaceutical Technology, 2012(43).
51. Killian, J.M. and G.H. Fromm, *Carbamazepine in the treatment of neuralgia: use and side effects*. Archives of neurology, 1968. **19**(2): p. 129-136.
52. Al-Hamidi, H., et al., *To enhance dissolution rate of poorly water-soluble drugs: glucosamine hydrochloride as a potential carrier in solid dispersion formulations*. Colloids and Surfaces B: Biointerfaces, 2010. **76**(1): p. 170-178.
53. Djuris, J., et al., *Preparation of carbamazepine–Soluplus® solid dispersions by hot-melt extrusion, and prediction of drug–polymer miscibility by thermodynamic model fitting*. European Journal of Pharmaceutics and Biopharmaceutics, 2013. **84**(1): p. 228-237.



54. Elqidra, R., et al., *Effect of polymorphism on in vitro-in vivo properties of carbamazepine conventional tablets*. Journal of Drug Delivery Science and Technology, 2004. **14**(2): p. 147-153.
55. Naima, Z., et al., *Interactions between carbamazepine and polyethylene glycol (PEG) 6000: characterisations of the physical, solid dispersed and eutectic mixtures*. European journal of pharmaceutical sciences, 2001. **12**(4): p. 395-404.
56. Zerrouk, N., et al., *In vitro and in vivo evaluation of carbamazepine-PEG 6000 solid dispersions*. International journal of pharmaceutics, 2001. **225**(1): p. 49-62.
57. Patterson, J.E., et al., *Melt extrusion and spray drying of carbamazepine and dipyridamole with polyvinylpyrrolidone/vinyl acetate copolymers*. Drug Dev Ind Pharm, 2008. **34**(1): p. 95-106.
58. A. Ashour, E., et al., *Influence of pressurized carbon dioxide on ketoprofen-incorporated hot-melt extruded low molecular weight hydroxypropylcellulose*. Drug development and industrial pharmacy, 2015(ahead-of-print): p. 1-8.
59. Elizondo, E., et al., *High loading of gentamicin in bioadhesive PVM/MA nanostructured microparticles using compressed carbon-dioxide*. Pharmaceutical research, 2011. **28**(2): p. 309-321.
60. Mendyk, A., et al., *KinetDS: an open source software for dissolution test data analysis*. J Dissolution Technology, 2012. **19**(1): p. 6-11.
61. Youn, Y.S., et al., *Improved intestinal delivery of salmon calcitonin by Lys 18-amine specific PEGylation: Stability, permeability, pharmacokinetic behavior and in vivo hypocalcemic efficacy*. Journal of controlled release, 2006. **114**(3): p. 334-342.

62. Guggi, D., A.H. Krauland, and A. Bernkop-Schnürch, *Systemic peptide delivery via the stomach: in vivo evaluation of an oral dosage form for salmon calcitonin*. Journal of controlled release, 2003. **92**(1): p. 125-135.
63. Pade, V. and S. Stavchansky, *Link between drug absorption solubility and permeability measurements in Caco-2 cells*. Journal of pharmaceutical sciences, 1998. **87**(12): p. 1604-1607.
64. Hörter, D. and J. Dressman, *Influence of physicochemical properties on dissolution of drugs in the gastrointestinal tract*. Advanced drug delivery reviews, 2001. **46**(1): p. 75-87.
65. Martinez, M.N. and G.L. Amidon, *A mechanistic approach to understanding the factors affecting drug absorption: a review of fundamentals*. Journal of Clinical Pharmacology, 2002. **42**(6): p. 620-643.
66. Varma, M.V. and R. Panchagnula, *Enhanced oral paclitaxel absorption with vitamin E-TPGS: effect on solubility and permeability in vitro, in situ and in vivo*. European journal of pharmaceutical sciences, 2005. **25**(4): p. 445-453.
67. Wu, Y., et al., *The role of biopharmaceutics in the development of a clinical nanoparticle formulation of MK-0869: a Beagle dog model predicts improved bioavailability and diminished food effect on absorption in human*. International journal of pharmaceutics, 2004. **285**(1): p. 135-146.
68. Chonpathompikunlert, P., J. Wattanathorn, and S. Muchimapura, *Piperine, the main alkaloid of Thai black pepper, protects against neurodegeneration and cognitive impairment in animal model of cognitive deficit like condition of Alzheimer's disease*. Food and Chemical Toxicology, 2010. **48**(3): p. 798-802.

69. Wattanathorn, J., et al., *Piperine, the potential functional food for mood and cognitive disorders*. Food and Chemical Toxicology, 2008. **46**(9): p. 3106-3110.
70. Khajuria, A., N. Thusu, and U. Zutshi, *Piperine modulates permeability characteristics of intestine by inducing alterations in membrane dynamics: influence on brush border membrane fluidity, ultrastructure and enzyme kinetics*. Phytomedicine, 2002. **9**(3): p. 224-231.
71. Gupta, S., et al., *Comparative anti-nociceptive, anti-inflammatory and toxicity profile of nimesulide vs nimesulide and piperine combination*. Pharmacological Research, 2000. **41**(6): p. 657-662.
72. Chithra, S., et al., *Piperine production by endophytic fungus Colletotrichum gloeosporioides isolated from Piper nigrum*. Phytomedicine, 2014. **21**(4): p. 534-540.
73. KONTUSH, A. and S. SCHEKATOLINA, *Vitamin E in neurodegenerative disorders: Alzheimer's disease*. Annals of the New York Academy of Sciences, 2004. **1031**(1): p. 249-262.
74. Selvendiran, K., et al., *Cytoprotective effect of piperine against benzo [a] pyrene induced lung cancer with reference to lipid peroxidation and antioxidant system in Swiss albino mice*. Fitoterapia, 2003. **74**(1): p. 109-115.
75. Borre, Y.E., et al., *Neuroprotective and cognitive enhancing effects of a multi-targeted food intervention in an animal model of neurodegeneration and depression*. Neuropharmacology, 2014. **79**: p. 738-749.
76. Kesarwani, K. and R. Gupta, *Bioavailability enhancers of herbal origin: An overview*. Asian Pacific journal of tropical biomedicine, 2013. **3**(4): p. 253-266.

77. Pattanaik, S., et al., *Effect of piperine on the steady-state pharmacokinetics of phenytoin in patients with epilepsy*. *Phytotherapy Research*, 2006. **20**(8): p. 683-686.
78. Pattanaik, S., et al., *Pharmacokinetic interaction of single dose of piperine with steady-state carbamazepine in epilepsy patients*. *Phytotherapy Research*, 2009. **23**(9): p. 1281-1286.
79. Atal, C., R. Dubey, and J. Singh, *Biochemical basis of enhanced drug bioavailability by piperine: evidence that piperine is a potent inhibitor of drug metabolism*. *Journal of Pharmacology and Experimental Therapeutics*, 1985. **232**(1): p. 258-262.
80. Majeed, M., V. Badmaev, and R. Rajendran, *Use of piperine as a bioavailability enhancer*, 1999, Google Patents.
81. Bajad, S., et al., *Piperine inhibits gastric emptying and gastrointestinal transit in rats and mice*. *Planta medica*, 2001. **67**(2): p. 176-179.
82. Brough, C., et al., *Pharmaceutical formulations of acetyl-11-keto-b-boswellic acid, diindolylmethane, and curcumin for pharmaceutical applications*, 2012, Google Patents.
83. Khajuria, A., U. Zutshi, and K. Bedi, *Permeability characteristics of piperine on oral absorption--an active alkaloid from peppers and a bioavailability enhancer*. *Indian journal of experimental biology*, 1998. **36**(1): p. 46-50.
84. Ribeiro, T.S., et al., *Toxic effects of natural piperine and its derivatives on epimastigotes and amastigotes of Trypanosoma cruzi*. *Bioorganic & medicinal chemistry letters*, 2004. **14**(13): p. 3555-3558.
85. Moorthi, C., et al., *Application of validated RP-HPLC-PDA method for the simultaneous estimation of curcumin and piperine in Eudragit E 100 nanoparticles*. *Journal of Pharmacy Research*, 2013. **7**(3): p. 224-229.

86. Vasanthavada, M., et al., *Phase behavior of amorphous molecular dispersions II: Role of hydrogen bonding in solid solubility and phase separation kinetics*. Pharmaceutical research, 2005. **22**(3): p. 440-448.
87. Schachter, D.M., J. Xiong, and G.C. Tirol, *Solid state NMR perspective of drug-polymer solid solutions: a model system based on poly (ethylene oxide)*. International journal of pharmaceutics, 2004. **281**(1): p. 89-101.
88. Glomme, A., J. März, and J. Dressman, *Comparison of a miniaturized shake-flask solubility method with automated potentiometric acid/base titrations and calculated solubilities*. Journal of pharmaceutical sciences, 2005. **94**(1): p. 1-16.
89. Van den Mooter, G., *The use of amorphous solid dispersions: A formulation strategy to overcome poor solubility and dissolution rate*. Drug Discovery Today: Technologies, 2012. **9**(2): p. e79-e85.
90. Blagden, N., et al., *Crystal engineering of active pharmaceutical ingredients to improve solubility and dissolution rates*. Advanced drug delivery reviews, 2007. **59**(7): p. 617-630.
91. Lakshman, J.P., et al., *Application of melt extrusion in the development of a physically and chemically stable high-energy amorphous solid dispersion of a poorly water-soluble drug*. Molecular pharmaceutics, 2008. **5**(6): p. 994-1002.
92. Kennedy, M., et al., *Enhanced bioavailability of a poorly soluble VRI antagonist using an amorphous solid dispersion approach: a case study*. Molecular pharmaceutics, 2008. **5**(6): p. 981-993.

93. Pignatello, R., et al., *Preparation, characterisation and photosensitivity studies of solid dispersions of diflunisal and Eudragit RS100® and RL100®*. International journal of pharmaceutics, 2001. **218**(1): p. 27-42.
94. Craig, D.Q., *The mechanisms of drug release from solid dispersions in water-soluble polymers*. International journal of pharmaceutics, 2002. **231**(2): p. 131-144.
95. Kawabata, Y., et al., *Formulation design for poorly water-soluble drugs based on biopharmaceutics classification system: basic approaches and practical applications*. International journal of pharmaceutics, 2011. **420**(1): p. 1-10.
96. Alonzo, D.E., et al., *Understanding the behavior of amorphous pharmaceutical systems during dissolution*. Pharmaceutical research, 2010. **27**(4): p. 608-618.
97. Overhoff, K.A., et al., *Solid dispersions of itraconazole and enteric polymers made by ultra-rapid freezing*. International journal of pharmaceutics, 2007. **336**(1): p. 122-132.
98. Shah, S., et al., *Melt extrusion with poorly soluble drugs*. International journal of pharmaceutics, 2013. **453**(1): p. 233-252.
99. Shamma, R.N. and M. Basha, *Soluplus®: A novel polymeric solubilizer for optimization of Carvedilol solid dispersions: Formulation design and effect of method of preparation*. Powder Technology, 2013. **237**: p. 406-414.
100. Hardung, H., D. Djuric, and S. Ali, *Combining HME & solubilization: Soluplus®—the solid solution*. Drug Deliv Technol, 2010. **10**(3): p. 20-7.
101. Thakral, N.K., et al., *Soluplus-solubilized citrated camptothecin—a potential drug delivery strategy in colon cancer*. AAPS PharmSciTech, 2012. **13**(1): p. 59-66.

102. Obata, T., et al., *Improvement of the Antitumor Activity of Poorly Soluble Sapacitabine (CS-682) by Using Soluplus® as a Surfactant*. Biological and Pharmaceutical Bulletin, 2014. **37**(5): p. 802-807.
103. Ruan, L.-P., et al., *Prediction of human absorption of natural compounds by the non-everted rat intestinal sac model*. European journal of medicinal chemistry, 2006. **41**(5): p. 605-610.
104. Le Ferrec, E., et al., *In vitro models of the intestinal barrier*. Atla, 2001. **29**: p. 649-668.
105. Volpe, D.A., *Application of method suitability for drug permeability classification*. The AAPS journal, 2010. **12**(4): p. 670-678.

## VITA

Eman Ashour received a Bachelor's degree in Pharmaceutical sciences from The University of Alexandria, Egypt. She joined The University of Mississippi and National Center of Natural Products Research (NCNPR) in 2006 as associate R&D chemist. She participated in the analysis of confiscated marijuana samples to determine the potency of those samples. During this period, she gained experience in the use of GC, GC-MS, HPLC, UV and column chromatography as a part of her job responsibility. During this period, she improved her organizational skills by maintaining accurate lab records as well as working under GMP guidelines. In 2011, she joined the Department of Pharmaceutics and Drug Delivery to pursue her Ph. D. Degree in pharmaceutics. She worked internally as research associate, teaching assistant and instructor in the "Hands on Tablet Course" (pre-formulation lab). Her research experience has focused on pre-formulation and formulation development of solid dosage forms using Hot Melt Extrusion technique to enhance the solubility and bioavailability of poorly water soluble APIs.

Eman is a member of the Honor Society Rho-Chi National Scholars Honorary Society. She is a recipient of several awards including; Travel Award from Formulation Design and Development (FDD) Section of AAPS sponsored by Astra Zeneca (2013), Travel Award from Nutraceutical and Natural Products Focus Group Section of AAPS sponsored by Amway (2014) and Travel Award from Formulation Design and Development (FDD) Section of AAPS (2015). Eman was also selected as oral presenter in Drug Discovery and Development Colloquium (DDDC) 2015.



She is also interested social work, so she served as the Senator for the Department of Pharmaceutics in Graduate Student Council (2013-2014), vice chair of the AAPS-University of Mississippi Student Chapter (2013), chair elect of the AAPS-University of Mississippi Student Chapter (2014) and chair of the AAPS-University of Mississippi Student Chapter (2015). Eman received the Doctor of Philosophy degree in Pharmaceutics in December 2015.